



FRACTUS2D

Release 8.0

Numerical and Experimental Evaluation of Fracture Mechanics Parameters

Claudio Ruggieri

Polytechnic School, University of São Paulo

A Research Project Sponsored by

São Paulo Research Foundation - FAPESP

Brazilian Scientific Research Council - CNPq

Petróleo Brasileiro S. A. - PETROBRAS

June 2021

Abstract

This document describes the theoretical aspects and commands necessary to use **FRACTUS2D**, a research code written in Fortran F77 and F90 to determine several key fracture mechanics parameters used in typical fracture mechanics applications for common fracture specimens and structural components containing stationary and growing cracks. **FRACTUS2D** is under continuing development to incorporate new capabilities that address recent advances in fracture mechanics procedures, test techniques and other crack problems. Specific features of the present version of **FRACTUS2D** include:

- *Numerical computation of J-Q trajectories for 2-D cracked bodies and structural components with stationary and growing cracks based on a modified boundary layer (MBL) reference solution;*
- *Numerical evaluation of η -factors to determine the elastic-fracture parameters J and CTOD (δ) in conventional fracture mechanics specimens, including C(T), 3P and 4P SE(B)s and SE(T)s under pin-load and clamp conditions;*
- *Experimental evaluation of fracture toughness in terms of critical values of J and CTOD at cleavage instability (J_c , δ_c) and fracture resistance data described by J-R or CTOD-R curves using experimentally measured load-displacement records provided by the MTS system MTS Landmark® Testing Solutions with 250 kN of capacity.;*

FRACTUS2D takes input commands to define the numerical (finite element) model, solution parameters, experimental toughness data and output requests in a format-free, English-like structure from a user-specified input file. This input file may include extensive user comments and is thus self-documenting. Finite element results required to compute the user-defined fracture parameters consist of displacements, reaction forces, stresses and strains in standard Patran format (binary or ASCII) MSC Patran® FEA Modeling Solution. written directly by the finite element code WARP3D.

Acknowledgements

The work described in this guide has been supported by grants principally from the The São Paulo Research Foundation - FAPESP, the Brazilian Scientific Research Council - CNPq, and Petróleo Brasileiro S. A. - (PETROBRAS)

Summary

1	Introduction	1
1.1	Fracture Mechanics in Structural Integrity Assessments	1
1.2	What is <i>FRACTUS2D</i> ?	2
2	Continuum Description of Constraint	4
2.1	The $J - Q$ Approach	4
2.2	The Modified Boundary Layer (MBL) Model	5
2.3	Computational Procedures	6
2.4	$J - Q$ Trajectories for Typical Crack Configurations	7
3	Evaluation of J and CTOD Parameters	10
3.1	J -Integral Analysis for Stationary and Growing Cracks	10
3.1.1	J Evaluation Procedure for a Stationary Crack	10
3.1.2	J Evaluation Procedure for a Growing Crack Based on LLD Data	12
3.1.3	J Evaluation Procedure for a Growing Crack Based on CMOD Data	14
3.2	CTOD Evaluation Procedure	15
3.2.1	CTOD for Stationary Cracks Based on the η -Method	16
3.2.2	J -CTOD Relation for Power Hardening Materials	16
3.2.3	J -CTOD Relation Under Large Scale Yielding Based on Fully Plastic Solutions	17
3.2.4	Extension to Include Stable Crack Growth	19
3.3	Geometric Evaluation of CTOD	20
3.3.1	The Plastic Hinge Model	20
3.3.2	The Double Clip-Gage Method	20
3.4	Computational Procedures	22
3.4.1	Plastic Area Under the Load-Displacement Curve	22
3.4.2	Numerical Evaluation of the Plastic η -Factor	23
3.4.3	Numerical Evaluation of the CTOD	24
3.4.4	Numerical Evaluation of the Plastic Rotational Factor	25
4	Experimental Evaluation of Fracture Toughness	26
4.1	J and CTOD Estimation Procedure Based on the η -Method	26
4.2	Crack Growth Resistance Curves	27
4.3	Evaluation of CTOD Using the Plastic Hinge Model	29
4.4	Computational Procedures	30

4.4.1	Cleavage Fracture Toughness	31
4.4.1.1	Evaluation Procedure of the J -Integral at Cleavage Instability, J_c	31
4.4.1.2	The CTOD at Cleavage Instability, δ_c	31
4.4.2	Fracture Resistance Curves	32
4.4.2.1	Evaluation Procedure of the J -Integral During Testing	32
4.4.2.2	Crack Growth Estimate Based on Unloading Compliance	32
4.4.2.3	Adjustment of Initial Crack Size and Initialization Procedure	33
5	Syntax of Commands and Input	
	Parameters	35
5.1	Using <i>FRACTUS2D</i>	35
5.2	Syntax Conventions	35
5.2.1	Descriptors	36
5.2.2	Command Structure	37
5.2.3	Other Syntaxes	38
5.3	Analysis Type Definition	38
5.4	Blocks of Subcommands	39
6	Evaluation of $J - Q$ Trajectories	40
6.1	Analysis Type Definition	40
6.2	Blocks of Subcommands	40
6.3	Small Scale Yielding (SSY) Model	40
6.3.1	Input File Directory	40
6.3.2	Nodal Coordinates and Element Incidences	41
6.3.3	Format for Finite Element Result Files	41
6.3.4	Crack Tip Node	41
6.3.5	Crack Plane Orientation	41
6.3.6	Near-Tip Elements	42
6.4	Finite Body	42
6.4.1	Specimen identification	42
6.4.2	Input File Directory	43
6.4.3	Nodal Coordinates and Element Incidences	43
6.4.4	Loading Parameter Results	43
6.4.5	Format for Finite Element Result Files	44
6.4.6	Crack Tip Node	44
6.4.7	Crack Flank Definition	45
6.4.8	Crack Plane Orientation	46
6.4.9	Model Symmetry	47
6.5	Analysis Parameters	48
6.5.1	WARP3D Release	48
6.5.2	Nondimensional Radius	48
6.5.3	Adaptive Factor	48
6.5.4	Reference J -Integral for the SSY Model	49
6.5.5	Material Properties	49

6.5.6	Node Search Tolerance	49
6.5.7	Specification of Load Steps for generation of $J - Q$ Trajectories	49
6.5.8	Output Options	49
6.6	Illustrative Example	50
7	<i>J</i> and CTOD Evaluation Procedures	52
7.1	Analysis Type Definition	52
7.2	Blocks of Subcommands	52
7.3	Crack Configuration	52
7.3.1	Specimen identification	52
7.3.2	Fracture Specimen Geometry	53
7.3.3	Specimen Dimensions	53
7.3.4	Format for Finite Element Result Files	54
7.3.5	Input File Directory	54
7.3.6	Loading Parameter Results	54
7.3.7	Nodal Coordinates and Element Incidences	55
7.4	Mesh Based Parameters	56
7.4.1	Crack Tip Node	56
7.4.2	Crack Flank Definition	56
7.4.3	CMOD and LLD Definition	57
7.4.4	Applied Load	58
7.4.5	Crack Plane Orientation	59
7.4.6	Model Symmetry	60
7.5	Analysis Parameters	60
7.5.1	WARP3D Release	60
7.5.2	Material Properties	61
7.5.3	Evaluation of the Plastic Area Under Load-Displacement Curve	61
7.5.4	CTOD and Rotational Factor Evaluation Procedure	62
7.5.5	Specification of Load Steps	62
7.5.6	Node Search Tolerance	63
7.5.7	Output Options	63
7.6	Illustrative Example	63
8	Cleavage Fracture Toughness Testing	66
8.1	Analysis Type Definition	66
8.2	Blocks of Subcommands	66
8.3	Crack Configuration	66
8.3.1	Specimen Identification	66
8.3.2	Fracture Specimen Geometry	66
8.3.3	Specimen Dimensions	67
8.3.4	Specimen Side Groove	68
8.4	Test Data Description	68
8.4.1	Test Data File Name	68
8.4.2	MTS Data File Structure	68

8.5	Analysis Parameters	69
8.5.1	Material Properties	69
8.5.2	Evaluation of the Elastic and Plastic Area Under the Load-Displacement Curve	70
8.5.3	Fracture Toughness Evaluation Procedure	71
8.5.4	User-Defined η -Factors	72
8.5.5	Test Data Units	72
8.6	Illustrative Example	72
9	Fracture Resistance Testing	74
9.1	Analysis Type Definition	74
9.2	Blocks of Subcommands	74
9.3	Crack Configuration	74
9.3.1	Specimen Identification	74
9.3.2	Fracture Specimen Geometry	74
9.3.3	Specimen Dimensions	75
9.3.4	Specimen Side Groove	76
9.4	Test Data Description	76
9.4.1	Test Data File Name	76
9.4.2	MTS Data File Structure	76
9.5	Analysis Parameters	79
9.5.1	Material Properties	79
9.5.2	Fracture Resistance Evaluation Procedure	79
9.5.3	Crack Extension Correction	80
9.5.4	Initialization Procedure	80
9.5.5	Test Data Units	81
9.6	Illustrative Example	81
A	Fracture Specimen Geometries	83
A.1	Homogeneous Fracture Specimens	83
A.2	Weld Centerline Fracture Specimens	83
B	Compliance Solutions for Fracture Specimens	87
B.1	Compact Tension Specimen - C(T)	88
B.2	3P Single Edge Notched Bend Specimen - 3P SE(B)	88
B.3	4P Single Edge Notched Bend Specimen - 4P SE(B)	89
B.4	Pin-Loaded Single Edge Notched Tension Specimen - SE(T) _P	89
B.5	Clamped Single Edge Notched Tension Specimen - SE(T) _C	89
C	η-Factors for Homogeneous Fracture Specimens	91
C.1	Compact Tension Specimen - C(T)	91
C.2	3P Single Edge Notched Bend Specimen - 3P S	

$$\eta_J^{\text{CMOD}} = 1.195 + 0.931(a/W) - 4.227(a/W)^2 + 3.072(a/W)^3 - 0.352M_y - 0.049M_y^2 , \quad H/W = 10 \quad (1)$$

E(B)	92
C.3 4P Single Edge Notched Bend Specimen - 4P SE(B)	92
C.4 Pin-Loaded Single Edge Notched Tension Specimen - SE(T) _P	92
C.5 Clamped Single Edge Notched Tension Specimen - SE(T) _C	93
D η-Factors for Weld Centerline Fracture Specimens	94
D.1 Compact Tension Specimen - C(T)	94
D.2 3P Single Edge Notched Bend Specimen - 3P SE(B)	95
D.3 Pin-Loaded Single Edge Notched Tension Specimen - SE(T) _P	95
D.4 Clamped Single Edge Notched Tension Specimen - SE(T) _C	95

1

Introduction

1.1 Fracture Mechanics in Structural Integrity Assessments

The fundamental importance of assessing fracture behavior in structural integrity analyses has stimulated a rapidly increasing amount of research on engineering procedures to quantify and analyze the influence of crack-like defects on the load carrying capacity of structural components such as, for example, cracks in critical weldments of aging structures and reactor pressure vessels (RPVs). Such methodologies play a key role in repair decisions and life-extension programs for in-service structures (e.g., nuclear and pressure vessel components) while, at the same time, ensuring acceptable safety levels during normal operation. Conventional fracture mechanics methodologies for structural integrity assessments rely on the correlation of fracture conditions across different crack geometries/loading modes as measured by the linear elastic stress intensity factor, K , or the elastic-plastic parameter defined by the J -integral and its corresponding value of the Crack Tip Opening Displacement, CTOD (δ) [1, 2]. The underlying concept is that the crack-tip stress and strain fields that develop over microstructurally significant size scales (*i.e.*, the fracture process zone of a few CTODs ahead of a macroscopic crack) can be adequately described by a single parameter, such as J , and, further, that this parameter sets the intensity of local deformation leading to material failure in various cracked structures having different levels of constraint. More recent efforts advanced the viewpoint of the continuum fracture mechanics framework by developing two-parameter fracture methodologies to describe the full range of Mode I, elastic-plastic crack-tip fields with varying near-tip stress triaxiality [3]. These approaches also make use of the J -integral (or, equivalently, the CTOD) to scale the crack-tip fields within the near-tip region over which large stresses and strains develop, while the second parameter defines a family of crack-tip fields of varying stress triaxiality [4, 5, 6, 7, 8, 9, 10].

Paralleling these efforts, substantial progress has been made in recent years in fitness-for-service (FFS) procedures applicable to defect assessments and life-extension programs of critical engineering structures. These methodologies, also referred to as Engineering Critical Assessment (ECA) procedures, provide a concise framework to correlate crack size with applied loading in terms of failure assessment diagrams (FAD) to evaluate the severity of crack-like flaws [11, 12, 13]. A key feature of these approaches lies in the use of fracture toughness data measured from deeply cracked specimens tested under bend loading to guarantee high levels of stress triaxiality which drive the fracture process. Under such conditions, a single geometry-independent failure locus then suffices to provide highly effective, albeit conservative, acceptance criteria for cracked structural components. Several flaw assessment methodologies based upon the FAD concept, such as the R6 procedure [14], BS7910 [15], API 579 [16] and SINTAP [17], among

others, are now well established and widely employed to analyze the significance of defects in terms of assessment of structural integrity.

The above arguments highlight the vital importance of determining accurate fracture parameters defining crack driving forces and fracture toughness for use in structural integrity assessment procedures. As a step in this direction, this work describes the computer program **FRACTUS2D** and the associated theoretical framework to evaluate several key fracture parameters for common fracture specimens and cracked configurations based on numerical simulations using the finite element method. **FRACTUS2D** is a research code that incorporates specific features to facilitate extensive fracture analyses of specimens and structural components with various cracked configurations, including experimental evaluation of fracture toughness using load-displacement records.

1.2 What is **FRACTUS2D**?

This document describes the theoretical aspects and commands necessary to use **FRACTUS2D**, a research code written in Fortran F77 and F90 to determine several key fracture mechanics parameters used in typical fracture mechanics applications for common fracture specimens and structural components containing stationary and growing cracks. **FRACTUS2D** is under continuing development to incorporate new capabilities that address recent advances in fracture mechanics procedures, test techniques and other crack problems. Specific features of the present version of **FRACTUS2D** include:

- Numerical computation of $J - Q$ trajectories for 2-D cracked bodies and structural components with stationary and growing cracks based on a modified bounday layer (MBL) reference solution;
- Numerical evaluation of η -factors to determine the elastic-fracture parameters J and CTOD em conventional fracture mechanics specimens, including C(T), 3P and 4P SE(B)s and SE(T)s under pin-load and clamp conditions;
- Experimental evaluation of fracture toughness in terms of critical values of J and CTOD at cleavage instability (J_c , δ_c) and fracture resistance data described by $J - R$ or CTOD – R curves using experimentally measured load-displacement records provided by the MTS system¹;

FRACTUS2D takes input commands to define the numerical (finite element) model, solution parameters, experimental toughness data and output requests in a format-free, English-like structure from a user-specified input file. This input file may include extensive user comments and is thus self-documenting. Finite element results required to compute the user-defined fracture parameters consist of displacements, reaction forces, stresses and strains in standard Patran format (binary or ASCII)² written directly by the finite element code WARP3D [18]. A convenient interface to manipulate finite element results written by the finite element code ABAQUS [19] is under development.

This manual is organized as follows. Chapter 2 provides the theoretical background for the $J - Q$ methodology and the basic procedures needed to determine parameter Q . Chapter 3 describes the evaluation procedure for parameters J and CTOD based on plastic work and the η -method. Chapter 4 provides the key procedures to evaluate experimental cleavage fracture toughness (J_c , δ_c) and fracture resistance curves in terms of $J - R$ and CTOD – R from measured values of load and displacement. Chapters 5-9 describe the commands and input data needed for execution of **FRACTUS2D**. Chapter

¹MTS Landmark® Testing Solutions with 250 kN capacity.

²MSC Patran® FEA Modeling Solution.

?? provides illustrative examples to describe the procedures and commands available to determine several fracture mechanics parameters covered in the current version of **FRACTUS2D**. The appendices describe additional details such as the functional forms of specimen compliance and η -factors implemented into the code.

2

Continuum Description of Constraint

2.1 The $J - Q$ Approach

The marked differences of toughness values (J_c , CTOD or δ_c) for shallow crack and deep crack specimen geometries having similar overall dimensions underlie the loss of one-to-one correspondence between J (and, equivalently, the CTOD) and the elastic-plastic crack-tip fields (see [20, 21, 22, 23, 24] for illustrative data) for ferritic steels at temperatures in the ductile-to-brittle transition (DBT) region. At increasing loads in common fracture specimens, the initially strong small scale yielding (SSY) fields gradually diminish as crack-tip plastic zones increasingly merge with the global bending plasticity on the nearby traction free boundaries. Stresses relax below the values determined uniquely by the J -integral for the high constraint, SSY conditions [1] which exist early in the loading. This loss of a unique relationship between the crack tip fields and J underlies the constraint loss phenomenon and contributes to the observed specimen geometry and loading mode dependence on measured values of cleavage fracture toughness (J_c , CTOD). Consequently, once SSY conditions no longer apply, the near-tip stresses (and strains) that develop ahead of a macroscopic crack cannot be described uniquely by J (or, equivalently, CTOD) [1, 3].

The above arguments motivated O'Dowd and Shih (OS) [7, 8] to propose an approximate two-parameter description for the elastic-plastic crack tip fields based upon a triaxiality parameter more applicable under large scale yielding (LSY) conditions for materials with elastic-plastic response described by a power hardening law given by $\epsilon/\epsilon_0 \propto (\sigma/\sigma_0)^n$. Here, n denotes the Ramberg-Osgood strain hardening exponent [2, 25], σ_0 and ϵ_0 are the reference (yield) stress and strain, respectively. Guided by detailed numerical analyses employing a modified boundary layer (MBL) model [26, 27], OS identified a family of self-similar fields in the form

$$\sigma_{ij} = \sigma_0 \tilde{f}_{ij} \left(\frac{r}{J\sigma_0}, \theta, Q \right) \quad (2.1)$$

where the dimensionless second parameter Q defines the amount by which σ_{ij} in fracture specimens differ from the adopted reference SSY solution with the T -stress term [5, 6, 26, 27, 28] set to zero. Here r and θ are polar coordinates centered at the crack tip with $\theta = 0$ corresponding to a line ahead of the crack.

Limiting attention to the forward sector ahead of the crack tip between the $SSY_{T=0}$ and the fracture specimen fields, OS showed that $Q\sigma_0$ corresponds effectively to a spatially uniform hydrostatic stress, *i.e.*, the *difference* field relative to a high triaxiality reference stress state

$$\sigma_{ij} = (\sigma_{ij})_{SSY, T=0} + Q\sigma_0 \delta_{ij} \quad ; \quad |\theta| < \pi/2, \quad J/\sigma_0 < r < 5J/\sigma_0 \quad . \quad (2.2)$$

Operationally, OS defined parameter Q as

$$Q \equiv \frac{\sigma_{\theta\theta} - (\sigma_{\theta\theta})_{SSY, T=0}}{\sigma_0} \quad , \quad \theta = 0, \quad r = 2J/\sigma_0 \quad (2.3)$$

where the difference field is conveniently evaluated at the microscale distance $r = 2J/\sigma_0$, which represents the location of the triggering cleavage mechanism ahead of crack tip. Construction of a $J - Q$ trajectory follows by the evaluation of Eq. (2.3) at each stage of loading in the finite body [3].

2.2 The Modified Boundary Layer (MBL) Model

The SSY reference fields used to evaluate Q by means of Eq. (2.3) are obtained from a plane-strain finite element analysis of an infinite domain, single-ended crack model under Mode I loading [21, 26, 27], which simplifies the generation of numerical solutions for stationary cracks under well-defined SSY conditions. With the plastic region limited to a small fraction of the domain radius, such as $R_p < R/20$, the general form of the asymptotic crack-tip stress fields well outside the plastic region is given by [3, 29]

$$\sigma_{ij} = \frac{K_I}{\sqrt{2\pi}r} f_{ij}(\theta) + T\delta_{1i}\delta_{1j} \quad (2.4)$$

where $K_I = \sqrt{EJ/(1-\nu^2)}$ is the stress intensity factor, f_{ij} define the angular variations of in-plane stress components and the non-singular term, T , represents a tension (or compression) stress parallel to the crack. Numerical solutions for different levels of K_I and T/σ_0 are generated by imposing displacements of the elastic, Mode I singular field on the outer circular boundary ($r = R$) which encloses the crack

$$u(R, \theta) = K_I \frac{1+\nu}{E} \sqrt{\frac{R}{2\pi}} \cos\left(\frac{\theta}{2}\right) (3 - 4\nu - \cos\theta) + T \frac{1-\nu^2}{E} R \cos\theta \quad (2.5)$$

$$v(R, \theta) = K_I \frac{1+\nu}{E} \sqrt{\frac{R}{2\pi}} \sin\left(\frac{\theta}{2}\right) (3 - 4\nu - \cos\theta) - T \frac{\nu(1+\nu)}{E} R \sin\theta \quad (2.6)$$

Figure 2.1 shows the plane-strain finite element model for an infinite domain, single-ended crack problem in which Mode I loading of the far field permits analysis using one-half of the domain as shown in the figure. Trovato and Ruggieri [30] employed this numerical model to generate SSY reference fields consistent with the above Eqs. (2.5) and (2.6). The finite element model utilizes a conventional mesh configuration having a focused ring of elements surrounding the crack front with a small key-hole at the crack tip; the radius of the key-hole, ρ_0 , is $2.5\mu\text{m}$ (0.0025mm). This SSY model has one thickness layer of 2065 8-node, 3-D elements with plane-strain constraints imposed ($w = 0$) on the nodes. The small initial root radius at the crack front (blunt tip) shown in Fig. 2.1(b) accelerates convergence of the finite-strain plasticity algorithms during the initial stage of blunting. Moreover, to limit effects of the initial root radius on the near-tip stress fields, the CTOD (δ) is required to equal four times the initial radius, ρ_0 , at a deformation consistent with $M = b\sigma_0/J = 250$, where M defines a nondimensional deformation limit, σ_0 is the reference yield stress and b is the remaining crack ligament.

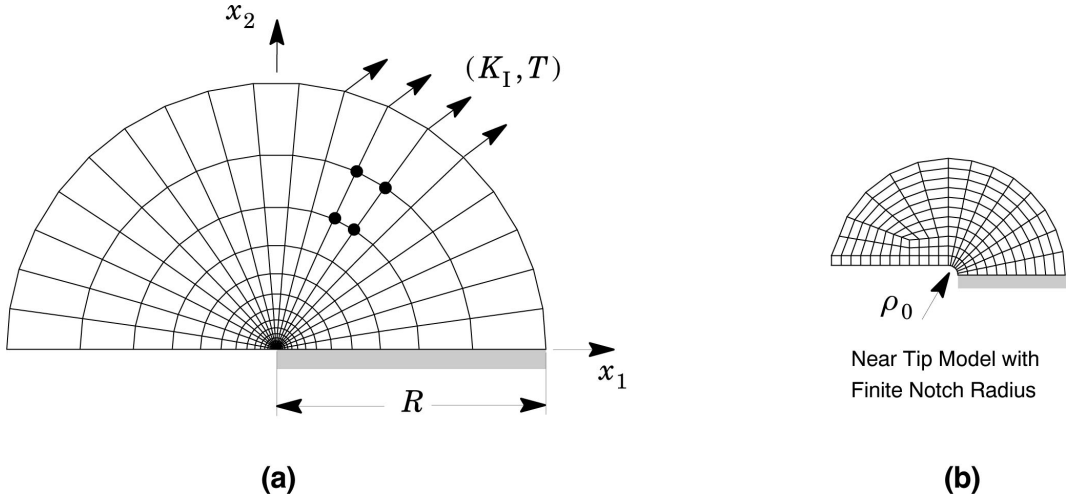


Figure 2.1: *SSY model with (K, T) fields imposed on the boundary.*

Figure 2.2(a-d) provides key results to verify the existence of such fields for well-contained, limited scale plasticity under varying levels of applied T -stress for an elastic-plastic material having flow properties defined by $n = 10$ and $E/\sigma_0 = 500$. In the plots, distances all scale with $(K/\sigma_0)^2$ whereas the opening stresses are normalized by σ_0 . At very low remote loading characterized by $K_I = 20$ and $40 \text{ MPa}\sqrt{\text{m}}$ for all levels of applied T -stress, the near-tip stresses increase as the process of crack-tip blunting takes place. After the notch root radius increases to several times the initial radius, ρ_0 , a *steady state* solution develops so that the near-tip fields under SSY conditions are simply a continuous series of self-similar states. These plane-strain fields thus define a family of reference fields for stationary cracks where specified values for K_I and T uniquely define the elastic-plastic fields along the crack tip when a vanishingly small plastic zone encloses the tip. The differences between the actual finite-body field and those of the comparison SSY field (having the applicable elastic T -stress) thus quantify the extent of large-scale yielding (LSY) effects. Despite the apparent small differences between these fields (differences between high and low constraint fields are of the order of $\sim 10\%$), the implications for fracture are enormous as demonstrated by several experimental observations. Indeed, factors exceeding 3-5 are often observed in toughness values (such as J_c or δ_c) for high constraint and low constraint fracture specimens. Further results regarding the generation of SSY near-tip fields are given by Dodds et al. [3], Trovato and Ruggieri [30] and Cravero and Ruggieri [31].

2.3 Computational Procedures

From the above discussion, it becomes clear that parameter Q represents a purely hydrostatic stress that measures the perturbation stress fields (from the SYY reference value) which is, thus, associated with the deviation in crack tip stress triaxiality (more adequately referred to as *crack-tip constraint*). Consequently, the generation of $J - Q$ trajectories for a cracked body or structural component is simply defined in terms of the Mode I difference fields at a reference distance from the crack tip for the cracked component and the MBL model. To illustrate the procedure, Fig. 2.3 shows the near-tip opening stresses for a representative cracked body with increasing loading levels, as characterized by J , in comparison with the corresponding SYY reference stress field. In this plot, the opening stresses are normalized by σ_0 whereas the crack tip distance is normalized by J/σ_0 .

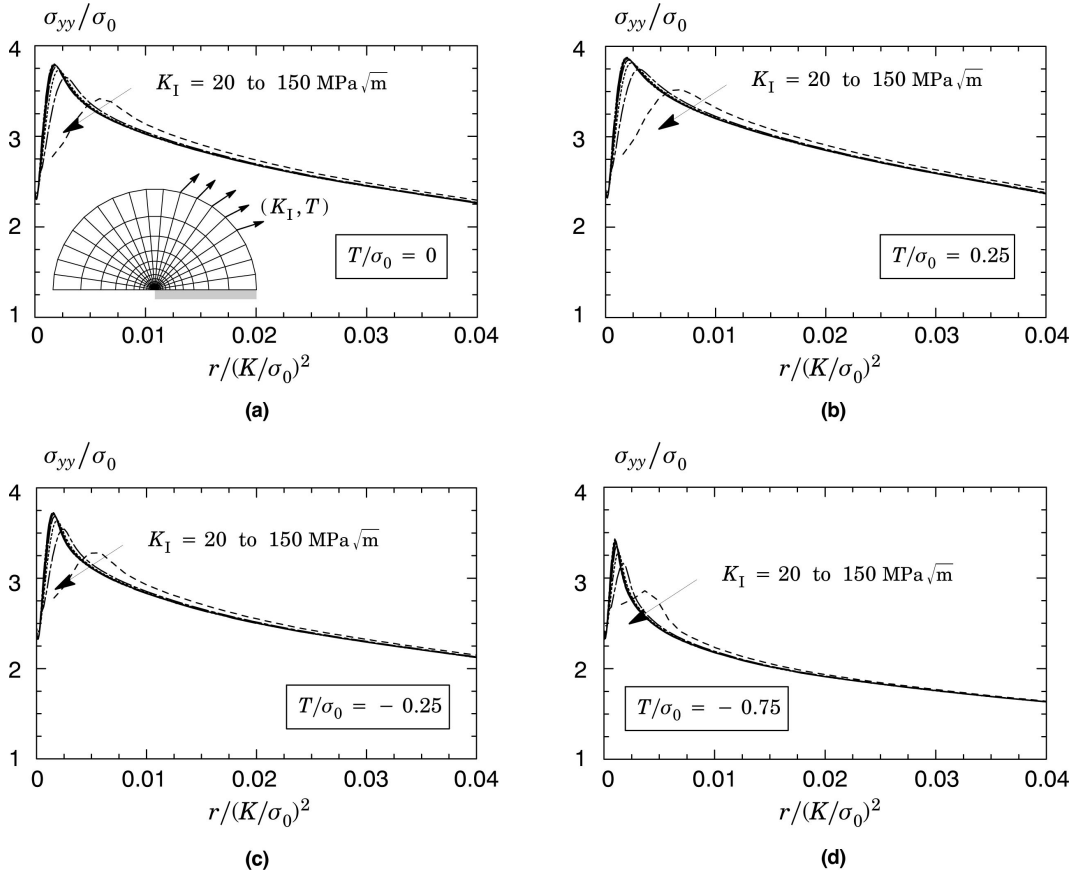


Figure 2.2: *Near-tip opening stresses under SSY conditions for an elastic-plastic material having flow properties defined by $n = 10$ and $E/\sigma_0 = 500$ with varying levels of applied T -stress. Plots are generated for load levels $K_I = 20, 40, 60, 80, 100, 125$ and $150 \text{ MPa}\sqrt{\text{m}}$.*

Within the present framework, parameter Q is operationally defined in **FRACHTUS2D** as

$$Q \equiv \frac{(\sigma_{yy})_{FB} - (\sigma_{yy})_{SSY, T=0}}{\sigma_0} \quad , \quad \theta = 0, \quad r/(J/\sigma_0) = \lambda \quad (2.7)$$

where the subscript *FB* refers to the finite body difference field and *SSY, T = 0* represents the MBL model with $T = 0$. While parameter Q is most often evaluated at the reference normalized distance defined by $\lambda = 2$, other values for λ can be specified in **FRACHTUS2D** as described later in this manual.

2.4 $J - Q$ Trajectories for Typical Crack Configurations

To illustrate the $J - Q$ methodology just outlined, this section provides representative $J - Q$ trajectories for typical crack configurations displayed in Fig. 2.4, including a standard compact C(T) specimen, a middle crack M(T) configuration loaded in tension, a standard three-point bend SE(B) specimen and a pin-loaded, single-edge notched tension SE(T) geometry. Figure 2.5 describes the evolution of Q with increased levels of applied J for an elastic-plastic material with stress-strain response following a power-law model given by $\epsilon/\epsilon_0 = (\sigma/\sigma_0)^n$ with $n = 10$ (moderate hardening material) and $n = 20$ (low hardening material). In those plots, parameter Q is defined by Eq. (2.7) and evaluated at the reference crack tip distance given by $r/(J/\sigma_0) = 2$ whereas J is normalized by $b\sigma_0$ with b denoting the remaining crack ligament, defined by $W - a$ (notice that $J/(b\sigma_0)$ is plotted against $-Q$ to maintain positive scales).

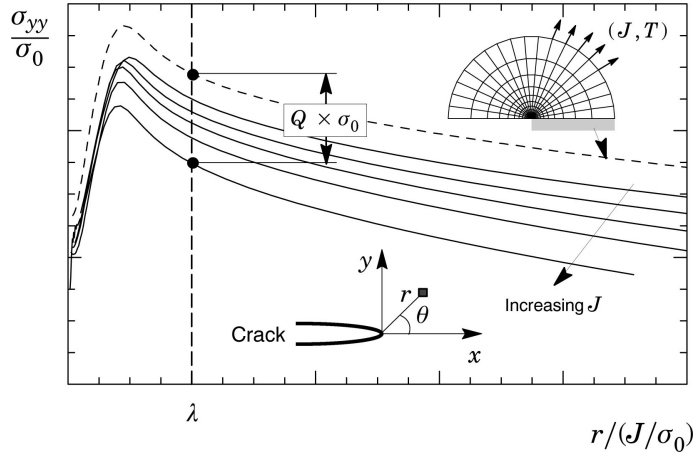


Figure 2.3: *Near-tip opening stresses for increasing levels of J in comparison with the SSY reference stress field.*

For each material, the evolution of Q as loading progresses depends markedly on the specimen geometry. For the deep notch C(T) specimen, parameter Q is positive at low load levels (which corresponds to positive elastic T -stresses for this geometry [3, 6]) and gradually change to negative (albeit small) values with increased levels of J . In all these plots, the deep notch SE(B) and SE(T) specimens display a relatively similar behavior with comparable $J - Q$ trajectories for almost the entire range of loading. In contrast, the deep notch M(T) specimen reveals large negative Q -values almost immediately upon loading for all considered strain hardening properties.

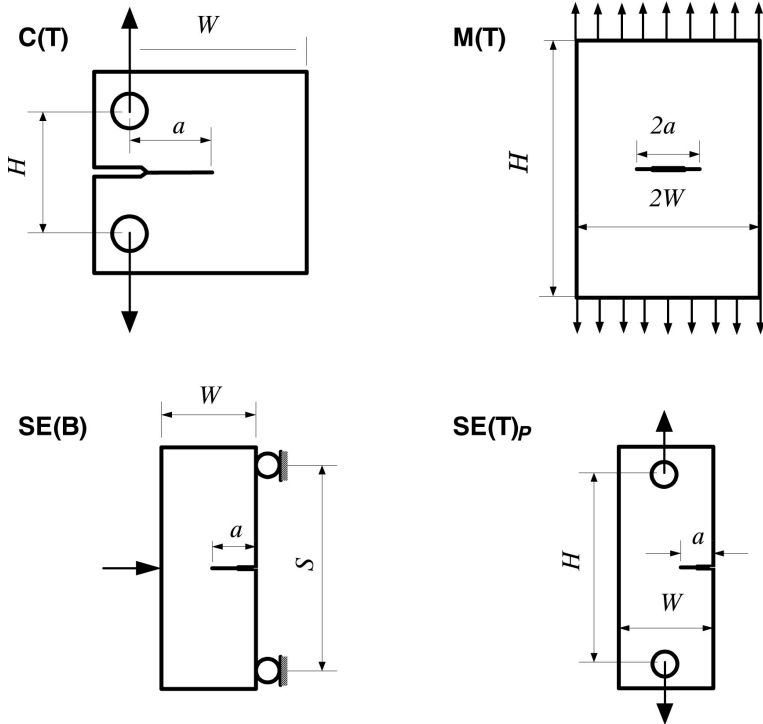
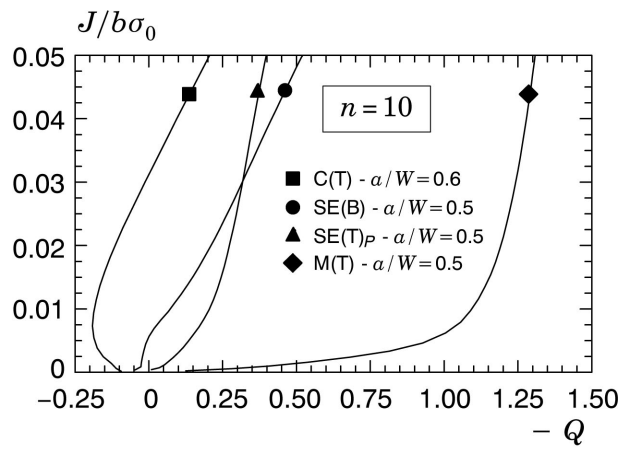
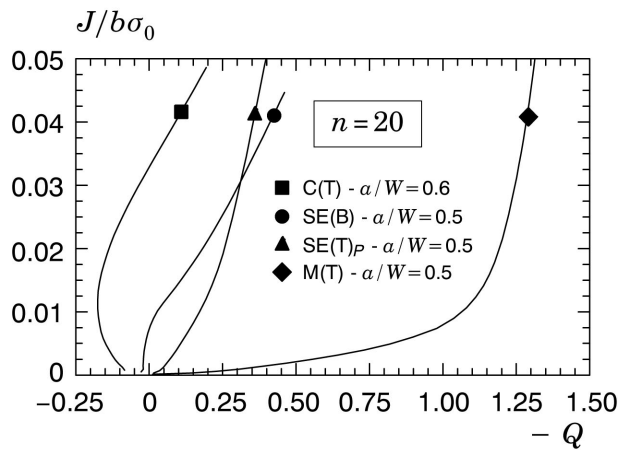


Figure 2.4: *Typical crack configurations including a standard compact C(T) specimen, a midle crack M(T) configuration loaded in tension, a standard three-point bend SE(B) specimen and a pin-loaded, single-edge notched tension SE(T) geometry.*



(a)



(b)

Figure 2.5: $J - Q$ trajectories for typical specimen configurations: (a) $n = 10$ material. (b) $n = 20$ material.

3

Evaluation of J and CTOD Parameters

3.1 J -Integral Analysis for Stationary and Growing Cracks

This section provides the essential features of the theoretical framework needed to determine J for stationary and growing cracks based upon load-displacement measurements. The description that follows draws heavily on the early work of Ernst et al. [32], Hutchinson and Paris [33] and Kanninen and Popelar [34]. The presentation begins with the J -integral analysis for a cracked body based upon the η -method and load-load line displacement (LLD or Δ) records. Attention is directed first to a stationary crack followed by the description of an incremental procedure to evaluate J for a growing crack. Subsequent development focuses on a simpler extension of the J evaluation procedure for growing cracks based upon crack mouth opening displacement (CMOD or V) records.

3.1.1 J Evaluation Procedure for a Stationary Crack

The energy release rate definition of J for a cracked body with unit thickness illustrated in Fig. 3.1(a) provides the basis to estimate the J -integral for a stationary crack based upon measured load-load line displacement records. Consistent with deformation theory, the path-independent J -integral is given by [33, 34]

$$J = \int_0^P \left(\frac{\partial \Delta}{\partial a} \right)_P dP = - \int_0^\Delta \left(\frac{\partial P}{\partial a} \right)_\Delta d\Delta \quad (3.1)$$

where P is the applied load, Δ is the load line displacement (LLD) and a is the crack size. Here, it is understood that the above integrals correspond to load control and displacement control conditions.

Upon consideration of the elastic, Δ_e , and plastic, Δ_p , components of the load line displacement given by

$$\Delta = \Delta_e + \Delta_p \quad (3.2)$$

and manipulating the first integral of Eq. (3.1), J can be expressed as

$$J = \int_0^P \left(\frac{\partial \Delta_e}{\partial a} \right)_P dP + \int_0^P \left(\frac{\partial \Delta_p}{\partial a} \right)_P dP = J_e + J_p \quad (3.3)$$

where J_e and J_p are the elastic and plastic components. Here, J_e is conveniently defined by the energy

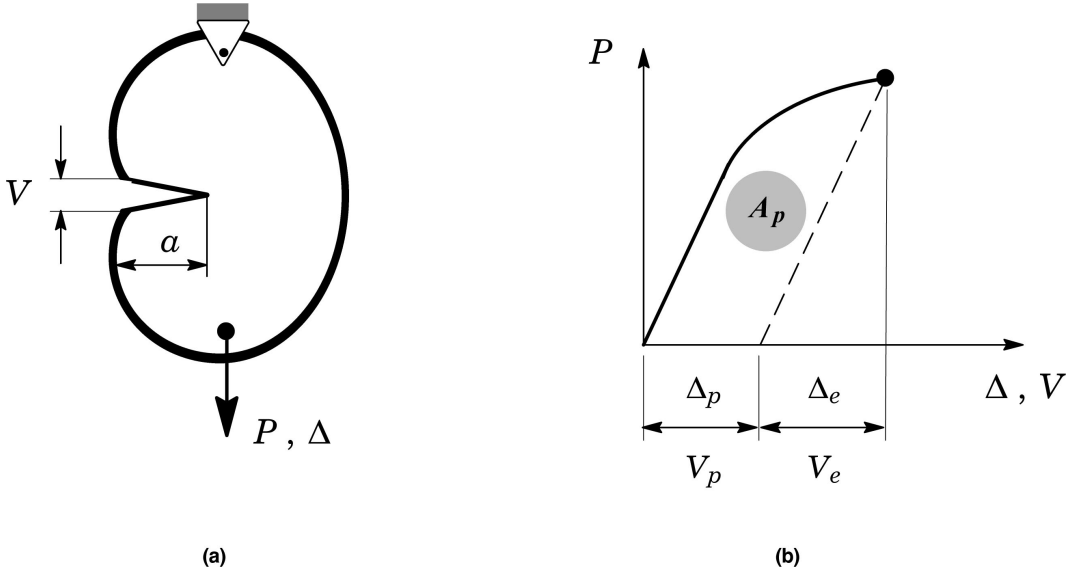


Figure 3.1: (a) Arbitrary cracked body with unit thickness subjected to remote loading. (b) Definition of the plastic area under the load-displacement curve.

release rate for a linear elastic cracked body under Mode I deformation in the standard form [2]

$$J_e = \frac{K_I^2}{E'} \quad (3.4)$$

where K_I denotes the (Mode I) elastic stress intensity factor for the cracked configuration and $E' = E/(1 - \nu^2)$ with E and ν representing the (longitudinal) elastic modulus and Poisson's ratio.

The plastic component, J_p , is derived from adopting the approach proposed by Sumpter and Turner [35] building upon the earlier work of Rice et al. [36] to relate the J -integral to the area under the load versus load-line displacement. Figure 3.1(b) illustrates the essential features of the estimation procedure for J_p . The approach simply relates the plastic contribution to the strain energy (due to the crack) and J in the form

$$J_p = \int_0^P \left(\frac{\partial \Delta_p}{\partial a} \right) dP = \frac{\eta_J^{LLD}}{b} \int_0^{\Delta_p} P d\Delta_p = \frac{\eta_J^{LLD} A_p^{LLD}}{b} \quad (3.5)$$

where A_p^{LLD} is the plastic area under the load versus load line displacement (Δ) and $b = W - a$ is the uncracked ligament. To arrive at Eq. (3.5), the equality $da = -db$ was used. Factor η_J^{LLD} introduced by Sumpter and Turner [35] represents a nondimensional parameter which relates the plastic contribution to the strain energy for the cracked body with J and is assumed to be a function of the flawed configuration and independent of loading [34]. Here, it is also noted that the specimen response (and, consequently, the plastic area under the load versus displacement curve) illustrated in Fig. 3.1(b) can be defined in terms of crack mouth opening displacement (CMOD) data. For definiteness, the corresponding η -factor is denoted η_J^{CMOD} so that J_p can be expressed as

$$J_p = \frac{\eta_J^{CMOD} A_p^{CMOD}}{b} \quad (3.6)$$

where A_p^{CMOD} is now the plastic area under the load versus crack mouth opening displacement (V).

The previous Eqs. (3.5) and (3.6) are equally applicable to a conventional fracture specimen with net

thickness B_N ($B_N = B$ if there are no side grooves where B is the gross thickness). Here, the plastic component of the J -integral is then given by

$$J_p = \frac{\eta_J^{LLD} A_p^{LLD}}{bB_N} \quad (3.7)$$

and

$$J_p = \frac{\eta_J^{CMOD} A_p^{CMOD}}{bB_N} \quad (3.8)$$

In the above, while both definitions for the η -factor serve essentially as a means to quantify the effect of plastic work on the J -integral, η_J -values based on LLD have a different character than the corresponding η_J -values based on CMOD.

3.1.2 J Evaluation Procedure for a Growing Crack Based on LLD Data

Conventional testing programs to measure crack growth resistance ($J - \Delta a$) curves routinely employ the unloading compliance (UC) method based upon testing of a single fracture specimen. Key advantages of the UC technique involve its relative simpler execution (when compared to the multi-specimen technique) [37] and, most importantly, the possibility to obtain fracture toughness data when severe limitations exist on material availability, for example, in nuclear reactor surveillance. However, application of the procedure requires accurate evaluation of the crack-tip driving force (as measured by J) and crack growth extension from laboratory measurements of load-displacement records.

The previous solution for J_p given by Eq. (3.5) retains strong contact with the deformation plasticity definition of J thereby assuming nonlinear elastic material response. However, the area under the actual load-displacement curve for a growing crack differs significantly from the corresponding area for a stationary crack (which the deformation definition of J is based on) - see discussion in Anderson [2]. Consequently, the measured load-displacement records must be corrected for crack extension to obtain an accurate estimate of J -values with increased crack growth. A convenient framework to evaluate J with crack extension follows from the earlier work of Ernst et al. [32]. Given the conditions of J -controlled crack growth and deformation plasticity are satisfied, the approach enables evaluation of J_p for arbitrary (small) increments of a and Δ_p .

Development of the evaluation procedure for J_p begins by considering the differential

$$dJ_p = \frac{\partial J_p}{\partial \Delta_p} d\Delta_p + \frac{\partial J_p}{\partial a} da \quad (3.9)$$

where it is understood that J_p is a function of crack size, a , and plastic displacement, Δ_p .

The plastic contribution to the strain energy for the cracked body, U_p , can be equally defined in terms of the plastic area under the load-displacement curve which permits recasting the previous Eq. (3.5) in the form

$$J_p = \frac{\eta_J^{LLD}}{b} \int_0^{\Delta_p} P d\Delta_p = \frac{\eta_J^{LLD} U_p}{b} \quad (3.10)$$

which upon differentiation with respect to Δ_p and a (after making $b = W - a$) gives

$$\frac{\partial J_p}{\partial \Delta_p} = \frac{\eta_J^{LLD}}{(W - a)} \frac{\partial U_p}{\partial \Delta_p} \quad (3.11)$$

and

$$\frac{\partial J_p}{\partial a} = \frac{1}{(W - a)} \frac{d\eta_J^{LLD}}{da} U_p + \frac{\eta_J^{LLD}}{(W - a)^2} U_p + \frac{\eta_J^{LLD}}{(W - a)} \frac{\partial U_p}{\partial a} \quad . \quad (3.12)$$

Noting that $J_p = -\partial U_p / \partial a$ and $P = \partial U_p / \partial \Delta_p$, the introduction of Eqs. (3.11) and (3.12) into Eq. (3.9) can be manipulated into the form

$$dJ_p = \frac{\eta_J^{LLD}}{b} P d\Delta_p - \frac{\gamma_{LLD}}{b} J_p da \quad (3.13)$$

where factor γ_{LLD} is given by

$$\gamma_{LLD} = \eta_J^{LLD} - 1 - \frac{b}{\eta_J^{LLD}} \frac{d\eta_J^{LLD}}{da} \quad . \quad (3.14)$$

In arriving at Eq. (3.13), $b = W - a$ and Eq. (3.10) were used.

Consider now the evolution of load, P , with plastic deformation, Δ_p , for a growing crack schematically illustrated in Fig. 3.2(a) where a_0 denotes the initial crack size. Because dJ_p is an exact differential, integration of Eq. (3.13) yields

$$J_p = \int_0^{\Delta_p} \frac{\eta_J^{LLD}}{b} P d\Delta_p - \int_{a_0}^a \frac{\gamma_{LLD}}{b} J_p da \quad (3.15)$$

which holds for any path leading to the current values of a and Δ_p [34]. It is clear that setting the crack growth ($\Delta a = a - a_0$) to zero reduces Eq. (3.15) to the previous Eq. (3.5) for a stationary crack.

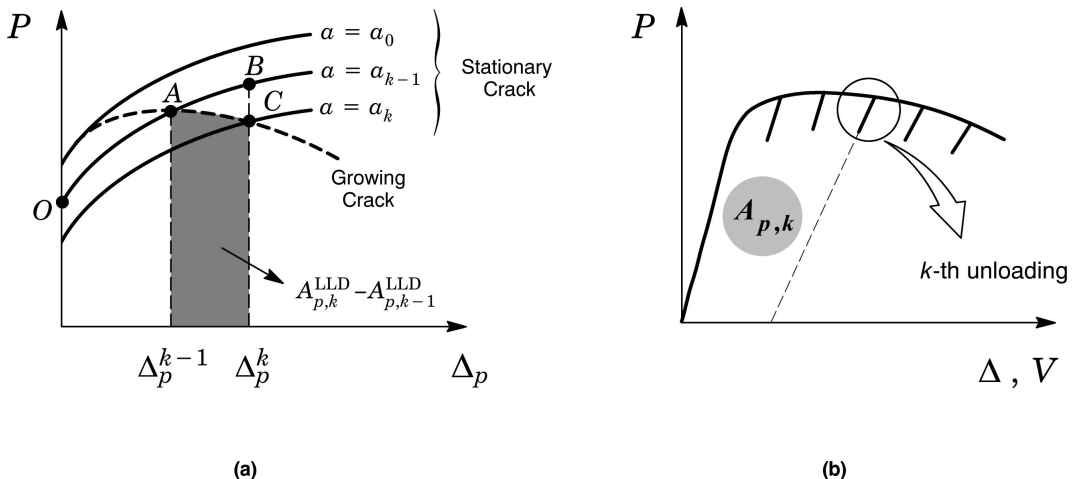


Figure 3.2: (a) Load-displacement trajectory for a stationary and growing crack; (b) Partial unloading during the evolution of load with displacement.

Now, limiting attention to a $P - \Delta_p$ curve for a fixed crack length, such as path **OAB** corresponding

to crack length $a = a_{k-1}$ in Fig. 3.2, the increase in J_p for a small increment in plastic deformation given by $\Delta_p^k - \Delta_p^{k-1}$ can be derived from Eq. (3.15) in the form

$$J_p^B - J_p^A = \frac{\eta_J^{LLD}}{b} \int_{\Delta_{k-1}}^{\Delta_k} P d\Delta_p \quad (3.16)$$

since $da = 0$ on this path and η_J^{LLD} is assumed constant throughout the loading.

When the crack has extended to the length $a = a_k$ for a fixed plastic displacement, Δ_p^k , the variation of J_p for a small increment in crack length is again derived from Eq. (3.15) as

$$J_p^C - J_p^B = - \int_{a_{k-1}}^{a_k} \frac{\gamma_{LLD}}{b} J_p da \approx - \frac{\gamma_{LLD, k-1}}{b_{k-1}} J_p^B (a_k - a_{k-1}) \quad (3.17)$$

in which now $d\Delta_p = 0$.

The previously developed formulations (which form the basis of current standards such as ASTM E1820 [38]) now lead to an incremental procedure which updates J_p at each partial unloading point, denoted k , during the measurement of the load vs. displacement curve illustrated in Fig. 3.2(b). Using Eqs. (3.16) and (3.17), and noting that $J_p^A \equiv J_p^{k-1}$ and $J_p^C \equiv J_p^k$, the k -th plastic term of J_p at crack length $a = a_k$ can be estimated by

$$J_p^k = \left[J_p^{k-1} + \frac{\eta_{J, k-1}^{LLD}}{b_{k-1}} (A_{p,k}^{LLD} - A_{p,k-1}^{LLD}) \right] \left[1 - \frac{\gamma_{LLD, k-1}}{b_{k-1}} (a_k - a_{k-1}) \right] \quad (3.18)$$

where $A_{p,k}^{LLD}$ and $A_{p,k-1}^{LLD}$ are the current plastic areas under the curve $P - LLD$ at crack length $a = a_k$ and $a = a_{k-1}$. It should be noted that the above treatment of the plastic contribution to the strain energy is applicable to a cracked body with unit thickness. For a cracked configuration with net thickness B_N (recall that $B_N = B$ if there are no side grooves where B is the gross thickness), the variation of plastic area ($A_{p,k}^{LLD} - A_{p,k-1}^{LLD}$) in previous Eq. (3.18) must be multiplied by $1/B_N$ to maintain agreement with the familiar ASTM E1820 [38] expression.

3.1.3 J Evaluation Procedure for a Growing Crack Based on CMOD Data

The J -correction for crack growth outlined previously derives from a J -integral analysis in which the strain energy is expressed in terms of load line displacement (LLD) measurements. When the crack growth response is evaluated by means of laboratory measurements of crack mouth opening displacement (CMOD) data, the above Eq. (3.18) to evaluate J at each partial unloading point does not hold true any longer. To provide a simpler extension of the previous procedure to correct J for crack growth effects based upon CMOD records, consider a constant relationship between the plastic components of LLD and CMOD, denoted Δ_p and V_p , in the form

$$\Delta_p = h_a V_p \quad (3.19)$$

where h_a is a factor dependent on crack size and relatively independent of loading and material properties. The extensive numerical analyses by Cravero and Ruggieri [39] demonstrate the applicability of this relationship in common fracture specimens.

Defining the plastic contribution to the strain energy for the cracked body in terms of the plastic area under the load-displacement curve (see Fig. 3.2(b)), it follows from Eq. (3.19) that $A_p^{LLD} = h_a A_p^{CMOD}$.

Then, by expressing the plastic component of the J -integral, J_p , in terms of CMOD as

$$J_p = \frac{\eta_J^{CMOD} A_p^{CMOD}}{b} \quad (3.20)$$

the relationship between η_J^{CMOD} and η_J^{LLD} yields

$$\eta_J^{CMOD} = h_a \eta_J^{LLD} \quad . \quad (3.21)$$

Now, taking the differential of Eq. (3.19) given by $d\Delta_p = h_a dV_p$ and using Eq. (3.13) coupled with Eq. (3.21), J_p can be expressed as

$$J_p = \frac{\eta_J^{CMOD}}{b} \int_0^{V_p} P dV_p - \int_0^a \frac{\gamma_{LLD}}{b} J_p da = \frac{\eta_J^{CMOD} A_p^{CMOD}}{b} - \int_{a_0}^a \frac{\gamma_{LLD}}{b} J_p da \quad (3.22)$$

which provides the crack growth correction for the plastic component of J when using laboratory measurements of P-CMOD data. A noteworthy feature of the previous formulation to evaluate J is that the connection between factor γ entering into Eq. (3.22) and η_J^{LLD} is preserved through Eq. (3.14). In other words, evaluation of based upon CMOD measurements through Eq. (3.22) consists of two terms (which is analogous to evaluation of based upon LLD data as previously developed): the first term represents the plastic contribution to the strain energy in terms of A_p^{CMOD} whereas the second term defines the crack extension correction in terms of LLD measurements.

Considering again the evolution of load, P , with plastic deformation, Δ_p , for a growing crack schematically illustrated in Fig. 3.2(a) and making use of the path independence of J , the k -th plastic term of J_p at crack length $a = a_k$ (corresponding to the k -th unloading point - see Fig. 3.2(b)) can be derived from CMOD records in the form

$$J_p^k = \left[J_p^{k-1} + \frac{\eta_{J,k-1}^{CMOD}}{b_{k-1}} (A_{p,k}^{CMOD} - A_{p,k-1}^{CMOD}) \right] \left[1 - \frac{\gamma_{LLD,k-1}}{b_{k-1}} (a_k - a_{k-1}) \right] \quad (3.23)$$

where $A_{p,k}^{CMOD}$ and $A_{p,k-1}^{CMOD}$ are current plastic areas under the curve P-CMOD at crack length $a = a_k$ and $a = a_{k-1}$. Similarly to previous Eq. (3.18), the variation of plastic area ($A_{p,k}^{CMOD} - A_{p,k-1}^{CMOD}$) in the above expression must be multiplied by $1/B_N$ to maintain agreement with the ASTM E1820 [38] yielding the familiar expression

$$J_p = \frac{\eta_J^{CMOD} A_p^{CMOD}}{b B_N} \quad (3.24)$$

3.2 CTOD Evaluation Procedure

Existing testing standards, including British Standard 7448 [40], ISO 12135 [41] and ISO 15653 [42], adopt a plastic hinge model [2] to provide estimation formulas for CTOD values which derive from laboratory measurements of load-displacement records using three-point bend specimens containing deep, through cracks ($a/W \geq 0.45 \sim 0.5$). The procedure considers that the test specimen rotates about a fixed plastic hinge located on the crack ligament which allows estimation of the CTOD from a simple geometric relationship between the plastic displacement at the crack mouth, V_p , and the plastic component of CTOD, δ_p , in which a constant plastic rotational factor, r_p , defines the relative position of the (apparent)

hinge point on the crack ligament (see details in [2, 43]). While used effectively in conventional testing programs to measure fracture toughness in a wide class of metallic materials, including their weldments, these formulas are most suitable for deeply-cracked bend specimens for which the plastic hinge model with a fixed r_p -value of $0.4 \sim 0.45$ describes reasonably well the global specimen rotation and deformation. Moreover, and perhaps more importantly, this estimation procedure does not address explicitly the effect of stable crack growth on the relationship between remotely applied loading and crack-tip driving forces, here characterized in terms of the CTOD. This section provides the essential features of the estimation procedure for CTOD while, at the same time, setting the necessary framework to construct improved relationships between J and CTOD derived from experimentally measured load-displacement data which are applicable for common fracture specimens with stationary and growing cracks.

3.2.1 CTOD for Stationary Cracks Based on the η -Method

Following the previous energy release rate interpretation of the J -integral and using the connection between J and CTOD (δ) [2, 44, 45], a similar formulation also applies when the CTOD is adopted to characterize fracture resistance. Experimental CTOD-values derived from $P - \text{CMOD}$ records are then evaluated by

$$\delta = \delta_e + \delta_p \quad (3.25)$$

where

$$\delta_e = \frac{K_I^2}{m_y \sigma_f E'} \quad (3.26)$$

and

$$\delta_p = \frac{\eta_{\delta}^{CMOD} A_p^{CMOD}}{b B_N \sigma_f} \quad (3.27)$$

where factor η_{δ}^{CMOD} represents a nondimensional parameter which describes the effect of plastic strain energy on the applied CTOD. In the above expressions, parameter m_y represents a plastic constraint factor which is most often assigned a value of 2 in current standards and σ_f denotes the flow stress defined as $\sigma_f = (\sigma_{ys} + \sigma_{uts})/2$, where σ_{ys} is the yield stress and σ_{uts} is the (ultimate) tensile strength.

3.2.2 J -CTOD Relation for Power Hardening Materials

A widely used procedure to evaluate the CTOD from laboratory measurements of load-displacement records lies on the rigorous equivalence of J and CTOD as elastic-plastic fracture parameters that are equally descriptive of the local conditions at the crack tip. For Mode I crack-tip deformation, the crack-tip opening displacement is accurately predicted by the small-scale yielding solution (associated with the HRR solution [46, 47]) as long as the crack-tip stress and strain fields that develop over microstructurally significant size scales (*i.e.*, the fracture process zone of a few CTODs ahead of a macroscopic crack) can be adequately described by the J -integral [1].

Development of a J -CTOD relation begins by considering an elastic-plastic power hardening model

to describe the true stress ($\bar{\sigma}$) vs true (logarithmic) strain ($\bar{\epsilon}$) behavior in the form [2, 48]

$$\frac{\bar{\epsilon}}{\epsilon_{ys}} = \frac{\bar{\sigma}}{\sigma_{ys}} + \alpha \left(\frac{\bar{\sigma}}{\sigma_{ys}} \right)^n \quad (3.28)$$

where α is a dimensionless constant, n defines the strain hardening exponent, σ_{ys} is the (reference) yield stress, most often assigned the value of the 0.2% proof stress, and $\epsilon_{ys} = \sigma_{ys}/E$ defines the corresponding (reference) yield strain. Often, the hardening exponent is estimated using the expression [?]

$$n = \left(\frac{1 + 1.3495Y_r - 5.3117Y_r^2 + 2.9643Y_r^3}{1.1249 + 11.0097Y_r - 11.7464Y_r^2} \right)^{-1} \quad (3.29)$$

where $Y_r = \sigma_{ys}/\sigma_{uts}$ defines yield stress to tensile strength ratio.

Using now the near-tip singularity displacements described by the HRR solution [1, 46, 47] as

$$u_i = \frac{\alpha\sigma_{ys}}{E} \left(\frac{EJ}{\alpha\sigma_{ys}^2 I_n r} \right)^{n/(n+1)} r^{1/(n+1)} \tilde{u}_i(\theta, n) \quad (3.30)$$

where (r, θ) are polar coordinates centered at the crack tip, I_n represents an integration constant that depends on n and \tilde{u}_i defines a dimensionless function of θ and n , and, further, defining the CTOD in terms of the 90° intercept procedure [2, 45], Shih [45] showed that the J vs CTOD relation is expressible as

$$\delta = d_n \frac{J}{\sigma_{ys}} \quad (3.31)$$

in which the proportionality factor d_n is given by

$$d_n = \left(\frac{\alpha\sigma_{ys}}{E} \right)^{1/n} (\tilde{u}_x + \tilde{u}_y)^{1/n} \left(\frac{2\tilde{u}_y}{I_n} \right) \quad (3.32)$$

where it is understood that \tilde{u}_x and \tilde{u}_y represent dimensionless displacement functions as described in Shih [45] and also Anderson [2]. While the above J vs CTOD relation defined by Eq. (3.31) strictly applies for the CTOD definition in terms of the 90° intercept procedure [2, 45], it is nevertheless a good approximation to other alternative definitions of CTOD, such as the displacement at the original crack tip [2].

Moreover, the previous J vs CTOD relation defined by Eq. (3.31) is essentially applicable for a stationary crack in a power hardening material in which SSY conditions hold true. Indeed, Shih [45] also showed that, apart from the case of very high hardening materials, Eq. (3.31) fails to accurately estimate the CTOD under large scale yielding conditions. A more convenient approach to extend the CTOD evaluation procedure over the full range of elastic-plastic loading follows from direct construction of the J vs CTOD relation based on numerical analyses as addressed later.

3.2.3 J-CTOD Relation Under Large Scale Yielding Based on Fully Plastic Solutions

Under conditions of large-scale yielding, a relationship between J and CTOD continues to hold along a wide range of applied loading but with no apparent analytic solution for the crack-tip displacement fields and, thus, to the CTOD. Indeed, dimensional considerations suggest that the J vs CTOD relation under large-scale yielding has similar form to previous Eq. (3.31) as δ should depend on J/σ_{ys} . Here, we

provide a formal justification for the equivalence between J and CTOD based on simple manipulation of the elastic-plastic crack-tip fields.

Solutions for J and CTOD applicable for fully plastic cracked configurations in which the elastic strains are vanishingly small within an annular region surrounding the crack tip have been given in earlier work by Shih and Hutchinson [49]. Assuming again an elastic-plastic power hardening model to describe the true stress ($\tilde{\sigma}$) vs true (logarithmic) strain ($\tilde{\epsilon}$) behavior in the form of previous Eq. (3.28) and employing the condition that the fully plastic crack-tip stresses, strains and displacements simply scale with the applied load, P , it can be shown that J and CTOD will be proportional to P^{n+1} [2, 49, 34, 50]. Thus, the fully plastic solutions for J and CTOD can be expressed as

$$J = J_e + J_p = \frac{K_I^2}{E'} + \alpha \epsilon_{ys} \sigma_{ys} b h_1 (a/W, \ell, n) \left(\frac{P}{P_0} \right)^{(n+1)} \quad (3.33)$$

$$\delta = \delta_e + \delta_p = \frac{K_I^2}{m_y \sigma_{ys} E'} + \alpha \epsilon_{ys} b h_2 (a/W, \ell, n) \left(\frac{P}{P_0} \right)^{(n+1)} \quad (3.34)$$

in which K_I is the (Mode I) elastic stress intensity factor, m_y is a dimensionless constant (often also termed as a plastic constraint factor) and $E' = E$ or $E' = E/(1-\nu^2)$ whether plane stress or plane strain conditions are assumed with E representing the (longitudinal) elastic modulus and ν is the Poisson's ratio. Here, a defines the crack size, W is specimen (component) width, $b = W - a$ denotes the uncracked ligament, ℓ represents a characteristic length for the cracked component and P_0 defines the (generalized) limit load. In the above fully plastic solutions for J and CTOD, h_1 and h_2 are dimensionless factors dependent upon crack size, component geometry and strain hardening properties. Chiodo and Ruggieri [50] provide further analyses of the fully plastic approach to evaluate J and CTOD in cracked configurations and discuss in detail the validity of the methodology under large scale yielding. In particular, they showed that a strong linear relationship between J and CTOD holds true for circumferentially cracked pipes under bending and large scale yielding conditions.

Upon manipulating Eqs. (3.33) and (3.34) and neglecting the elastic components, J_e and δ_e , the J vs CTOD relation under large scale yielding can be approximated by

$$\delta = \frac{J}{m\sigma_f} = \frac{1}{m\sigma_f} \left[\frac{K_I^2}{E'} + \frac{\eta_J^{CMOD} A_p^{CMOD}}{B_N(W - a_0)} \right] \quad (3.35)$$

in which m represents a proportionality coefficient strongly dependent on the material strain hardening. Here, we note that the material yield stress has been replaced by the flow stress, $\sigma_f = (\sigma_{uts} + \sigma_{ys})/2$ in which σ_{uts} denotes the tensile strength, to incorporate the effects of strain hardening on the J vs CTOD relation. The above expression has also been adopted earlier by Kirk and Dodds [44] and Kirk and Wang [51] to develop improved CTOD estimation formulas for 3P bend fracture specimens. Moreover, it follows from the previous relationship between J and CTOD given by Eq. (3.35) that $m \approx h_1/h_2$ when the fully-plastic solutions described by Eqs. (3.33) and (3.34) are defined in terms of σ_f rather than σ_{ys} .

The J – CTOD relationship defined by the above Eq. (3.35) has also been incorporated into recent revisions of ASTM E1820 [38] and ISO 15653 [42]. The methodology determines the CTOD value from first evaluating the plastic component of J using the plastic work defined by the area under the load vs. CMOD curve and then converting it into the corresponding value of plastic CTOD. The approach has the potential to simplify evaluation of CTOD-values while, at the same time, relying on a rigorous energy release rate definition of J for a cracked body.

3.2.4 Extension to Include Stable Crack Growth

A central result emerging from the previous analyses is that a linear relationship between J and CTOD holds true under large scale yielding conditions as long as the fully plastic solutions described by Eqs. (3.33) and (3.34) are sufficiently descriptive of the crack-tip conditions. Moreover, for restricted conditions of small amounts of stable crack growth accompanied by limited scale plasticity, the J -integral and thus the CTOD still characterize the crack-tip conditions provided the region where large strain effects prevail is small compared to the in-plane dimensions of the cracked body [1, 2]. Under such conditions, Eq. (3.35) should describe relatively well the J vs CTOD relation for a growing crack. However, in typical fracture test specimens, the yielded region extends over a large portion of the crack ligament with increased applied J during crack growth thereby violating the conditions for J -controlled growth.

For a growing crack, the extending crack-tip develops a sharp opening profile at the length-scale characteristic of the CTOD at onset of tearing as shown in Fig. 3.3. After a transitional behavior corresponding to the initiation of stable crack growth, crack extension takes place under a nearly constant crack-tip opening angle (CTOA) which also implies a linear resistance curve for which the tearing modulus is constant. To illustrate this issue, consider the crack configuration depicted in Fig. 3.3 and let $d\delta/da$ be the CTOA where da is the incremental amount of crack extension. By taking the derivative of Eq. (3.35) with respect to a and manipulating the resulting expression yields

$$\frac{dJ}{da} = m\sigma_f \text{CTOA} \quad (3.36)$$

where dJ/da is the slope (tearing modulus) of the resistance curve [52, 33, 32, 34]. When the CTOA is invariant with crack extension, the above expression then defines a linear resistance curve for which the slope dJ/da is constant. Newman et al. [53] provides an extensive review of the CTOA and CTOD parameters as suitable fracture criteria to model stable crack growth and instability during the ductile fracture process. While a number of experimental studies support the assumption of a nearly constant CTOA value (or, equivalently, a constant $d\delta/da$ value) during stable crack growth, the tearing modulus is usually not constant during crack growth in many structural material, including typical pipeline steels.

These previous arguments underline the difficulty (and perhaps some ambiguity) in adopting a proper and meaningful definition for the CTOD in the case of a growing crack. However, since the interest here lies primarily in developing an evaluation procedure for the CTOD to characterize crack growth resistance properties applicable in ECA methodologies, a similar intercept procedure illustrated in Fig. 3.3 can be advantageously adopted in which the intercept between a straight line at 45° from the *original* crack tip and the deformed crack flanks defines the current value of CTOD for an extending crack. This definition makes strong contact with the widely utilized intercept procedure for stationary crack analysis and, at the same time, with current fracture toughness testing protocols to characterize ductile fracture behavior in terms of crack growth resistance curves.

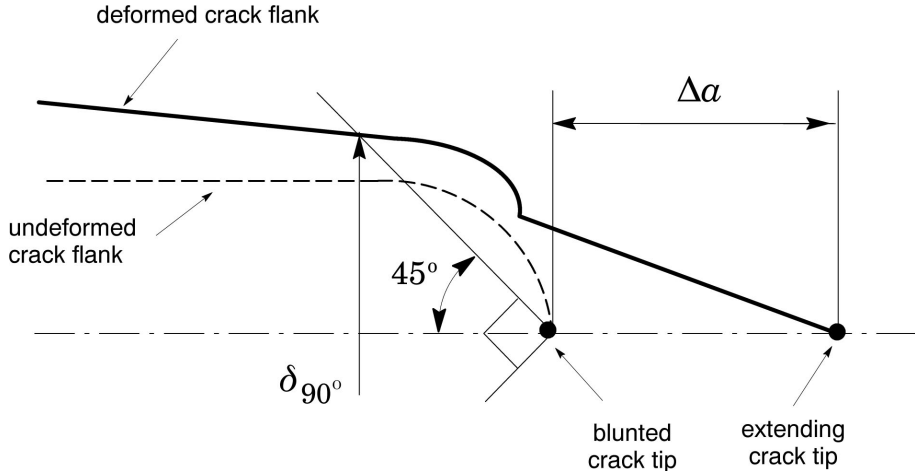


Figure 3.3: Schematic of the intercept procedure to determine the CTOD for a growing crack.

3.3 Geometric Evaluation of CTOD

3.3.1 The Plastic Hinge Model

As mentioned before, current standards to estimate the crack tip opening displacement from measured load-CMOD records for homogeneous fracture specimens, such as BS 7448 [40] and ISO 12135 [41], also adopt separation of the CTOD parameter into its elastic and plastic components as given by the previous Eq. (3.25). Within this methodology, the plastic component of CTOD, defined by δ_p , is derived from considering that the test specimen rotates about a plastic hinge located in the crack ligament as illustrated schematically in Fig. 3.4.

By assuming straight crack flanks and using a similar triangle construction, δ_p is simply related to the plastic displacement at the crack mouth, V_p , through the expression

$$\delta_p = \frac{r_p(W - a)V_p}{r_p(W - a) + a + z} \quad (3.37)$$

where z is the knife edge height ($z = 0$ if the clip gage is attached directly in the specimen - see [40, 41]) and r_p represents the plastic rotational factor which defines the relative position of the (apparent) hinge point on the crack ligament - see Fig. 3.4(b). For deeply cracked, homogeneous SE(B) specimens, r_p takes on the value of 0.4 in BS 7448 [40] and ISO 12135 [41].

3.3.2 The Double Clip-Gage Method

As already noted, the plastic hinge model adopted by current standardized techniques [40, 41] to measure the CTOD for structural steels assumes a constant plastic rotational factor, r_p , to define the relative position of the (apparent) hinge point on the crack ligament [2, 43]. Since application of the methodology to evaluate the CTOD for other crack configurations, such as clamped and pin-loaded SE(T) specimens, requires accurate knowledge of the r_p -value for the analyzed geometry and, further, the assumption that r_p does not change with increased specimen deformation, direct use of the plastic hinge model becomes limited.

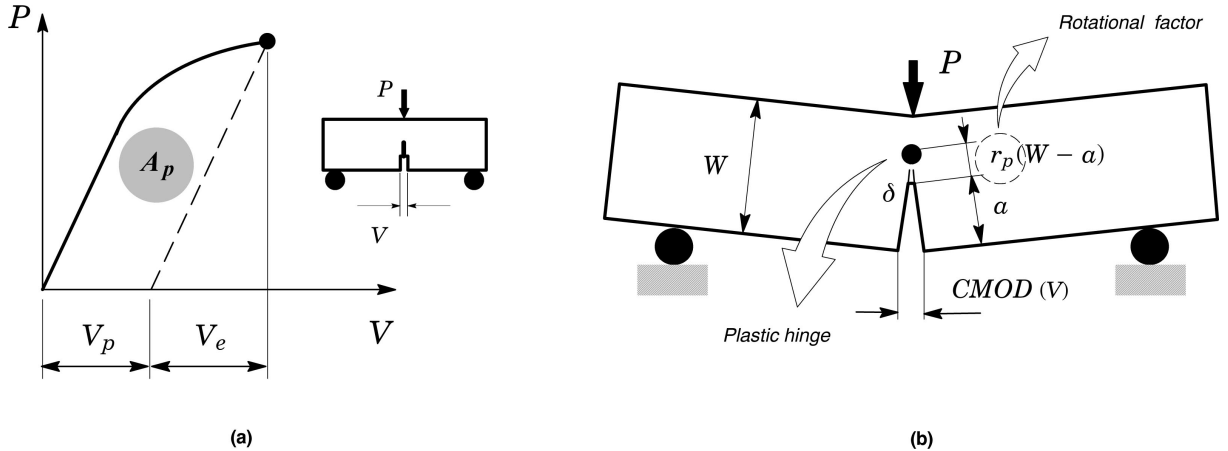


Figure 3.4: (a) Definition of the plastic area under the load-displacement curve. (b) Plastic hinge model employed to estimate CTOD.

To provide a simpler extension of the plastic hinge concept applicable to broader crack configurations, a double clip-gage arrangement can also be used as an alternative method to estimate the CTOD from adequate measurements of crack opening displacements (COD) at two different points. Figure 3.5(a-b) schematically illustrates the procedure. By measuring two COD-values, V_1 and V_2 , at two locations on a straight line passing through the crack flank of the specimen and assuming rigid body rotation, the specimen rotation angle yields

$$\sin \theta = \frac{V_1 - \delta}{2(z_1 + a_0)} = \frac{V_2 - V_1}{2(z_2 - z_1)} \quad (3.38)$$

from which a geometrical relationship between the CTOD (δ) and both measured COD-values is obtained in the form

$$\delta = V_1 - \frac{z_1 + a_0}{z_2 - z_1} (V_2 - V_1) \quad (3.39)$$

where z_1 and z_2 represent the distance of the measuring points for V_1 and V_2 from the specimen surface as depicted in Fig. 3.5(b). Here, we note that the crack size, a_0 , entering into Eq. (3.39) represents the initial crack length not the current crack size measured at the extending tip as indicated in previous Fig. 3.5(b).

Undoubtedly, use of previous Eq. (3.39) associated with the double clip-gage method simplifies the procedure to evaluate the CTOD but at an extra cost of measuring two crack opening displacements. Moreover, since the geometrical relationship between the CTOD (δ) and the measured COD-values is constructed on the basis of the initial crack length, a_0 , we can anticipate that the CTOD-values estimated from using Eq. (3.39) and Eq. (3.35) should compare well. Indeed, observe the similarities between the CTOD determined from the scheme illustrated in Fig. 3.4(b) and the CTOD derived from the procedure shown in Fig. 3.5(b).

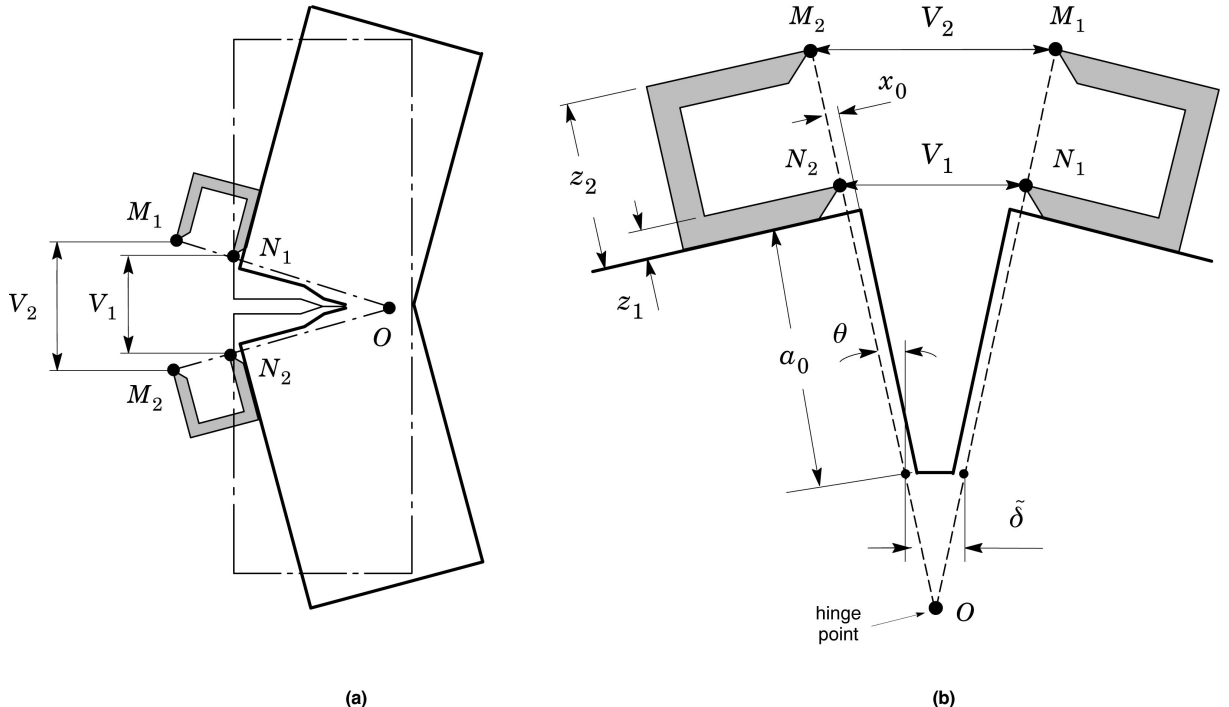


Figure 3.5: *Double clip-gage method to estimate the CTOD using measurements of crack opening displacements (COD) at two different points.*

3.4 Computational Procedures

This section briefly describes the numerical procedures implemented in **FRACTUS2D** to determine the η -factors and CTOD presented previously from finite element solutions of the nodal forces and nodal displacements obtained from numerical models for conventional fracture specimens. These results are generally provided at user-defined load steps, which are associated with the finite element analysis from which **FRACTUS2D** reads the finite element results.

3.4.1 Plastic Area Under the Load-Displacement Curve

The accurate and consistent evaluation of the area under the load-displacement (P – LLD or P – CMOD) curve, with subsequent separation into its elastic, A_e , and plastic, A_p , represents a key step in the numerical computation of the η -factor for the cracked configuration. Figure 3.6(a) illustrates a typical load-displacement curve defined in terms of k load steps, from which a summary of the computational procedures to determine A_p from P – LLD or P – CMOD records follows.

1. First, the linear slope, Φ_e , corresponding to the elastic region of the load-displacement curve is determined. Φ_e can be evaluated by performing an adequate linear regression over j load steps which belong to the linear region of the load-displacement curve. In general, it is simpler and more accurate to determine Φ_e based on the compliance expressions for the specimen configuration under analysis implemented in **FRACTUS2D** as provided in Appendix B.
2. The total area, A_t , at the k -th load step is evaluated by summing the partial areas, A_k , corresponding

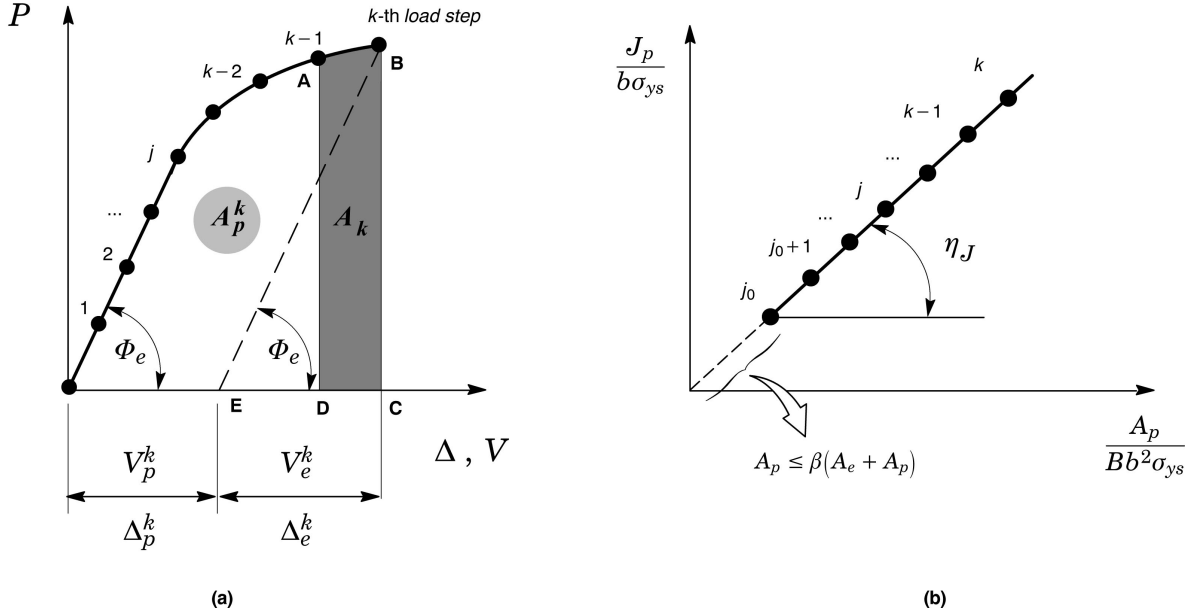


Figure 3.6: (a) Numerical procedure to determine the plastic area, A_p , under the load-displacement curve applicable to either LLD or CMOD data. (b) Numerical scheme based on a standard linear regression performed over discrete points in the load step range defined between j_0 and k to determine the η -factor.

to the interval $[k-1, k]$, as indicated by the area **ABCD** in Fig. 3.6(a) in the form

$$A_t = \sum A_k \quad (3.40)$$

in which A_k is evaluated by Simpson's rule [54] by

$$A_k = \frac{(b-a)}{6} \left[f(a) + 4f\left(\frac{a+b}{2}\right) + f(b) \right] \quad (3.41)$$

where it is readily understood that $[a, b]$ represents the interval defining a given area **ABCD**.

3. Once A_t corresponding to the total area, the plastic area, A_p , is computed by subtracting the elastic area, A_e , defined by the triangle **BEC** as indicated in Fig. 3.6(a), from A_t .

3.4.2 Numerical Evaluation of the Plastic η -Factor

A simple manipulation of previous Eqs. (3.7) and (3.8) or, equivalently, Eq. (3.27) allows evaluation of the corresponding η -factor. Omitting the superscripts LLD and CMOD for clarity and assuming $B_N = B$ for simplicity, J_p and δ_p can be recast as

$$\frac{J_p}{b\sigma_{ys}} = \frac{\eta_J A_p}{Bb^2\sigma_{ys}} \quad (3.42)$$

and

$$\frac{\delta_p}{b} = \frac{\eta_\delta A_p}{Bb^2\sigma_f} \quad (3.43)$$

from which it is understood that η_J and, equivalently, η_δ represent the (linear) slope of the straight line defined by $J_p/(b\sigma_{ys})$ vs. $A_p/(Bb^2\sigma_{ys})$ and δ_p/b vs. $A_p/(Bb^2\sigma_f)$ as illustrated in Fig. 3.6(b).

To evaluate η_J and, equivalently, η_δ , **FRACTUS2D** employs a standard linear regression performed over discrete points in the load step range defined between j_0 and k . The implemented numerical scheme defines the initial load step, j_0 , as the one at which $A_p = \beta(A_e + A_p) = \beta A_t$, where the value of $\beta = 0.1$ is often adopted.

3.4.3 Numerical Evaluation of the CTOD

FRACTUS2D determines the CTOD from direct evaluation of the crack opening at the crack tip using selected nodal displacements defining the deformed crack flank. Currently, **FRACTUS2D** employs two procedures to evaluate the CTOD as follows.

- *90° Intercept Procedure*

The method was originally proposed by Rice [55] and evaluates the CTOD as the intercept of the crack flanks with a 90° vertex originating at the deformed crack tip, as illustrated in Fig. 3.7(a). The procedure is widely employed to determine the CTOD in finite element analysis and its actually the CTOD method most often adopted in numerical analyses addressing computation of near-tip stress-strain fields, η -factors and J -CTOD relationships, among others.

- *Tangent Intersection to the Notch Flanks*

This method is a modification of the 90° intercept procedure to represent more closely the CTOD derived from the plastic hinge model described next. Because the notch flanks tend to remain straight during crack opening, the intersections of the tangent line to the deformed notch flanks and a vertical line originating at the deformed crack tip shown in Fig. 3.7(b) defines the CTOD. To facilitate the numerical computation and, at the same time, increased accuracy, the tangent line to the notch flank is described by a least square fitting to the nodal displacements defining the deformed crack flank.

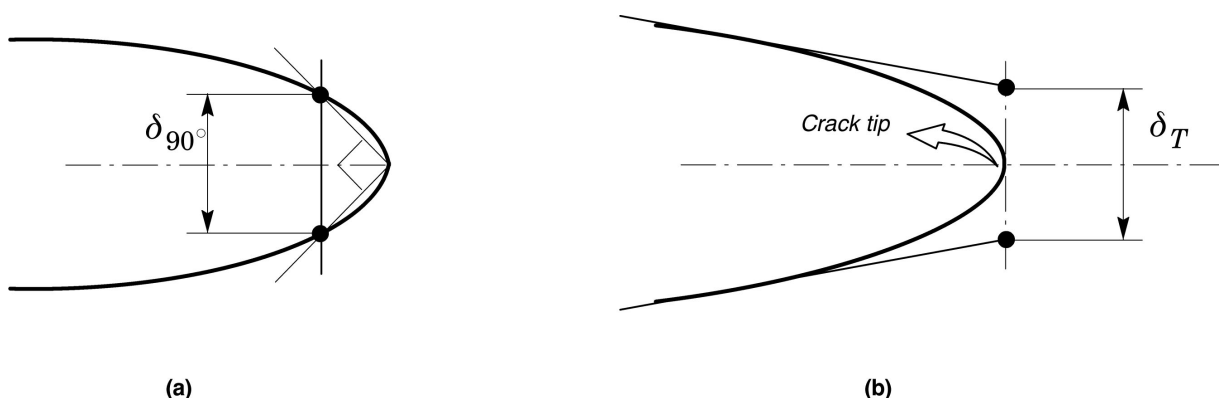


Figure 3.7: (a) 90° intercept method based on the deformed crack tip to define the CTOD, denoted δ_{90° . (b) CTOD defined by the tangent intersection to the deformed notch flanks, denoted δ_T .

3.4.4 Numerical Evaluation of the Plastic Rotational Factor

Numerical evaluation of the plastic rotational factor, r_p , follows directly from solving previous Eq. (3.37) for each load step. First, the total CTOD is computed using the tangent intersection to the deformed notched flanks, δ_T , as outlined above. Next, by separating the CTOD into its elastic, $\delta_{T,e}$, and plastic, $\delta_{T,p}$, components and, further, by evaluation the plastic component of the CMOD, V_p , parameter r_p is simply determined as illustrated in Fig. 3.8. While the rotational factor concept associated with the plastic hinge model was originally developed for deeply-cracked bend specimens under 3P bending, it is also applicable to other fracture specimen configurations, such as shallow crack SE(B) specimens, C(T) geometries and SE(T) configurations.

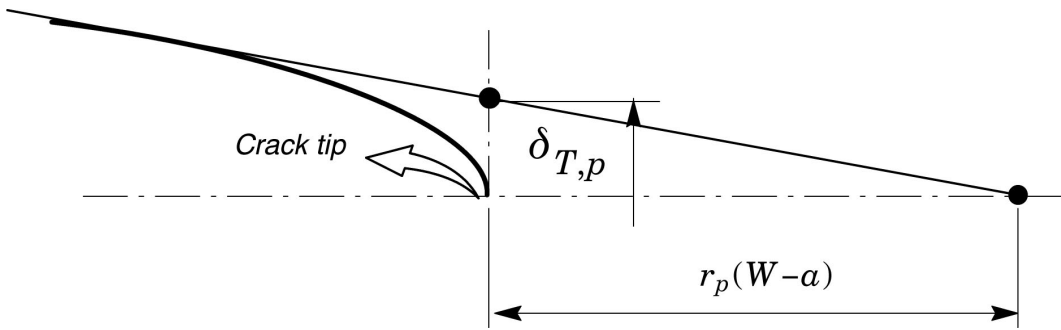


Figure 3.8: General scheme to determine the plastic rotational factor, r_p , at each load step.

4

Experimental Evaluation of Fracture Toughness

This section provides the necessary background for measuring elastic-plastic fracture toughness data, here characterized in terms of the J -integral and CTOD, from laboratory tests of conventional fracture specimens using experimentally measured load-displacement records. To a large extent, the procedure outlined here follows ASTM 1820 [38] standard in the case of conventional C(T) and 3P SE(B) specimens, which are standardized specimen geometries. However, the method is equally applicable to other selected specimen configurations, such as pin-loaded and clamped SE(T) geometries. Moreover, much of the procedures described here follow closely the theoretical framework already described in previous Chapter 3.

4.1 J and CTOD Estimation Procedure Based on the η -Method

Evaluation of the J -integral from laboratory measurements of load-displacement records is most often accomplished by considering the elastic and plastic contributions to the strain energy for a cracked body under Mode I deformation [2] as follows

$$J = J_e + J_p \quad (4.1)$$

where the elastic component, J_e , is given by

$$J_e = \frac{K_I^2}{E'} \quad (4.2)$$

in which $E' = E$ or $E' = E/(1 - \nu^2)$ whether plane stress or plane strain conditions are assumed with E and ν representing the (longitudinal) elastic modulus and Poisson's ratio. Further, K_I is the (Mode I) elastic stress intensity factor which is defined for a conventional fracture specimen as [2, 38, 56]

$$K_I = \left[\frac{P}{(BB_NW)^{1/2}} \right] F(a/W) \quad (4.3)$$

where P is the applied load, B represents the specimen thickness, B_N is the net thickness in side-grooved specimens ($B_N = B$ when side groove are not used), W denotes the specimen width and $F(a/W)$ defines a nondimensional stress intensity factor given by Tada et al. [56], Anderson [2] and ASTM E1820 [38].

The plastic component, J_p , is conveniently evaluated from the plastic area under the load-displacement

curve as

$$J_p = \frac{\eta_J A_p}{B_N(W - a_0)} \quad (4.4)$$

where a_0 is the original crack size (fatigue precrack notch size), A_p represents the plastic area under the load-displacement curve and factor η_J is a nondimensional parameter which describes the effect of plastic strain energy on the applied J . Figure 4.1 illustrates the procedure to determine the plastic area to calculate J from a typical load-CMOD (V) curve. While A_p (and consequently η_J) can be defined in terms of load-load line displacement (LLD or Δ) data, current testing protocols to measure fracture toughness values employing conventional fracture specimens favor the use of load-crack mouth opening displacement (CMOD or V) data; here, this quantity is denoted η_J^{CMOD} . Moreover, the above Eq. (4.4) is essentially applicable to a stationary crack in which factor η_J is assumed to be a function of the cracked configuration and independent of loading [34].

Following the previous energy release rate interpretation of the J -integral and using the connection between J and δ [44, 2, 45], a similar formulation also applies when the CTOD is adopted to characterize the material's fracture resistance. Experimental CTOD-values are then evaluated by

$$\delta = \frac{J}{m\sigma_f} = \frac{1}{m\sigma_f} \left[\frac{K_I^2}{E'} + \frac{\eta_J A_p}{B_N(W - a_0)} \right] \quad (4.5)$$

in which m is a dimensionless constant and σ_f denotes the flow stress defined as $\sigma_f = (\sigma_{ys} + \sigma_{uts})/2$, where σ_{ys} is the yield stress and σ_{uts} is the (ultimate) tensile strength.

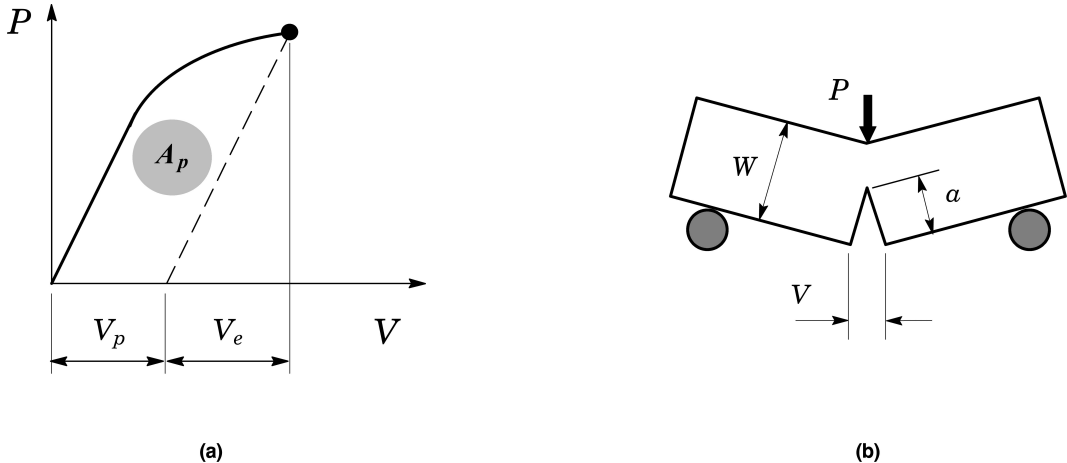


Figure 4.1: *Definition of the plastic area under the load-CMOD curve for a 3-P bend specimen. Similar definition holds true for other crack configurations, includion a C(T) specimen and a clamped SE(T) geometry.*

4.2 Crack Growth Resistance Curves

Conventional testing programs to measure crack growth resistance ($J - \Delta a$) curves in metallic materials routinely employ the unloading compliance (UC) method based on a single specimen test. A key step in the experimental evaluation of the fracture resistance response for these specimens involves the

estimation procedure for the J -integral as a function of applied (remote) loading and crack size. This section provides the essential features of the analytical framework needed to determine J and Δa for common fracture specimens, including the SE(T) and SE(B) configurations, from laboratory measurements of load-displacement records. Attention is directed to an incremental procedure to obtain estimates of J and crack length for an extending crack based on crack mouth opening displacement (CMOD) data.

Similar to the previous section, the procedure to estimate crack growth resistance data also considers the elastic and plastic contributions to the strain energy for a cracked body under Mode I deformation [2, 37] so that J can be conveniently defined in terms of its elastic component, J_e , and plastic component, J_p , as

$$J = J_e + J_p = \frac{K_I^2}{E'} + \frac{\eta A_p}{bB_N} \quad (4.6)$$

where K_I is the elastic stress intensity factor for the cracked configuration, A_p represents the plastic area under the load-displacement curve, B_N is the net specimen thickness at the side groove roots ($B_N = B$ if the specimen has no side grooves where B is the specimen gross thickness), b denotes the uncracked ligament ($b = W - a$ where W is the width of the cracked configuration and a is the crack length). In writing the first term of Eq. (4.6), plane-strain conditions are adopted such that $E' = E/(1 - \nu^2)$ where E and ν are the (longitudinal) elastic modulus and Poisson's ratio, respectively.

Factor η appearing in the second term of Eq. (4.6) represents a nondimensional parameter which relates the plastic contribution to the strain energy for the cracked body with J . Fig. 4.2(a) illustrates the essential features of the estimation procedure for the plastic component J_p . Here, we note that A_p (and consequently, η_J) can be defined in terms of load-load line displacement (LLD or Δ) data or load-crack mouth opening displacement (CMOD or V) data. For definiteness, these quantities are denoted η_{J-LLD} and η_{J-CMOD} .

The previous Eq. (4.6) defines the key quantities driving the evaluation procedure for J as a function of applied (remote) loading and crack size. However, the area under the actual load-displacement curve for a growing crack differs significantly from the corresponding area for a stationary crack (which the deformation definition of J is based on) [2, 39, ?]. Consequently, the measured load-displacement records must be corrected for crack extension to obtain accurate estimates of J -values with increased crack growth (see further details in [39]). A widely used approach (which forms the basis of current standards such as ASTM E1820 [38]) to evaluate J with crack extension follows from an incremental procedure which updates J_e and J_p at each partial unloading point, denoted k , during the measurement of the load vs. displacement curve illustrated in Fig. 4.2(b) as

$$J^k = J_e^k + J_p^k \quad (4.7)$$

where the current elastic term is simply given by

$$J_e^k = \left(\frac{K_I^2}{E'} \right)_k \quad (4.8)$$

For standard SE(B) and C(T) configurations, solutions for K_I can be found in several previously published works, such as Tada et al. [56], whereas Cravero and Ruggieri [57] provide K_I -solutions for clamped SE(T) specimens.

Evaluation of the plastic term, J_p^k , deserves further discussion. Early methods to measure J -resistance curves adopted an incremental equation to estimate J_p based entirely on load-load line displacement (LLD) records [?]. In addition to the η -factor introduced previously, the approach relies on a geometric γ -factor to correct the incremental plastic work for crack growth. Given the conditions of J -controlled crack growth and deformation plasticity are satisfied, the methodology enables approximate (but highly accurate) estimates of J_p for arbitrary (small) increments of crack length and load line displacement. However, when crack growth response is measured using load-crack mouth opening displacement (CMOD) records, direct application of such incremental formulation to evaluate J_p at each partial unloading point does not hold true. Recognizing this limitation, Cravero and Ruggieri [39] and Zhu et al. [58] introduced an incremental formulation to determine J_p which is more applicable to CMOD data in the form

$$J_p^k = \left[J_p^{k-1} + \frac{\eta_{J-CMOD}^{k-1}}{b_{k-1} B_N} (A_p^k - A_p^{k-1}) \right] \left[1 - \frac{\gamma_{LLD}^{k-1}}{b_{k-1}} (a_k - a_{k-1}) \right] \quad (4.9)$$

where factor γ_{LLD} is evaluated from

$$\gamma_{LLD}^{k-1} = \left[-1 + \eta_{J-LLD}^{k-1} - \left(\frac{b_{k-1}}{W \eta_{J-LLD}^{k-1}} \frac{d\eta_{J-LLD}^{k-1}}{d(a/W)} \right) \right] \quad (4.10)$$

The incremental expression for J_p defined by Eq. (4.9) contains two contributions: one is from the plastic work in terms of CMOD and, hence, η_{J-CMOD} and the other is due to crack growth correction in terms of LLD by means of η_{J-LLD} . While the resulting J -estimation procedure based on CMOD may appear a little more complex, evaluation of Eq. (4.9) coupled with Eq. (4.10) is also relatively straightforward provided the two geometric factors, η_{J-CMOD} and η_{J-LLD} , are known.

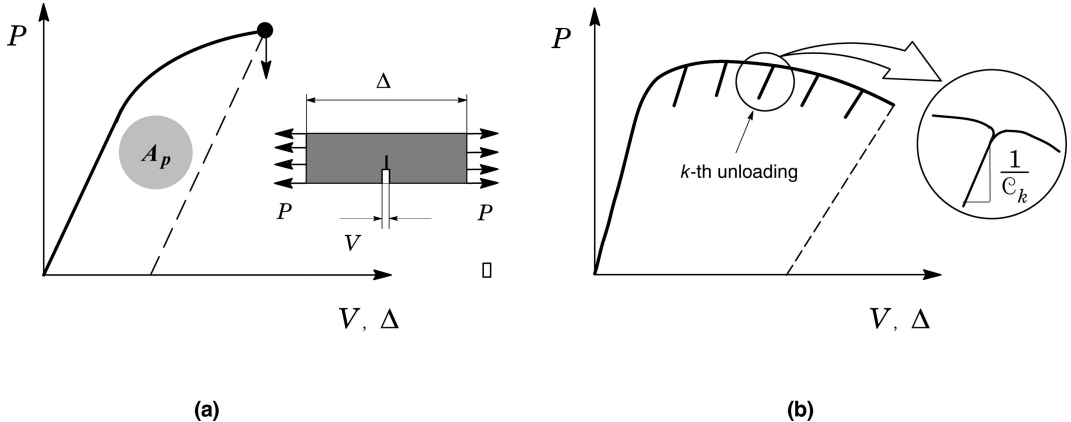


Figure 4.2: (a) Typical representation of the plastic area under the load-displacement curve. (b) Partial unloading during the evolution of load with displacement.

4.3 Evaluation of CTOD Using the Plastic Hinge Model

A widely adopted laboratory procedure to evaluate the CTOD from experimental measurements of load-CMOD records, including BS 7448 [40] and ISO 12135 [41], employs the plastic hinge model. Within this

methodology, the CTOD (δ) is given by

$$\delta = \frac{K_I^2}{m_y \sigma_{ys} E'} + \frac{r_p(W - a_0)V_p}{r_p(W - a_0) + a_0 + z} \quad (4.11)$$

in which the key quantities of interest, represented by parameter K_I and the plastic component of CMOD, V_p , are often defined at the instability point as illustrated in Fig. 4.3. In the above, factor m_y is assigned a value of 2, σ_{ys} represents the 0.2 % proof strength at the temperature of the fracture test and a_0 is average original crack length as defined by a 9-point measurement procedure [38, 40, 41].

The plastic rotational factor, r_p , appearing in previous Eq. (4.11) deserves further discussion. As already discussed, r_p takes on the value of $0.4 \sim 0.45$ in current testing protocols for deeply cracked, 3P SE(B) specimens [40, 41]. However, the plastic rotational factor concept to determine the CTOD from load-CMOD records is also equally applicable to other fracture specimens, including shallow crack SE(B) specimens and SE(T) configurations, provided the plastic hinge model can be shown to describe reasonably well the mechanical and fracture behavior of the specimen. Appendix ?? provides revised plastic rotational factors for standard 3P SE(B) specimens with different a/W -ratios employed by **FRACTUS2D** to determine the CTOD using the previous Eq. (4.11).

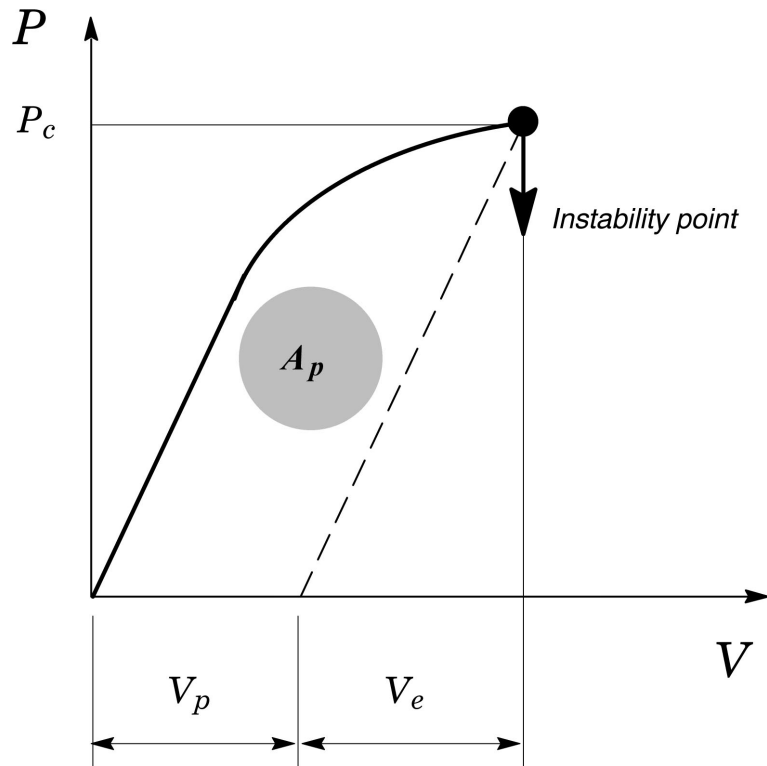


Figure 4.3: *Typical load-CMOD record and definition of the applied load and plastic component of CMOD, V_p , at the instability point.*

4.4 Computational Procedures

This section briefly describes the numerical procedures implemented in **FRACTUS2D** to determine the experimental values of fracture toughness in terms of critical values of J and CTOD at cleavage

instability (J_c , δ_c) and fracture resistance data described by $J - R$ or CTOD – R curves, discussed previously from experimentally measured load-displacement records provided by the MTS system¹, in which displacement is described in terms of CMOD for convenience and operational simplicity. These measured load-displacement records are provided as ASCII text files directly output from the MTS System from which **FRACTUS2D** evaluates the experimental fracture toughness and, in the case of crack growth resistance curves, the amount of ductile tearing.

4.4.1 Cleavage Fracture Toughness

4.4.1.1 Evaluation Procedure of the J -Integral at Cleavage Instability, J_c

Starting from Eq. (4.1), the plastic component, J_p , expressed by Eq. (4.4), is determined from the plastic area under the experimentally measured load-CMOD curve, A_p , as illustrated in Fig. 4.4. To evaluate A_p , **FRACTUS2D** adopts a simple strategy in which the slope of the linear relationship between P and CMOD derives directly from the elastic compliance, C , for the tested specimen geometry as given in Appendix B. Once the elastic area, A_e , defined by the triangle **ABC** in Fig. 4.4 is determined, the plastic area simply derives from $A_p = A_t - A_e$, in which the total area, A_t , is evaluated by Simpson's rule [54] in a similar fashion as expressed by previous Eq. (3.41).

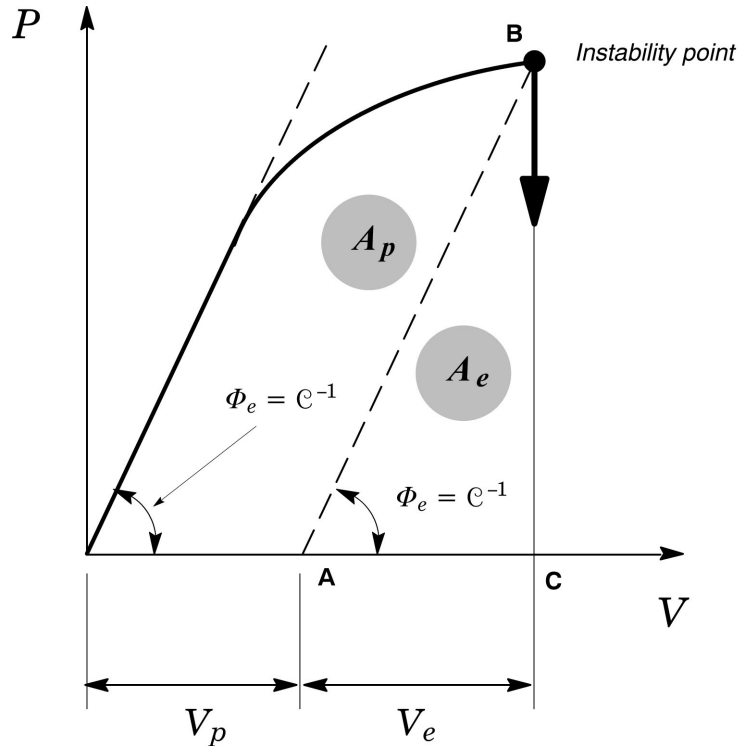


Figure 4.4: Illustrative example of experimentally measured load-CMOD records from which the plastic area, A_p , is extracted to evaluate the critical value of fracture toughness at cleavage instability, J_c .

4.4.1.2 The CTOD at Cleavage Instability, δ_c .

Evaluation of the critical value of CTOD follows directly from Eq. (4.11) in which the plastic component of CMOD, here defined by V_p , is evaluated from elastic compliance, C , for the tested specimen geometry

¹MTS Landmark® Testing Solutions with 250 kN capacity.

as given in Appendix B and illustrated in Fig. 4.4. Once V_e is determined, the quantity V_p entering into Eq. (4.11) simply derives from $V_p = V - V_e$, in which V represents the total CMOD. Moreover, the plastic rotational factors appearing Eq. (4.11) is given in Appendix ?? for standard 3P SE(B) specimens with different a/W -ratios.

4.4.2 Fracture Resistance Curves

4.4.2.1 Evaluation Procedure of the J -Integral During Testing

The procedure to evaluate the J -integral during the testing follows essentially the same strategy already outlined previously in Section 4.4.1.1. Starting from Eq. (4.9), the plastic component, J_p , at each partial unloading point, denoted k , during the measurement of the load vs. displacement curve illustrated in Fig. 4.5 is determined from the plastic area at the k -th unloading step given by $A_{p,k} = A_{t,k} - A_{e,k}$, in which the total area, $A_{t,k}$, is also evaluated by Simpson's rule [54] in a similar fashion as expressed by previous Eq. (3.41).

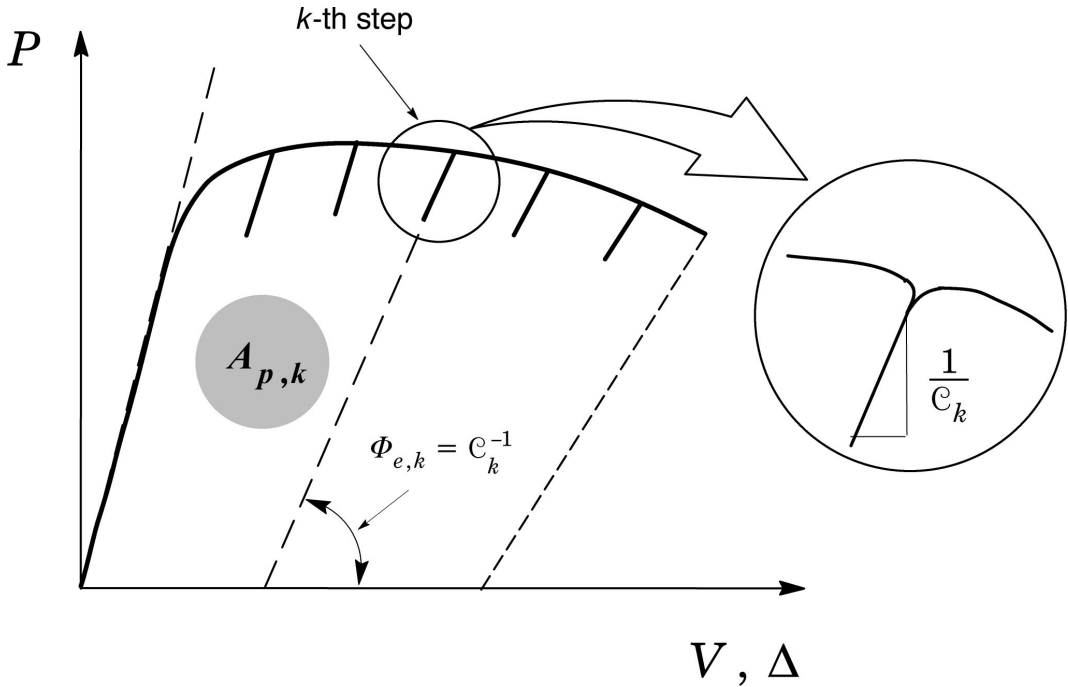


Figure 4.5: *Illustrative example of experimentally measured load-displacement records corresponding to UC testing from which the plastic area at the k -th unloading step, $A_{p,k}$, is extracted to evaluate the current value of the J -integral.*

4.4.2.2 Crack Growth Estimate Based on Unloading Compliance

The procedure to estimate the increased amount of ductile crack growth during the testing relies on the evaluation of the change in specimen compliance at each partial unloading point, denoted k , during the measurement of the load vs. displacement curve. Figure 4.6 shows an enlarged view of the unload-reload sequence and illustrate the procedure to determine the change in specimen compliance by a linear fitting to selected points including both unloading and reloading data. Computation of the (current) specimen compliance is performed in **FRACTUS2D** by using the following procedure. After identifying the unload-reload data, a number of CMOD values pertaining to the bottom and top of the unloading are

excluded from the fitting process - these values correspond to data points within V_{ex} in Fig. 4.6. With the remaining CMOD values, which correspond to data points within V_c , a linear least square fitting is conducted to determine the current specimen compliance, C_k . It is clear from the figure that the total CMOD, V_t , defining the unload-reload sequence region is given by $V_t = V_c + 2V_{ex}$, in which $V_{ex} = \lambda V_t$ and parameter λ defines the fraction of excluded data points within the unload-reload sequence region. In general, $\lambda = 0.1$ which implies that only 80 % of the data points corresponding to V_c are included into the fitting procedure.

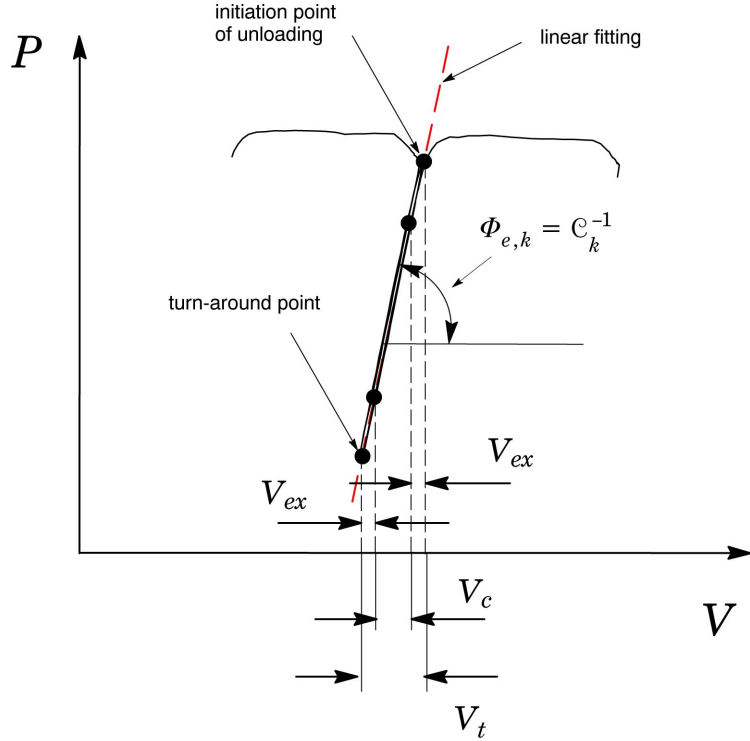


Figure 4.6: *Enlarged view of the unload-reload sequence illustrating the procedure to determine the change in specimen compliance by a linear fitting to selected data points.*

4.4.2.3 Adjustment of Initial Crack Size and Initialization Procedure

An important step in the experimental evaluation of the fracture resistance curve for the tested specimen involves the determination of an improved value for the initial crack size. In general, when the measured average fatigue crack length differs from the crack size initially predicted, the resistance curve often displays a rather anomalous behavior in which either a crack backup phenomenon or an initial offset at the start of the test occur (see discussion in Joyce [37]). Presumably, a better description of the fracture resistance data is obtained by using the following initialization procedure.

First, the data are plotted as crack length, a , versus J to establish a polynomial dependence of crack size (as determined from the uncompliance procedure) with the experimentally measured crack driving force in the form

$$a = a_{0q} + \frac{J}{2\sigma_f} + BJ^2 + CJ^3 \quad (4.12)$$

where a_{0q} is the improved value for the initial crack size and $\sigma_f = (\sigma_{ys} + \sigma_{uts})/2$ represents the flow stress. Then, by using the experimentally measured pairs of (J_k, a_k) data with n records for which $P < P_{max}$,

where P_{max} defines the maximum load attained in the test, and ignoring any spurious apparent *negative* crack growth during the initial part of loading, a least square method [[59]] yields the following system of equations

$$\left\{ \begin{array}{l} \sum a_k - \sum J_k / 2\sigma_f \\ \sum a_k J_k^2 - \sum J_k^3 / 2\sigma_f \\ \sum a_k J_k^3 - \sum J_k^4 / 2\sigma_f \end{array} \right\} = \left[\begin{array}{ccc} n & \sum J_k^2 & \sum J_k^3 \\ \sum J_k^2 & \sum J_k^4 & \sum J_k^5 \\ \sum J_k^3 & \sum J_k^5 & \sum J_k^6 \end{array} \right] \left\{ \begin{array}{l} a_{0q} \\ B \\ C \end{array} \right\} \quad (4.13)$$

Once the above system is solved for a_{0q} , an adjusted set of data can be replotted to produce an improved fracture resistance curve. The above adjustment procedure follows closely ASTM E1820 [38] which also provides further requirements regarding the quality of the fitting procedure which, in turn, may affect the determination of a_{0q} as a valid estimate for the initial crack size. However, as addressed in Section 9.5.4, the current implementation of **FRACTUS2D** does not check for the validity of the estimated a_{0q} nor the quality of the fitting procedure.

5

Syntax of Commands and Input Parameters

5.1 Using *FRACTUS2D*

FRACTUS2D takes input commands in a free-form command language from a file to define the model, material properties, solution parameters and experimental data. Input files may include extensive user comments and thus are generally self-documenting. Input finite element results consist of files stored in Patran binary or ASCII format associated with WARP3D [18] finite element code. Future versions of *FRACTUS2D* will have the capability of handling finite element results from ABAQUS [19] finite element code.

The current version of *FRACTUS2D* executes in foreground mode on DOS environment using the shell command

```
fractus2d < input_file > output_file
```

or

```
fractus2d < input_file
```

where the last command simply displays the results to the standard output device defined by the screen Windows command line (DOS shell).

5.2 Syntax Conventions

The input translators for *FRACTUS2D* provide a problem oriented language (POL) command structure to simplify specification of model and solution parameters. This section describes the conventions and notation employed throughout the manual to explain commands.

Input to *FRACTUS2D* appears as a sequence of English-like commands in the form

```
crack size < 10.2 >
```

where the words **crack** and **size** form a command which is followed by a descriptor (in the above example a real number).

The appearance within a **FRACTUS2D** command of a descriptor of the form

```
< integer >
```

or

```
< real >
```

implies that the user should enter a data within that position in the statement of the class described by the descriptor, such as an *integer* or *real* in the above examples. The command

```
crack size < real >
```

implies that the word *size* is to be followed by a real number, such as 25 or 10.2.

5.2.1 Descriptors

The following are definitions of most of the descriptors used within the language. Those not described below are explained when they first occur in the text.

```
< integer >
```

a series of digits of integer character optionally preceded by a plus or minus sign.

Examples are 121, +300, -410.

```
< real >
```

a series of digits with a decimal point included, or series of digits with a decimal point followed by an exponential indicating a power of 10. Real numbers may be optionally signed. Examples are 1.0, -2.5, 4.3e-01 or 25.

```
< number >
```

is either a

```
< real >
```

 or an

```
< integer >
```

. The input translator performs mode conversion as needed for internal storage.

```
< label >
```

is a series of letters and digits. The sequence must begin with a letter. Input translators also accept the character underbar, _, as a valid letter. Labels may have the form **sebaw5_a515**, for example, to give the appearance of multiple words for readability.

```
< string >
```

is any textual information enclosed in apostrophes ('') or quotes (""). An example is "this is a string".

< list >

is the notation used to indicate a sequence of positive integer values - usually node and element numbers. Lists generally contain two forms of data that may be intermixed with the same list. The first form of data is a series of integers optionally separated by commas. An example is 1, 3, 6, 10, 12. The second common form of a list implies a consecutive sequence of integers and consists of two integers separated by a hyphen. An example is 1-10, which implies all integers in the sequence 1 through 10. An extension of this form implies a constant increment, e.g., 1-10 by 2 implies 1, 3, 5, 7, 9. A third form defined by the key word **all** is sometimes permitted, and implies all physically meaningful integers. The forms of lists are often combined as in ... nodes 1-100 by 3, 200-300, 500-300 by - 3.

5.2.2 Command Structure

In many instances, more than one word is acceptable in a given position within a command. The choices are listed one above the other in the command definition. The command definition

fracture specimen geometry { ct
 3p seb
 clamped set }

indicates that each of the following commands are acceptable

fracture specimen geometry ct

fracture specimen geometry 3p seb

fracture specimen geometry clamped set

Optional words and phrases are enclosed with parentheses, (), like in the command

format (of) fe - results patran type binary

In order to be more descriptive within the command definitions, actual data items (those denoted with < > in the definition) are sometimes described in terms of their physical meaning and followed by the type or class of data item which can be used in the command. For example the command,

structure < name of structure : label >

implies that the data item following the word **structure** is the name of the structure and must be a

descriptor of type < label >. Examples of acceptable commands are

```
structure bend_bar
```

or

```
structure seb
```

while

```
structure 1tseb
```

is not acceptable since the name of the structure is not a label (*labels must begin with a letter*).

5.2.3 Other Syntaxes

The following are definitions of other syntaxes used within the language.

Continuation Lines

A comma (,) placed at the end of a line causes the subsequent data line to be considered a logical continuation of the current line. There is no limit on the number of continuation lines. Continuation can be invoked at any point in any command.

Comment Lines

Comments may be placed in the input following a Fortran style. The letter c or C appearing in physical column 1 of the data line marks it as a comment line. The line is read and (possibly) echoed by the input translator. The content is ignored and the next data line read.

Line Termination

Line termination is accomplished in one of three ways. First, the last column examined by the input translators is column 72. Secondly, after encountering the first data item on a card, the translators count blanks between data items. If 40 successive blanks are found, the remainder of the line is assumed blank. Finally, a \$ or ! indicate an end of line. Spaces following the \$ or ! are ignored by the input translators and are often used for short comments.

5.3 Analysis Type Definition

FRACTUS2D includes several capabilities to support some key applications related to the computation of selected fracture parameters for typical crack configurations. In particular, **FRACTUS2D** provides extensive features to support the evaluation of $J - Q$ trajectories and plastic η -factors for key fracture specimen geometries, including compact tension C(T) and single edge notch bend SE(B) specimens. To drive the correct execution of the code, a specific analysis type must be assigned to **FRACTUS2D** before any other command in the inpput file.

The first command line of the input file defines the analysis type in the form

```
crack analysis type < analysis type : label >
```

The current version of **FRACTUS2D** implements four types of analyses: 1) Computation of $J - Q$ trajectories; 2) Evaluation of the plastic η -factors to determine the elastic-plastic parameters, J and CTOD, including CTOD evaluation based on the plastic hinge model; 3) Evaluation of experimentally measured fracture toughness at cleavage instability, J_c and CTOD, from laboratory testing of common fracture specimens using load-displacement records and 4) Evaluation of experimentally measured crack growth resistance curves, $J - R$ and CTOD – R , from laboratory testing of common fracture specimens using load-displacement records. These analysis types and related parameter definitions will be defined later in subsequent chapters.

5.4 Blocks of Subcommands

Following the definition of the analysis type described above, the input file syntax is composed by blocks of subcommands, which must necessarily be specified (otherwise a syntax error will occur), followed by the keyword **end** as shown in the illustrative examples provided at the end of each Chapter. Scanning of input parameters stops when the keyword **end** is found by the translator. Each block is delimited by the braces { and } as also shown in the illustrative examples provided in next chapters.

6

Evaluation of $J - Q$ Trajectories

6.1 Analysis Type Definition

Evaluation of $J - Q$ trajectories for the cracked configuration under analysis is requested with the command

```
crack analysis type jq - curve
```

The above command line must be the first command interpreted by the input processor. The `crack analysis type` command initiates the input sequence to specify information about the specimen geometry, mesh information and general parameters related to the computation of the Q -parameter with increased J -values.

6.2 Blocks of Subcommands

To perform evaluation of $J - Q$ trajectories for the cracked configuration under analysis, the next blocks of subcommands must be specified following the definition of the analysis type in the order defined below (see illustrative example in Chapter ??):

- ssy model
- finite body
- analysis parameters

6.3 Small Scale Yielding (SSY) Model

This block of commands defines key parameters related to the finite element model for the small scale yielding (SSY) configuration, including crack tip node and crack plane orientation, among others. This SSY model provides the reference solution from which parameter Q is evaluated. The following input sequence of commands are used to define the SSY model.

6.3.1 Input File Directory

To facilitate manipulation of the required input files and to avoid having these files in the current working directory, users should specify the directory where the input files for each crack configuration are located through the command:

```
get files from directory < directory name : label >
```

6.3.2 Nodal Coordinates and Element Incidences

Element incidences (connectivities) and nodal coordinates referenced to the undeformed configuration are required for the computations of the $J - Q$ trajectories. Moreover, the model size (number of nodes and elements) is specified in the input mesh file. In general, it is simpler to edit the original input file used for the finite element analysis in a format compatible with the translator of **FRACTUS2D** as shown next in Fig 6.1. The command syntax is:

```
input mesh (from) file < file name : label >
```

6.3.3 Format for Finite Element Result Files

This command defines the source from which **FRACTUS2D** will obtain the finite element results for the computations of the $J - Q$ trajectories. As currently implemented, only results files in standard Patran ASCII or binary format can be taken as input data. The command syntax is:

```
format (of) fe - results patran type { ascii  
                                         { binary }
```

FRACTUS2D defaults to the naming convention of Patran results files adopted in WARP3D FE code [18]. Patran binary files of nodal displacement results and element stress and strain results are termed according to the release of the FE code WARP3D [18]. For versions 17.x (and earlier), the file name convention is *wndxxxxx*, *websxxxx* and *webxxxx*, respectively, where “xxxx” represents the 5-digit load step number. Similarly, Patran ASCII files of nodal displacement results and element stress and strain results are termed *wndxxxxx*, *websxxxxx* and *wefxxxx*, respectively. For recent, updated versions from V18.x, the file name convention is *wndxxxxxxxx*, *websxxxxxxxx* and *webxxxxxxxx*, respectively, where “xxxxxxxx” represents the 7-digit load step number. Likewise, Patran ASCII files of nodal displacement results and element stress and strain results are termed *wndxxxxxxxx*, *websxxxxxxxx* and *wefxxxxxxxx*, respectively. The default format for finite element result files follows the file name convention for V18.x.

6.3.4 Crack Tip Node

The crack tip node defines the origin of the (stationary) crack tip from which the CMOD, CTOD and the deformed crack flank are determined for the fracture specimen. The command to specify the crack tip node is simply:

```
crack tip node < integer >
```

6.3.5 Crack Plane Orientation

To evaluate the correct displacements and loads, including the CTOD and CMOD, **FRACTUS2D** requires specification of the crack plane orientation as well as the normal to the crack plane. The crack plane angle, φ , is defined by the direction cosines, n_x and n_y , of a two-dimensional vector on the XY -plane defining the crack orientation as illustrated in Fig. 6.5(a). Moreover, the normal to the crack plane shown

in Fig. 6.5(b) is also defined by the corresponding direction cosine. The command to specify the crack plane orientation has the form

$$\text{crack plane angle } \begin{cases} \text{nx} \\ \text{ny} \end{cases} < \text{number} > \begin{cases} \text{nx} \\ \text{ny} \end{cases} < \text{number} > \text{normal} \begin{cases} \text{nx} \\ \text{ny} \end{cases} < \text{number} >$$

6.3.6 Near-Tip Elements

Specification of near-tip elements are required to process the stress distribution ahead of crack tip on the plane $\theta = 0$ - refer to Eq. (2.7) in previous Section 2. While it is not necessary to specify the elements in ascending order (*i.e.*, from the closest element to the crack tip) as **FRACTUS2D** automatically orders them, the user must ensure that the specified list of elements covers the nondimensional radius, λ , during the entire loading history (*i.e.*, up to the maximum J -value used in the construction of the $J - Q$ trajectory). Observe that, while parameter λ remains fixed throughout the analysis, the physical crack-tip distance, r , increases with increased values of applied J as $r = \lambda J/\sigma_0$. The command to specify the near-tip elements is

```
near tip elements < integer list >
```

Alternatively, **FRACTUS2D** allows the automatic generation of the near-tip element list using the command

```
near tip elements automatic maximum radius adaptive
```

in which the subcommand `maximum radius adaptive` defines the crack-tip distance inside which the automatic list of near-tip elements is generated. Here, **FRACTUS2D** determines an adaptive radius, which actually incorporates an additional margin to the maximum radius calculated at the onset of the computations, using an adaptive factor specified later in Section 6.5.3.

6.4 Finite Body

This block of commands defines key parameters related to the finite element model, including crack tip node and crack plane orientation, among others, which are used in the post-processing of nodal displacements, crack tip stresses and associated mesh file information. The following input sequence of commands are used to define the analyzed crack configuration.

6.4.1 Specimen identification

Computation of $J - Q$ trajectories requires the specification of an alphanumeric identifier for the crack configuration or structural component. The syntax for assigning a name to the crack configuration under analysis is as follows:

```
structure < name : label >
```

6.4.2 Input File Directory

To facilitate manipulation of the input files and to avoid having these files in the current working directory, users should specify the directory where the input files for each crack configuration are located through the command:

```
get files from directory < directory name : label >
```

6.4.3 Nodal Coordinates and Element Incidences

Element incidences (connectivities) and nodal coordinates referenced to the undeformed configuration are required for the computations of the $J - Q$ trajectories. Moreover, the model size (number of nodes and elements) is specified in the input mesh file. In general, it is simpler to edit the original input file used for the finite element analysis in a format compatible with the translator of **FRACTUS2D** as shown in Fig 6.1. The command syntax is:

```
input mesh (from) file < file name : label >
```

1260 575 1 - .145000000E+02 .700000000E+02 .250000000E+00 2 - .145000000E+02 .700000000E+02 .000000000E+00 3 -.108750000E+02 .700000000E+02 .250000000E+00 ' ' ' ' ' ' ' ' ' ' ' ' 1257 -.440890379E-01 .829215795E-01 .250000000E+00 1258 -.292893108E-01 .707106888E-01 .250000000E+00 1259 -.292893108E-01 .707106888E-01 .000000000E+00 1260 -.440890379E-01 .829215795E-01 .000000000E+00 1 173 174 146 145 175 176 148 147 2 175 176 148 147 177 178 150 149 3 177 178 150 149 179 180 152 151 ' ' ' ' ' ' ' ' ' ' ' ' 573 929 930 928 927 897 898 896 895 574 963 964 962 961 931 932 930 929 575 931 932 930 929 899 900 898 897	{ Mesh information { Nodal Coordinates { Element Incidences
---	---

Figure 6.1: *Input file for nodal coordinates and element incidences.*

6.4.4 Loading Parameter Results

The computed J -values at the specified load steps (which must be consistent with the finite element results generated by the FE-analysis) are also input through a result file. The command syntax to provide the file name is:

```
input j - values from file < file name : label >
```

in which the format-free input lines are described in Fig 6.2.

Step Number	Loading Parameter
10	0.555
20	1.145
30	2.008
'	'
'	'
'	'

Figure 6.2: *Input file format for loading parameter results in terms of J-values.*

6.4.5 Format for Finite Element Result Files

This command defines the source from which **FRACTUS2D** will obtain the finite element results for the computations of the $J - Q$ trajectories. As currently implemented, only results files in standard Patran ASCII or binary format can be taken as input data. The command syntax is:

```
format (of) fe - results patran type { ascii  
                                         | binary }
```

FRACTUS2D defaults to the naming convention of Patran results files adopted in WARP3D FE code [18]. Patran binary files of nodal displacement results and element stress and strain results are termed according to the release of the FE code WARP3D [18]. For versions 17.x (and earlier), the file name convention is *wndxxxxx*, *websxxxx* and *webxxxx*, respectively, where “xxxxx” represents the 5-digit load step number. Similarly, Patran ASCII files of nodal displacement results and element stress and strain results are termed *wndxxxxx*, *wefsxxxx* and *wefxxxx*, respectively. For recent, updated versions from V18.x, the file name convention is *wndxxxxxxxx*, *websxxxxxxxx* and *webxxxxxxxx*, respectively, where “xxxxxxxx” represents the 7-digit load step number. Likewise, Patran ASCII files of nodal displacement results and element stress and strain results are termed *wndxxxxxxxx*, *wefsxxxxxxxx* and *wefxxxxxxxx*, respectively. The default format for finite element result files follows the file name convention for V18.x.

6.4.6 Crack Tip Node

The crack tip node defines the origin of the (stationary) crack tip from which the CMOD, CTOD and the deformed crack flank are determined for the fracture specimen. The command to specify the crack tip node is simply:

```
crack tip node < integer >
```

FRACTUS2D was originally developed for 2-D analyses and, thus, all displacement quantities, including CMOD, CTOD and nodal displacements describing the deformed crack flanks refer to a specific

plane of the finite element model as defined by the crack tip node. In the half-symmetric, 3-D finite element model for a conventional 3P SE(B) specimen illustrated in Fig. 6.3, the plane $Z = 0$ defines the specimen center plane. Here, if the origin of the 3-D finite element model coincides with the location of the crack tip node (which is the recommended procedure when constructing the finite element model), then the crack tip node has cartesian coordinates $(0, 0, 0)$ and, thus, all displacement quantities will be computed for the XY -plane at $Z = 0$. Consequently, it follows that **FRACTUS2D** can also compute the η -factors and CTOD for any plane along the crack front once an appropriate crack tip node is specified.

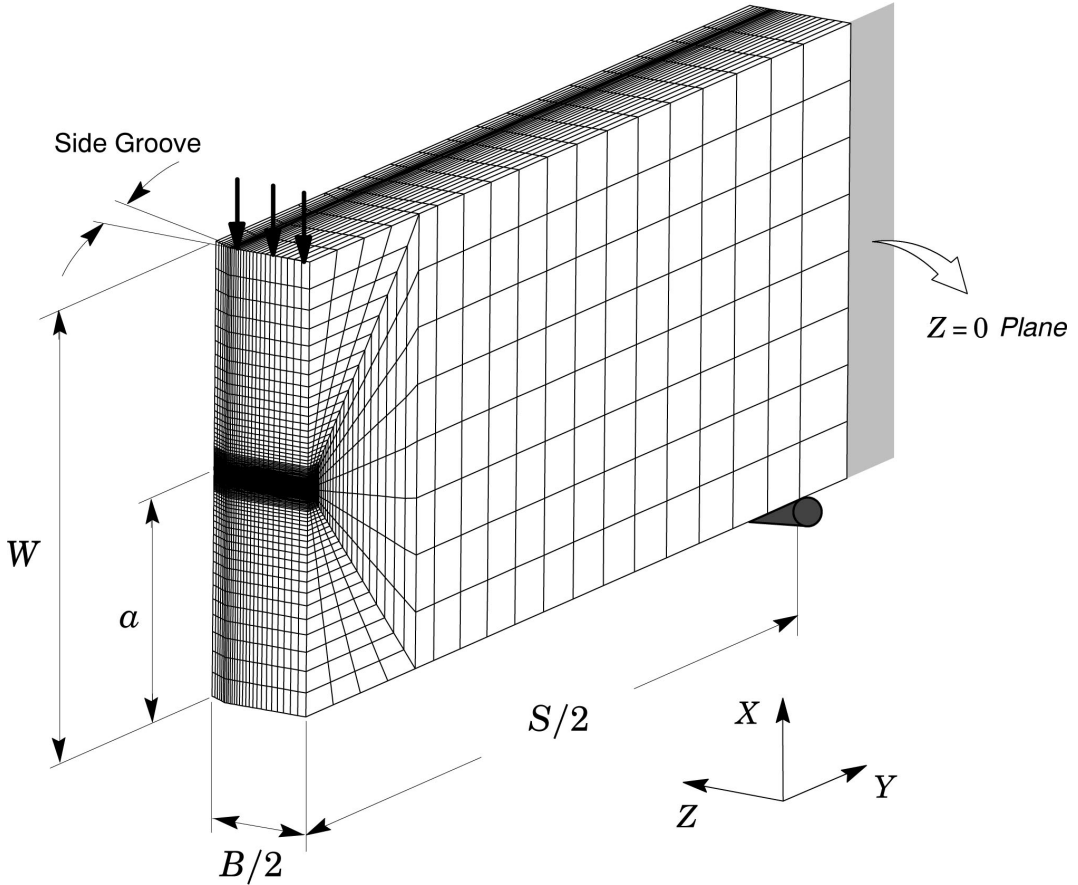


Figure 6.3: *Half-symmetric, 3-D finite element model for a conventional 3P SE(B) specimen in which $Z = 0$ defines the specimen center plane and the location of the crack tip node coinciding with the origin of the numerical model.*

6.4.7 Crack Flank Definition

The numerical procedures to determine the CTOD-values implemented in **FRACTUS2D** require evaluation of the current nodal displacements at each load step for the deformed crack flank - refer to previous Sections 3.4.3 and 3.4.4. This is accomplished by constructing a straight line through selected nodes defining the crack flank based on a conventional least-square method as illustrated in Fig. 6.4. Moreover, because of potentially large distortion occurring at the crack tip region, the nodes at the crack tip blunt region and associated displacements need to be excluded from the fitting process. The procedure thus ensures a very good description of the straight, deformed crack flank which, in turn, provides essentially no adverse impact on the CTOD and r_p computations. The command syntax to define the crack flank is:

```
crack flank node set automatic blunt radius < number > exclusion radius < number >
```

In the above command, the specified blunt radius, ρ_0 , must have the same size as the initial blunt radius used in the finite element model and finite element analysis. The exclusion radius, ρ_e , should be large enough to exclude, at least, all nodes defining the crack tip blunt region and perhaps any other nodes that belong to the highly distorted crack flank in the neighborhood of the crack tip blunt region. Since the numerical strategy to determine the CTOD-values implemented in **FRACTUS2D** relies on a straight line defining the crack flank, it is recommended to use a sufficiently large value for ρ_e . Values of $\rho_e = 100 \sim 200\rho_0$ are often adopted in most analyses.

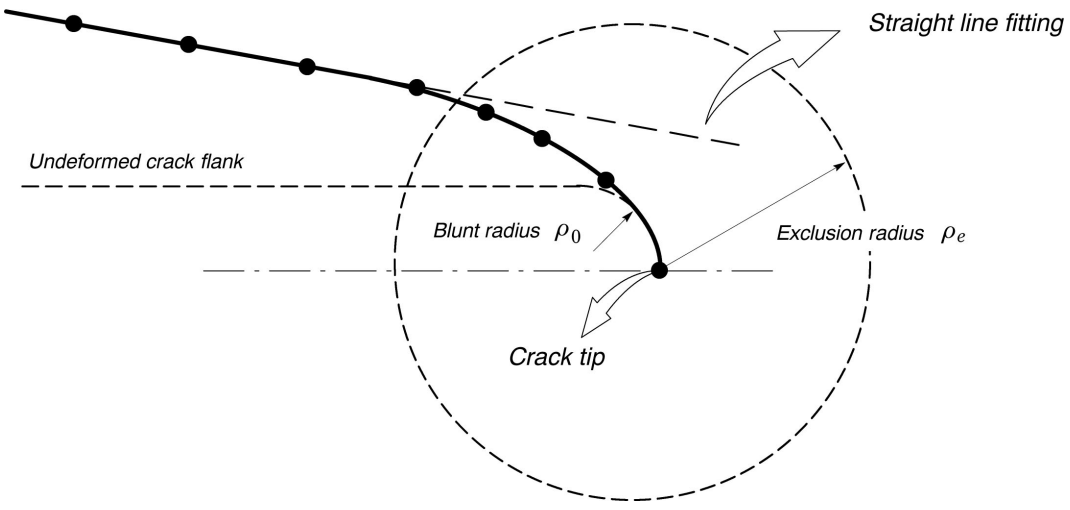
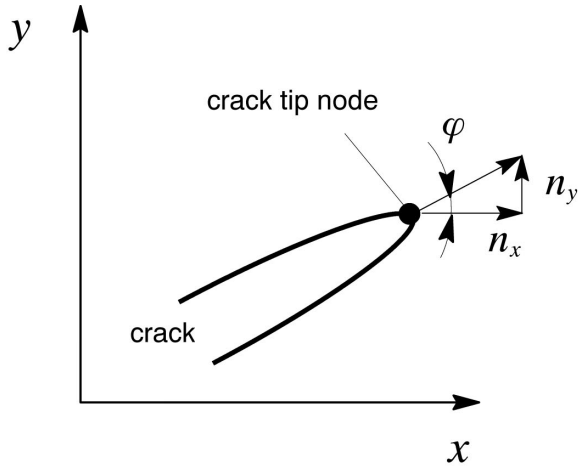


Figure 6.4: Numerical procedure to construct a straight line through selected nodes defining the crack flank based on a conventional least-square method.

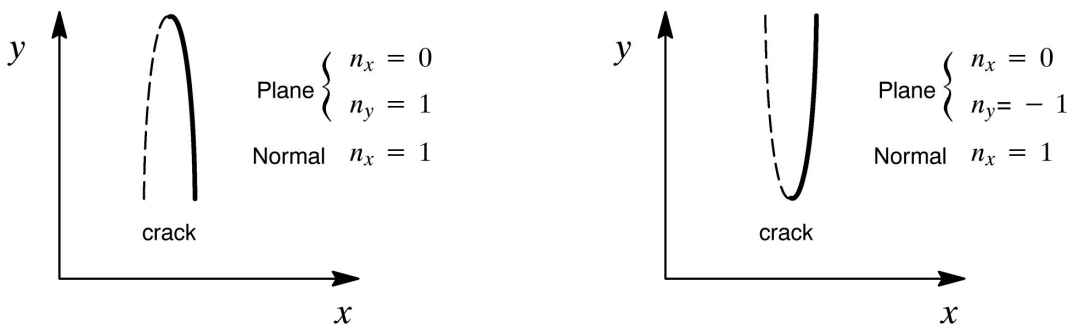
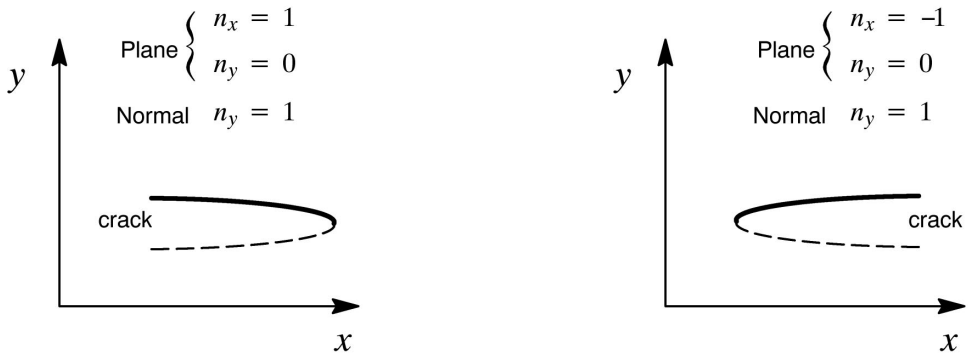
6.4.8 Crack Plane Orientation

To evaluate the correct displacements and loads, including the CTOD and CMOD, **FRACTUS2D** requires specification of the crack plane orientation as well as the normal to the crack plane. The crack plane angle, φ , is defined by the direction cosines, n_x and n_y , of a two-dimensional vector on the XY -plane defining the crack orientation as illustrated in Fig. 6.5(a). Moreover, the normal to the crack plane shown in Fig. 6.5(b) is also defined by the corresponding direction cosine. The command to specify the crack plane orientation has the form

```
crack plane angle {nx      < number > {nx      < number > normal {nx      < number >
ny      < number > } ny      < number > } ny      < number > }
```



(a)



(b)

Figure 6.5: Definition of crack plane orientation and the normal to the crack plane.

6.4.9 Model Symmetry

Many structures and associated finite element models have planes of symmetry with respect to loading and geometry. Symmetry properties, if used for generation of the finite element results, must be taken into account for the correct computation of quantities associated with the η -factors and CTOD. **FRA**C-

TUS2D uses a *scale* or *multiplication factor* to correctly compute the load and displacements as needed based upon the number of symmetry planes in the model. The symmetry factor enters into the evaluation of load and displacements based upon the FE model and specimen geometry. For example, if geometrical and loading conditions permit modeling of only one half of a C(T) specimen, such as the configuration shown in previous Fig. 7.6(b), then the symmetry factor for displacements is 2 and for load is 1. The command is simply

```
symmetry factor displacement < number > load < number >
```

6.5 Analysis Parameters

This block of commands specifies all parameters controlling the analysis to compute the $J-Q$ trajectories. It also allows the user to control key output requests and the load steps over which the near-tip stress and strains are plotted.

6.5.1 WARP3D Release

Recent releases of WARP3D [18] (Release 18.x and later) generate the Patran compatible result files with assigned names that begin with four letters (nodal result files begin with the letters *wn* whereas element result files begin with the letters *we*) followed by the 7 digit load step number. However, older versions of WARP3D (Releases 17.x and 16.x) adopted a 5 digit form to reference the load step number. Since each form of the assigned file name must be manipulated slightly differently by the open file routines in **FRACTUS2D**, the WARP3D release used to generate the finite element results needs to be specified by the command

warp3d release	$\begin{cases} \text{V18} \\ \text{V17} \end{cases}$
----------------	--

where the default option is V18 thereby allowing users to simply omit this command when Release 18.x and later are used.

6.5.2 Nondimensional Radius

Computation of $J-Q$ trajectories requires the specification of the nondimensional radius, λ at which parameter Q is evaluated - refer to Eq. (2.7). The syntax for specifying parameter λ is:

```
nondimensional radius < number >
```

in which the default value is $\lambda = 2$.

6.5.3 Adaptive Factor

To incorporate an additional margin to the maximum radius calculated at the onset of the $J-Q$ computations, an adaptive factor, which actually increases the size of the maximum radius, should be specified as follows:

```
adaptive radius factor < number >
```

where a value of 1.25 implies that the radius ahead of the crack tip from which the near-tip element list is generated is 25 % larger than the maximum radius determined at the onset of the computations.

6.5.4 Reference J -Integral for the SSY Model

Following the operational definition of parameterer Q as expressed by previous Eq. (2.7), a reference opening stress corresponding to the small scale yielding (SSY) solution derived from the MBL model is employed to compute Q at a given nondimensional radius, λ . This reference opening stress for the SSY model is evaluated at a given value of the J -integral corresponding to a given load step specified by the command

```
reference j - int < number > at load step < integer >
```

6.5.5 Material Properties

Computation of parameter Q essentially requires specification of the reference stress, σ_0 , which is generally assumed as the material yield stress, σ_{ys} . *The yield stress specified in **FRACTUS2D** must be the same as the one used in the finite element analysis.* The command to specify the yield stress has the form

```
yield stress < number >
```

6.5.6 Node Search Tolerance

To generate the list of near-tip elements from which the near-tip stress distribution and, consequently, parameter Q are evaluated, **FRACTUS2D** also invokes a node search algorithm based on the nodal coordinates. The search algorithm requires a node search tolerance which is specified by the commad

```
node tolerance < number >
```

where the default value is 0.001 (10^{-3}).

6.5.7 Specification of Load Steps for generation of $J - Q$ Trajectories

The range of load steps over which the computations are performed must be consistent with the results available from the finite element analysis (Patran results files). Users should specify any valid integer between the minimum and the maximum number of load steps available from the finite element analysis. The command syntax is:

```
compute j - q curves {on  
off} steps < lstep list : integer >
```

6.5.8 Output Options

As a further convenience, the user may request creation of a text (ASCII) file of the near-tip stress and strain distribution with increased crack-tip distance. To output these quantities, use the command

```
plot stress strain {on
                   off}      steps < lstep list: integer >
```

where the default option is `off`. The data file created with this command has the name: *fname*_ldisp where *fname* denotes the first 8 characters of the `structure < name >` (see Section 7.3.1).

The above command requires that *both* output stress and strain files derived from WARP3D FE code [18] are available. In the case that only one of them are available or the user wants to output only one of them, then the command syntax is simply

```
plot stress {on
             off}      steps < lstep list: integer >
```

or

```
plot strain {on
              off}      steps < lstep list: integer >
```

6.6 Illustrative Example

The following example illustrates the ***FRACTUS2D*** input file to compute the $J - Q$ trajectories for a standard SE(B) specimen with $a/W = 0.5$ and $n = 10$ material .

```

c
c      FRACTUS Example
c
c      Computation of J-Q curves for Standard SE(B) specimen
c      with a/W = 0.5 and S/W=4
c
c      Elastic-plastic analysis with SGC - n = 10
c
c
c      crack analysis type jq-curves
c
c
c      ssy model {
        get files from directory ssy_small_n10
        input mesh from file ssy_small_coor
        format fe-results patran type ascii
        crack tip node 1
        crack plane angle nx 1 ny 0
        near tip elements automatic maximum radius adaptive }

c
c
c      finite body {
        structure sebaw5_sw4
        get files from directory sebaw5_n10
        input mesh from file sebaw5_sw4_coor
        input j-values from file sebaw5_sw4_jvalues
        format fe-results patran type ascii
        crack tip node 2614
        crack flank node set automatic blunting radius 0.0025 ,
                           exclusion radius 0.5
        crack plane angle nx 1 ny 0
        near tip elements automatic maximum radius adaptive
        symmetry factor displacement 2 load 1 }

c
c
c      analysis parameters {
        warp3d release V18
        nondimensional radius 2.0
        adaptive radius factor 1.25
        yield stress 412
        node tolerance 0.0001
        reference j-int 44.53 at load step 100
        compute j-q curves on steps 10-500 by 10
        plot stress strain on steps 100-1000 by 100 }

c
end

```

Figure 6.6: Illustrative example of **FRACTUS2D** input file to compute the $J - Q$ trajectories for a standard SE(B) specimen with $a/W = 0.5$ and $n = 10$ material.

7

J and CTOD Evaluation Procedures

7.1 Analysis Type Definition

Evaluation of the η -factors to evaluate the elastic-plastic parameters, J and CTOD, including J – CTOD relationships and the plastic rotational factor (which is based on the plastic hinge model) to determine the CTOD, is requested with the command

```
crack analysis type eta-factor
```

The above command line must be the first command interpreted by the input processor. The `crack analysis type` command initiates the input sequence to specify information about the specimen geometry, mesh information and general parameters related to the computation of η -factors and CTOD

7.2 Blocks of Subcommands

To perform evaluation of the η -factors and associated parameters following the definition of the analysis type, the next blocks of subcommands must be specified in the following order (see illustrative example in Chapter ??):

- crack configuration
- mesh based parameters
- analysis parameters

7.3 Crack Configuration

This block of commands defines the fracture specimen geometry used in the numerical analysis and associated mesh file information. The following input sequence of commands are used to define the analyzed specimen geometry.

7.3.1 Specimen identification

The definition of the η -factor analysis begins with specification of an alphanumeric identifier for the fracture specimen or structural component. The syntax for assigning a name to the specimen employed in the analysis is as follows:

```
structure < name : label >
```

7.3.2 Fracture Specimen Geometry

FRACTUS2D currently supports the following fracture specimen geometries: 1) compact tension specimen - C(T); 2) three-point bend specimen - 3P SE(B) ; 3) four-point bend specimen - 4P SE(B); 4) clamped and pin-loaded single notch edge tensile specimens - SE(T). The specimen geometry utilized in the analysis must be specified so that the correct evaluation procedures routines for the η -factors, CTOD and other associated parameters are invoked in **FRACTUS2D**. The specimen geometry is defined with a command having the form

```
fracture specimen (geometry) {  
    3p seb  
    4p seb  
    ct  
    pin_loaded set  
    clamped set}
```

When analyzing a precracked Charpy V-notch (PCVN) specimen under 3P or, eventually, under 4P bending, specify a specimen geometry corresponding to a 3P SE(B) or 4P SE(B) configuration. **FRACTUS2D** will invoke the same routines applicable to an SE(B) specimen in the case of a PCVN configuration.

7.3.3 Specimen Dimensions

Evaluation of the η -factors, CTOD and other associated parameters requires specification of the specimen dimensions, including specimen thickness, specimen width and crack size. The commands to define the specimen dimensions are:

```
specimen thickness < number >
```

```
specimen width < number >
```

```
crack size < number >
```

For SE(B) and SE(T) specimens, the analysis also requires specification of the specimen span for bend geometries and the load point distance (also known as *day-light distance* between grips or pins) for the SE(T) geometries. Each of these dimensions is specified using the commands

```
specimen span < number >
```

```
specimen day light < number >
```

As currently implemented in FRACTUS2D, the specimen inner span for 4-point bend specimens is set to half the specimen span, $D = S/2$ - refer to Appendix A.

7.3.4 Format for Finite Element Result Files

This command defines the source from which **FRACTUS2D** will obtain the finite element results for the computations of the η -factors, CTOD and other associated parameters. As currently implemented, only results files in standard Patran ASCII or binary format can be taken as input data. The command syntax is:

```
format (of) fe - results patran type { ascii  
                                         { binary }
```

FRACTUS2D defaults to the naming convention of Patran results files adopted in WARP3D FE code [18]. Patran binary files of nodal displacement results and element stress and strain results are termed according to the release of the FE code WARP3D [18]. For versions 17.x (and earlier), the file name convention is *wndxxxxx*, *websxxxx* and *webxxxx*, respectively, where “xxxx” represents the 5-digit load step number. Similarly, Patran ASCII files of nodal displacement results and element stress and strain results are termed *wndxxxxx*, *wefsxxxx* and *wefexxxx*, respectively. For recent, updated versions from V18.x, the file name convention is *wndxxxxxxxx*, *websxxxxxxxx* and *webxxxxxxxx*, respectively, where “xxxxxxxx” represents the 7-digit load step number. Likewise, Patran ASCII files of nodal displacement results and element stress and strain results are termed *wndxxxxxxxx*, *wefsxxxxxxxx* and *wefxxxxxxxx*, respectively. The default format for finite element result files follows the file name convention for V18.x.

7.3.5 Input File Directory

To facilitate manipulation of the input files and to avoid having these files in the current working directory, users should specify the directory where the input files for each crack configuration are located through the command:

```
get files from directory < directory name : label >
```

7.3.6 Loading Parameter Results

The computed J -values at the specified load steps (which must be consistent with the finite element results generated by the FE-analysis) are also input through a result file. The command syntax to provide the file name is:

```
input loading parameter from file < file name : label >
```

in which the format-free input lines are described in Fig 7.1.

Step Number	Loading Parameter
10	0.555
20	1.145
30	2.008
.	.
.	.
.	.

Figure 7.1: *Input file format for loading parameter results (J or CTOD).*

7.3.7 Nodal Coordinates and Element Incidences

Element incidences (connectivities) and nodal coordinates referenced to the undeformed configuration are required for the computations of the η -factors, CTOD and other associated parameters. Moreover, the model size (number of nodes and elements) is specified in the input mesh file. In general, it is simpler to edit the original input file used for the finite element analysis in a format compatible with the translator of **FRACTUS2D** as shown in Fig 7.2. The command syntax is:

```
input mesh (from) file < file name : label >
```

1260 575 1 - .145000000E+02 .700000000E+02 .250000000E+00 2 - .145000000E+02 .700000000E+02 .000000000E+00 3 - .108750000E+02 .700000000E+02 .250000000E+00 . . . 1257 -.440890379E-01 .829215795E-01 .250000000E+00 1258 -.292893108E-01 .707106888E-01 .250000000E+00 1259 -.292893108E-01 .707106888E-01 .000000000E+00 1260 -.440890379E-01 .829215795E-01 .000000000E+00 1 173 174 146 145 175 176 148 147 2 175 176 148 147 177 178 150 149 3 177 178 150 149 179 180 152 151 . . . 573 929 930 928 927 897 898 896 895 574 963 964 962 961 931 932 930 929 575 931 932 930 929 899 900 898 897	{ Mesh information { Nodal Coordinates { Element Incidences
--	---

Figure 7.2: *Input file for nodal coordinates and element incidences.*

7.4 Mesh Based Parameters

This block of commands defines key parameters related to the finite element model, including crack tip node and crack plane orientation, among others, which are used in the post-processing of nodal displacements and nodal reactions. The following input sequence of commands are used to define the finite element mesh employed in the analysis.

7.4.1 Crack Tip Node

The crack tip node defines the origin of the (stationary) crack tip from which the CMOD, CTOD and the deformed crack flank are determined for the fracture specimen. The command to specify the crack tip node is simply:

```
crack tip node < integer >
```

FRACTUS2D was originally developed for 2-D analyses and, thus, all displacement quantities, including CMOD, CTOD and nodal displacements describing the deformed crack flanks refer to a specific plane of the finite element model as defined by the crack tip node. In the half-symmetric, 3-D finite element model for a conventional 3P SE(B) specimen illustrated in Fig. 7.3, the plane $Z = 0$ defines the specimen center plane. Here, if the origin of the 3-D finite element model coincides with the location of the crack tip node (which is the recommended procedure when constructing the finite element model), then the crack tip node has cartesian coordinates $(0, 0, 0)$ and, thus, all displacement quantities will be computed for the XY -plane at $Z = 0$. Consequently, it follows that **FRACTUS2D** can also compute the η -factors and CTOD for any plane along the crack front once an appropriate crack tip node is specified.

7.4.2 Crack Flank Definition

The numerical procedures to determine the CTOD-values implemented in **FRACTUS2D** require evaluation of the current nodal displacements at each load step for the deformed crack flank - refer to previous Sections 3.4.3 and 3.4.4. This is accomplished by constructing a straight line through selected nodes defining the crack flank based on a conventional least-square method as illustrated in Fig. 7.4. Moreover, because of potentially large distortion occurring at the crack tip region, the nodes at the crack tip blunt region and associated displacements need to be excluded from the fitting process. The procedure thus ensures a very good description of the straight, deformed crack flank which, in turn, provides essentially no adverse impact on the CTOD and r_p computations. The command syntax to define the crack flank is:

```
crack flank node set automatic blunt radius < number > exclusion radius < number >
```

In the above command, the specified blunt radius, ρ_0 , must have the same size as the initial blunt radius used in the finite element model and finite element analysis. The exclusion radius, ρ_e , should be large enough to exclude, at least, all nodes defining the crack tip blunt region and perhaps any other nodes that belong to the highly distorted crack flank in the neighborhood of the crack tip blunt region. Since the numerical strategy to determine the CTOD-values implemented in **FRACTUS2D** relies on a straight line defining the crack flank, it is recommended to use a sufficiently large value for ρ_e . Values of $\rho_e = 100 \sim 200\rho_0$ are often adopted in most analyses.

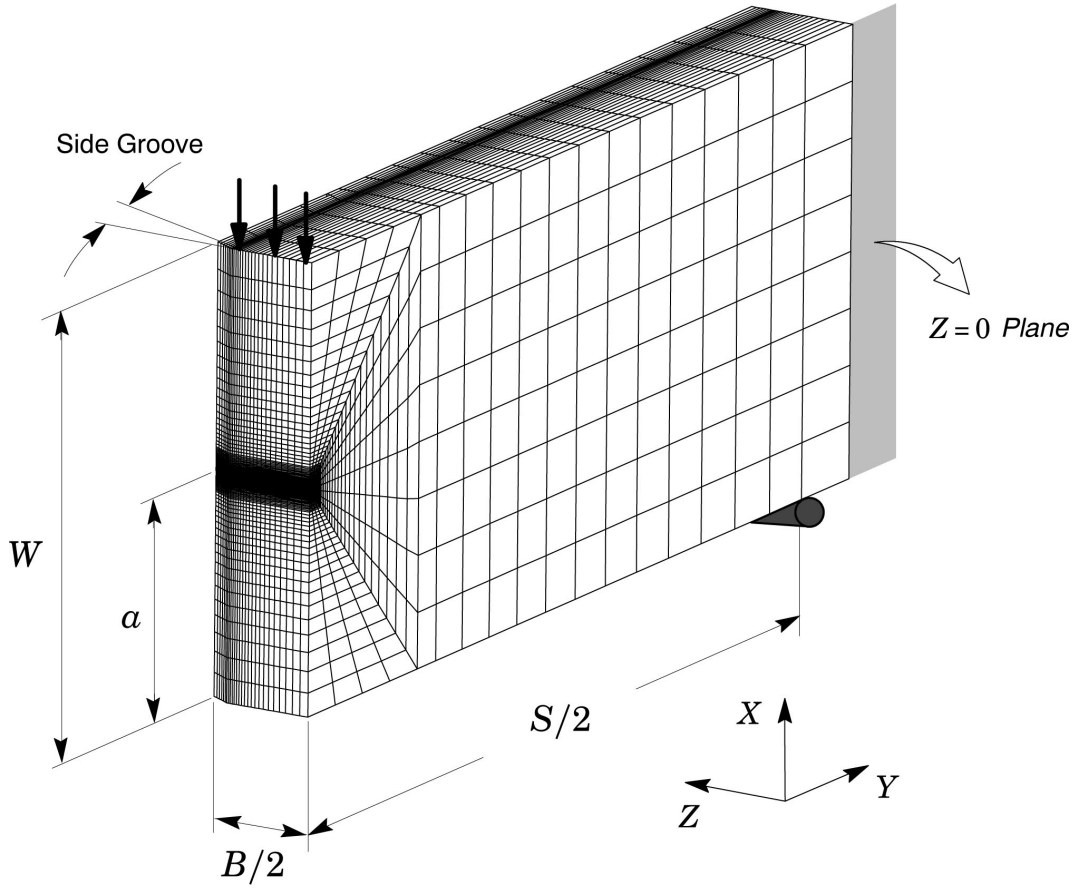


Figure 7.3: Half-symmetric, 3-D finite element model for a conventional 3P SE(B) specimen in which $Z = 0$ defines the specimen center plane and the location of the crack tip node coinciding with the origin of the numerical model.

7.4.3 CMOD and LLD Definition

The η -method to determine J and CTOD is entirely based on the plastic area under the load-displacement curve, in which displacements are characterized by the load line displacement (LLD or Δ) and the crack mouth opening displacement (CMOD). These quantities are extracted from the finite element result files for each specified load step by reading the corresponding displacements at the LLD and CMOD nodes. The commands to specify the LLD and CMOD nodes has the form

```
lld node < integer >
```

```
cmod node < integer >
```

For numerical models of SE(B) specimens, evaluation of the load line displacement also requires specification of a reference node as shown in Fig. 7.5. Here, the load line displacement is taken as the relative displacement in the loading direction of a node on the symmetry plane located $\approx 0.4(W - a)$ from the crack tip in the remaining ligament and of a node located a distance $\approx W/2$ above the support. This

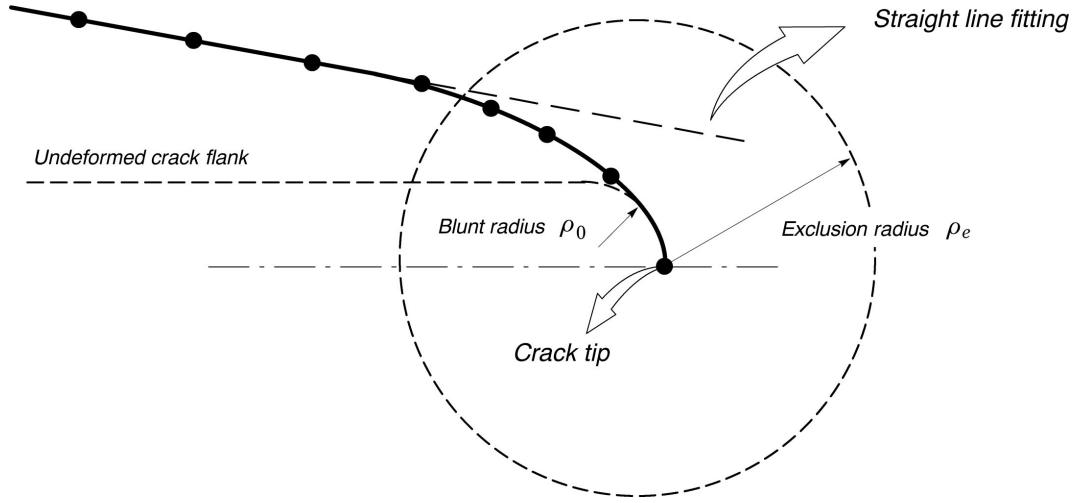


Figure 7.4: *Numerical procedure to construct a straight line through selected nodes defining the crack flank based on a conventional least-square method.*

procedure eliminates the effect of locally high displacements in the vicinity of both the load and support points on the LLD. The command to specify a reference node is

```
lld reference node < integer >
```

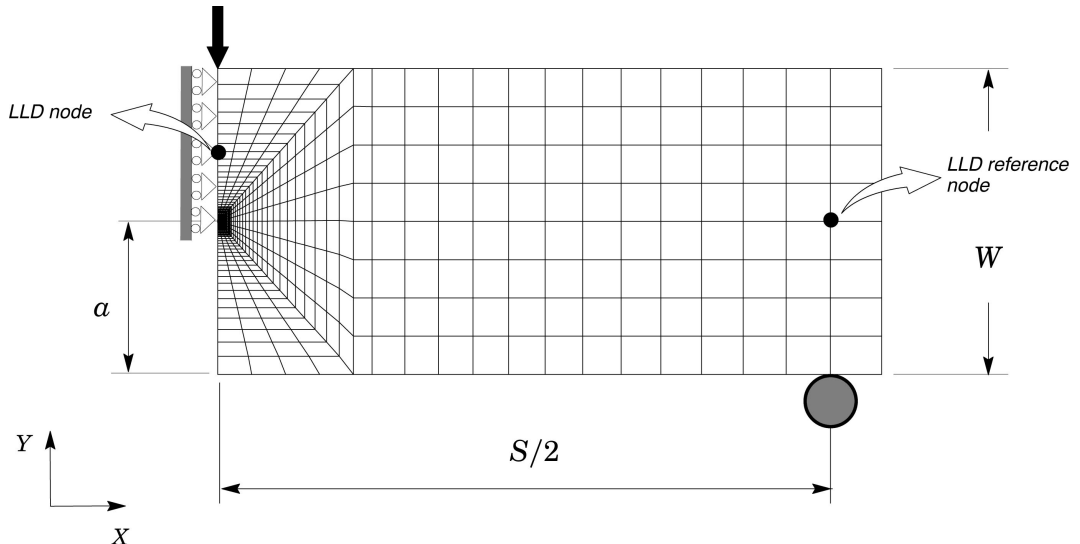


Figure 7.5: *Definition of load line displacement as the relative displacement between the LLD and a reference node.*

7.4.4 Applied Load

Evaluation of the applied load in the FE model is required to determine J and CTOD from the plastic area under the load-displacement curve. Similarly to the above command, this quantity is extracted from the finite element result files for each specified load step by reading the corresponding (internal) reaction forces at appropriate nodes. The command to specify the nodes at which the reaction forces are evaluated

has the form

```
reaction force node set < integer list >
```

where `< integer list >` typically defines the list of reaction nodes or nodes at the crack ligament plane as shown in Fig. 7.6(a). For the FE model of the 3P SE(B) specimen illustrated in this figure, the list of reaction nodes includes all nodes along the Z -direction that belong to the support point - for example, for a one-layer, plane-strain model with thickness, $B = 1$ mm, only the 2 nodes at $Z = 0$ and $Z = 1$ mm are required.

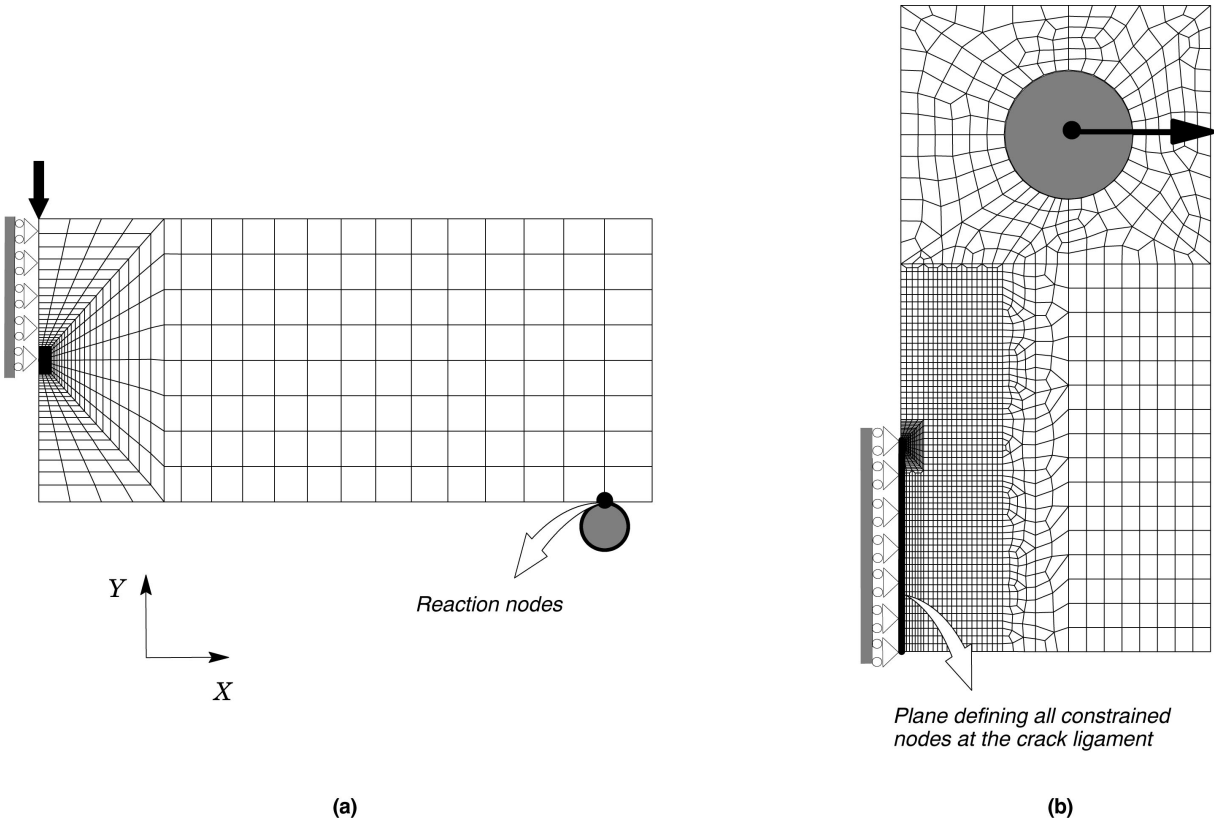


Figure 7.6: *Definition of reaction nodes which are used to determine the applied load.*

For tension-loaded geometries, such as the C(T) specimen shown in Fig. 7.6(b) or an SE(T) configuration, it is simpler to include all nodes that belong to the (constrained) crack ligament as illustrated in the figure. **FRACTUS2D** searches for the nodes of the plane defining the constrained crack ligament and automatically computes the internal reaction forces thereby assigning the resulting value to the applied load. Here, the command syntax is

```
reaction force node set automatic
```

7.4.5 Crack Plane Orientation

To evaluate the correct displacements and loads, including the CTOD and CMOD, **FRACTUS2D** requires specification of the crack plane orientation as well as the normal to the crack plane. The crack

plane angle, φ , is defined by the direction cosines, n_x and n_y , of a two-dimensional vector on the XY -plane defining the crack orientation as illustrated in Fig. 7.7(a). Moreover, the normal to the crack plane shown in Fig. 7.7(b) is also defined by the corresponding direction cosine. The command to specify the crack plane orientation has the form

$$\text{crack plane angle } \begin{cases} \text{nx} \\ \text{ny} \end{cases} < \text{number} > \begin{cases} \text{nx} \\ \text{ny} \end{cases} < \text{number} > \text{normal } \begin{cases} \text{nx} \\ \text{ny} \end{cases} < \text{number} >$$

7.4.6 Model Symmetry

Many structures and associated finite element models have planes of symmetry with respect to loading and geometry. Symmetry properties, if used for generation of the finite element results, must be taken into account for the correct computation of quantities associated with the η -factors and CTOD. **FRACTUS2D** uses a *scale* or *multiplication factor* to correctly compute the load and displacements as needed based upon the number of symmetry planes in the model. The symmetry factor enters into the evaluation of load and displacements based upon the FE model and specimen geometry. For example, if geometrical and loading conditions permit modeling of only one half of a C(T) specimen, such as the configuration shown in previous Fig. 7.6(b), then the symmetry factor for displacements is 2 and for load is 1. The command is simply

```
symmetry factor displacement < number > load < number >
```

7.5 Analysis Parameters

This block of commands specifies all parameters that control the analysis to compute the η -factors, the J – CTOD relationships and the plastic rotational factor to determine the CTOD. It also allows the user to control key output requests and the load steps over which the η -factors and associated quantities are computed.

7.5.1 WARP3D Release

Recent releases of WARP3D [18] (Release 18.x and later) generate the Patran compatible result files with assigned names that begin with four letters (nodal result files begin with the letters *wn* whereas element result files begin with the letters *we*) followed by the 7 digit load step number. However, older versions of WARP3D (Releases 17.x and 16.x) adopted a 5 digit form to reference the load step number. Since each form of the assigned file name must be manipulated slightly differently by the open file routines in **FRACTUS2D**, the WARP3D release used to generate the finite element results needs to be specified by the command

$$\text{warp3d release } \begin{cases} \text{V18} \\ \text{V17} \end{cases}$$

where the default option is V18 thereby allowing users to simply omit this command when Release 18.x and later are used.

7.5.2 Material Properties

A specific set of mechanical properties must be assigned to the analysis to correctly compute the η -factors, CTOD and the $J - \text{CTOD}$ relationships. *This set of mechanical properties must be the same as the one used in the finite element analysis.* The commands to specify the material properties have the form

```
yield stress < number >

tensile strength < number >
```

In particular, specification of the tensile strength is required in all CTOD-related calculations as the flow stress, defined in the present work as $\sigma_f = (\sigma_{ys} + \sigma_{uts})/2$, enters directly into the evaluation of $\eta_\delta^{\text{CMOD}}$ and the dimensionless constant, m - see Previous Eqs. (3.27) and (3.35). Often, an elastic-plastic model incorporating a power hardening law to describe the stress-strain behavior is adopted in the finite element analysis, in which case the tensile strength is not immediately available. For this case, specify the Ramberg-Osgood hardening exponent using the command

```
hardening exponent < number >
```

which prompts **FRACTUS2D** to estimate the tensile strength using Eq. (3.29) appearing in Section 3.2.2. However, when *both* the tensile strength and hardening exponent are specified, **FRACTUS2D** ignores the input of the hardening exponent and proceeds with the analysis by using the user-defined tensile strength value.

7.5.3 Evaluation of the Plastic Area Under Load-Displacement Curve

Evaluation of the plastic area under the load-displacement curve represents a key step in the numerical procedure to determine factors η_J and η_δ . As already outlined in Section 3.4.2, **FRACTUS2D** employs a standard linear regression performed over discrete points in the load step range beginning at a certain value of the plastic area defined by $A_p = \beta(A_e + A_p) = \beta A_t$, where the β -value is specified by the command

```
plastic area ratio < number >
```

where a ratio od $\beta = 0.1$ is most often adopted.

Moreover, the elastic area, A_e , from which the plastic area is calculated by making $A_p = A_t - A_e$, requires evaluation of the linear slope, Φ_e , corresponding to the elastic region of the load-displacement curve. As outlined in Section 3.4.1, Φ_e can be evaluated by performing an adequate linear regression the load steps belonging to the linear region of the load-displacement curve or by simply using the compliance expressions for the specimen configuration under analysis implemented in **FRACTUS2D** (see Appendix B). This is specified by the command

```
use elastic compliance {on {plane stress  
plane strain}  
off number (of) elastic steps < integer >}
```

where the default value is `on` with stress state condition defined by `plane strain`.

In the above command, when specifying the option `off`, the elastic compliance is determined on the basis of a linear regression over a given number of load steps describing the elastic region of the load-displacement curve - see Section 3.4.1. Here, the default number of elastic load steps is 3 and therefore the number of elastic steps can be omitted by the user.

7.5.4 CTOD and Rotational Factor Evaluation Procedure

The CTOD evaluation procedure in **FRACTUS2D** includes two definitions for the crack tip opening displacement (see Section 3.4.3): 1) 90° intercept method and 2) tangent intersection to the deformed notch flank. The input command to specify the CTOD evaluation procedure is thus:

$$\text{ctod model} \begin{cases} \text{ninety degree (vertex)} \\ \text{tangent intersection} \end{cases}$$

After **FRACTUS2D** computes the current CTOD (δ) using one of the above options, the plastic component, δ_p , is evaluated by simply subtracting δ from its elastic component, δ_e . Evaluation of this quantity requires specification of the plastic constraint factor, m_e , appearing in Eqs. (3.26) and (3.34), by using the command:

```
ctod constraint factor < number >
```

in which the default value is 2.0.

FRACTUS2D also supports evaluation of the plastic rotational factor to locate a hinge point in the fracture specimen based on a simple idealization of the specimen rotation as outlined in Section 3.4.4. This option is requested with the command

$$\text{compute rotational factor} \begin{cases} \text{on} \\ \text{off} \end{cases}$$

where the default value is `off`. *Here, it is important to note that the rotational factor evaluation procedure derives from computation of CTOD based on the tangent intersection to the deformed notch flank. Consequently, when this option is invoked with the value `on`, the ctod model will switch to the tangent intersection method.*

7.5.5 Specification of Load Steps

The range of load steps over which the computations are performed must be consistent with the results available from the finite element analysis (Patran results files). Users should specify any valid integer between the minimum and the maximum number of load steps available from the finite element analysis. The command syntax is:

```
compute eta factors (for) steps < lstep list : integer >
```

7.5.6 Node Search Tolerance

When the applied load is evaluated using automatic computation of internal reaction forces at constrained nodes (see Section 7.4.4), a list of specific nodes is created using a node search algorithm based on the nodal coordinates. The search algorithm requires a node search tolerance which is specified by the command

```
node tolerance < number >
```

where the default value is 0.001 (10^{-3}).

7.5.7 Output Options

By default, some key quantities for each specified load step, including CTOD values, plastic area under the load-displacement curve, η -factors based on CMD and LLD, among others, are printed onto the output file. However, the user can invoke the output of more detailed information to trace the entire evolution of the load *vs.* displacement curve, including the applied load, CMOD and LLD for each load step. To explicitly request this level of output, use the command

```
plot load - disp {on off} format {short long}
```

where the format options `short` and `long` prompt **FRACTUS2D** to print a short / long list of the pertinent data. Here, the default option is `on` with format specified as `short`.

Moreover, because the instantaneous and average η -factors display some variation with increased deformation, it may prove more convenient to specify a reference load level, as characterized by the J -integral value, upon which a reference η -factor is evaluated and printed onto the output file. Evaluation of a reference η -factor is invoked with the command

```
print reference eta factor at j - value < number >
```

for which there is no default for the J -integral value at which a reference η -factor is computed.

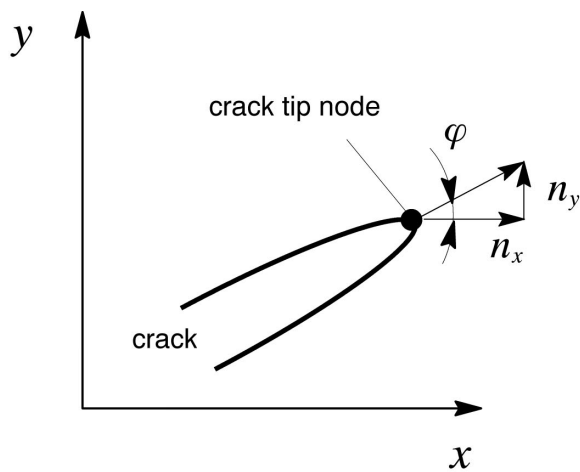
As a further convenience, the user may request creation of a text (ASCII) file of all key quantities for the load *vs* displacement curve. To save the load *vs* displacement data, use the command

```
save load - disp {on off}
```

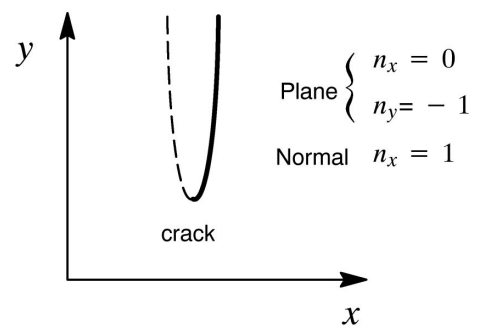
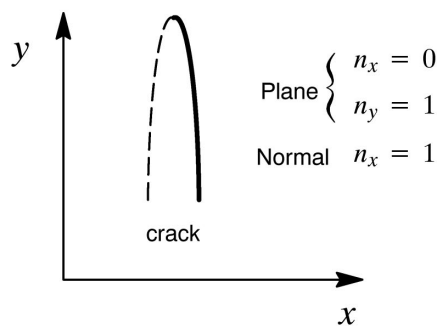
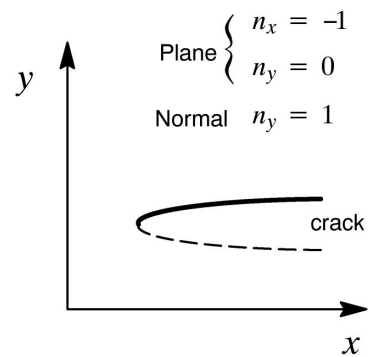
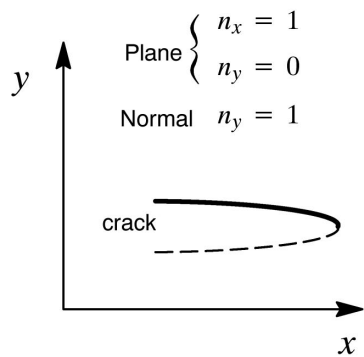
where the default option is `on`. The data file created with this command has the name: *fname_ldisp* where *fname* denotes the first 8 characters of the `structure < name >` (see Section 7.3.1).

7.6 Illustrative Example

The following example illustrates the **FRACTUS2D** input file to compute the η -factors for a standard SE(B) specimen with $a/W = 0.5$ and $n = 10$ material .



(a)



(b)

Figure 7.7: Definition of crack plane orientation and the normal to the crack plane.

```

c
c      Eta-Factor Analysis
c
c      Computation of eta-factor for a Standard SE(B) specimen
c      with a/W = 0.5 and S/W=4
c
c      1-T 2-D Plane-Strain Model
c
c
c      crack analysis type eta-factor
c
c
c      crack configuration {
        structure sebaw5_sw4
        fracture specimen geometry 3p seb ! SE(B) Specimen
        specimen thickness 1.0 ! Espessura do modelo FE
        specimen width 50.8
        specimen span 203.2
        crack size 25.4
        get files from directory sebaw5
        input mesh from file sebaw5_sw4_coor
        input j-values from file sebaw5_sw4_jvalues
        format fe-results patran type ascii    }
c
c      mesh based parameters {
        crack tip node 2614
        crack flank node set automatic blunting radius 0.0025 ,
                           exclusion radius 0.5
        lld node 614
        lld reference node 28
        cmod node 344
        reaction forces node set 19 20
        crack plane angle nx 1 ny 0 normal ny 1
        symmetry factor displacement 2 load 2  }
c
c
c      analysis parameters {
        warp3d release V17
        yield stress 412
        tensile strength 551
        poisson ratio 0.3
        young modulus 206000
        ctod constraint factor 2
        ctod model ninety degree vertex ! 90 degree intercept procedure
        node tolerance 0.0001
        plastic area ratio 0.10
        use elastic compliance on
        plot load-disp on format long
        save load-disp on
        print reference eta factor at j-value 200
        compute eta factors steps 10-500 by 10  }
c
c      end

```

Figure 7.8: Illustrative example of **FRACTUS2D** input file to compute the η -factors for a standard SE(B) specimen with $a/W = 0.5$ and $n = 10$ material.

8

Cleavage Fracture Toughness Testing

8.1 Analysis Type Definition

Evaluation of cleavage fracture toughness based on load *vs.* displacement data provided by the MTS system is requested with the command

```
crack analysis type cleavage fracture testing
```

The above command line must be the first command interpreted by the input processor. The `crack analysis type` command initiates the input sequence to specify information about the specimen geometry, the test data output from the MTS system and general parameters related to the fracture toughness test procedure.

8.2 Blocks of Subcommands

To perform evaluation of fracture toughness following the definition of the analysis type, the next blocks of subcommands must be specified in the following order (see illustrative example in Chapter ??):

- crack configuration
- test data description
- analysis parameters

8.3 Crack Configuration

8.3.1 Specimen Identification

The definition of fracture toughness test begins with specification of an alphanumeric identifier for the fracture specimen. The syntax for assigning a name to the specimen employed in the analysis is as follows:

```
structure < name : label >
```

8.3.2 Fracture Specimen Geometry

FRACTUS2D currently supports the following fracture specimen geometries: 1) compact tension specimen - C(T); 2) three-point bend specimen - 3P SE(B) ; 3) four-point bend specimen - 4P SE(B); 4)

clamped and pin-loaded single notch edge tensile specimens - SE(T). The specimen geometry utilized in the fracture tests must be specified so that the correct evaluation procedures routines for J_c -values (or, equivalently, CTODvalues) are invoked in **FRACTUS2D**. The specimen geometry is defined with a command having the form

fracture specimen (geometry)	{ 3p seb 4p seb ct pin_loaded set clamped set }
------------------------------	--

When analyzing a precracked Charpy V-notch (PCVN) specimen under 3P or, eventually, under 4P bending, specify a specimen geometry corresponding to a 3P SE(B) or 4P SE(B) configuration. **FRACTUS2D** will invoke the same routines applicable to an SE(B) specimen in the case of a PCVN configuration or any other similar bend configuration.

8.3.3 Specimen Dimensions

Evaluation of fracture toughness (cleavage fracture instability or crack growth resistance) requires determination of fracture test parameters, such as the η -factor and the stress intensity factor, K_I , for the analyzed test geometry which, in turn, depend upon the specimen dimensions. The commands to define the specimen dimensions and geometry are:

```
specimen thickness < number >
```

```
specimen width < number >
```

```
initial crack size < number >
```

The initial crack size, a_0 , usually refers to the *post-mortem* measurement of the actual fatigue precrack based on a convenient average technique, such as the 9-point average procedure specified in ASTM E1820 [38]. However, the routines and procedures implemented into **FRACTUS2D** do not distinguish between the actual initial crack size and any other user-specified value, such as the nominal machined notch size. Consequently, the user should specify an appropriate and, possibly, the best value defining the initial crack size, a_0 , for subsequent use in the analysis to determine J or CTOD.

For SE(B) and SE(T) specimens, the evaluation procedure of fracture toughness also requires specification of the specimen span for bend geometries and the load point distance (also known as *day-light distance* between grips or pins) for SE(T) geometries. Each of these dimensions is specified using the commands

```
specimen span < number >
```

```
specimen day light < number >
```

As currently implemented in **FRACTUS2D**, the specimen inner span for 4-point bend specimens is set to half the specimen span, $D = S/2$ - refer to Appendix A.

8.3.4 Specimen Side Groove

Experimental procedures to evaluate fracture toughness most often recommend equipping the specimen with side grooves to maintain high constraint levels over the crack front [60]. Moreover, 3-D finite element analyses by Nevalainen and Dodds [60] have shown that side grooves tend to make the J -integral at the crack tip more uniform across the specimen crack front, thereby mitigating the effects of low J -values near the specimen surfaces. The input command to specify the side-groove depth machined into the test specimen (which thus defines the specimen net thickness) is:

```
side groove depth < number >
```

In the above command, the side-groove depth is defined as the fraction of total thickness reduction. For example, a 20 % side groove (10 % each side) corresponds to a $0.2B$ in total thickness reduction with B denoting the specimen thickness - consequently, the side groove depth is 0.2.

8.4 Test Data Description

8.4.1 Test Data File Name

To facilitate manipulation of the input file and to improve data management and organization, users should specify the directory where the MTS input file for the tested specimens is located through the command:

```
get files from directory < directory name : label >
```

Once the directory is defined, the MTS file name is specified using the following command syntax:

```
input test data from file < file name : label >
```

in which the test data MTS file is a text (ASCII) file containing basically the evolution of applied force (load) with increased displacement (CMOD and LLD) as recorded by the MTS system - see next section.

8.4.2 MTS Data File Structure

The test data file provided by the MTS system is basically a text (ASCII) file in which each line of the test data file contains records of time, applied force (load) and corresponding displacements (CMOD and LLD) as shown in Fig. 8.1. The raw data file generated by the MTS system actually contains several initial lines with key information and test parameters related to the fracture toughness test procedure. The user should edit this raw test data file and produce another text file containing *only* records of time, applied force (load) and displacements as displayed in Fig. 8.1 (observe that the characters **Time**, **Force**, **Displ_1** and **Displ_2** are provided in the input test data file only for clarity). Also observe that the

output test data file provided by the MTS system displays negative values of force and displacement. The internal routines implemented in **FRACTUS2D** correct these negative values to positive ones as needed.

Depending on the MTS setup at the start of the fracture test, the CMOD data can commonly be assigned to either column 3 or column 4 in the test data file. Since the present implementation of **FRACTUS2D** determines J_c -values and CTOD values *only* from experimentally measured load-CMOD records, the user must specify the column of records corresponding to CMOD and load data through the commands:

```
assign cmod to column < integer >
```

```
assign load to column < integer >
```

Moreover, quite often during the fracture toughness test, the load reaches a maximum value from which point it decreases even though the displacements are increasing. Another case of interest related to a drop in applied load is the occurrence of *pop-ins* during the fracture toughness test. Since the primary interest in the fracture test is to evaluate the toughness at fracture instability, it proves convenient and useful to specify at which point on the load-displacement curve the fracture toughness value should be evaluated. This is easily accomplished by using the command

```
number of data points at fracture < integer >
```

8.5 Analysis Parameters

8.5.1 Material Properties

A specific set of mechanical properties must be assigned to the analysis to evaluate the fracture toughness value, including the J -integral and CTOD. *This set of mechanical properties must correspond to the properties of the tested material at the test temperature.* The commands to specify the material properties have the form

```
yield stress < number >
```

```
tensile strength < number >
```

```
young modulus < number >
```

```
poisson ratio < number >
```

In particular, specification of the tensile strength is required in all CTOD-related calculations as the flow stress, defined in the present work as $\sigma_f = (\sigma_{ys} + \sigma_{uts})/2$, enters directly into the $J - \text{CTOD}$ relationship dimensionless constant, m - see previous Eq. (3.35). Moreover, since **FRACTUS2D** sets

the Poisson's ratio to a default value of 0.3, specification of ν may be omitted in the analysis.

Time	Force	Displ_1	Displ_2
17.8164	-1.20014	-0.0315834	0.00681442
35.7568	-2.45393	-0.0564237	-0.00115496
53.7334	-3.70442	-0.0789943	-0.00955269
63.2363	-4.34811	-0.0931241	-0.0142189
71.7051	-4.95481	-0.105351	-0.0179387
89.5576	-6.20527	-0.126361	-0.0264185
107.636	-7.45711	-0.147868	-0.0344248
125.538	-8.70806	-0.171124	-0.0426431
128.728	-8.90167	-0.17574	-0.0442209
143.485	-9.95891	-0.192092	-0.0508186
161.57	-11.2148	-0.216164	-0.0591914
179.459	-12.4655	-0.238943	-0.0673672
193.355	-13.3949	-0.255699	-0.0742215
197.491	-13.7181	-0.261671	-0.0756988
215.457	-14.97	-0.281999	-0.0842514
233.353	-16.2203	-0.303831	-0.0930171
251.328	-17.4711	-0.328963	-0.101762
256.097	-17.7736	-0.334813	-0.104228
.....			
501.99	-34.8842	-0.681373	-0.254385
502.834	-34.9917	-0.684911	-0.254939
520.838	-36.246	-0.717487	-0.271675
532.832	-37.0317	-0.74068	-0.284391
538.933	-37.4983	-0.753797	-0.291096
556.866	-38.7521	-0.796409	-0.313815
557.197	-38.7307	-0.797422	-0.314422
574.919	-40.0029	-0.844067	-0.341222
576.785	-40.0918	-0.850182	-0.344452
592.095	-41.1585	-0.901015	-0.374512
592.929	-41.2547	-0.903246	-0.376107
604.452	-42.0154	-0.948069	-0.404617
610.804	-42.5048	-0.980629	-0.423578
613.829	-42.6694	-0.996969	-0.434641
620.865	-43.1547	-1.04206	-0.464677
626.29	-43.5408	-1.08809	-0.494691
628.814	-43.7549	-1.11457	-0.512709

Figure 8.1: Structure of the MTS data file for fracture toughness testing in which Displ_1 and Displ_2 can define either CMOD or LLD records.

8.5.2 Evaluation of the Elastic and Plastic Area Under the Load-Displacement Curve

Evaluation of the plastic area under the load-displacement curve represents a key step in the evaluation procedure of fracture toughness, specifically in the case of the J -integral, based on the η -methodology. The procedure to evaluate A_p is similar to the method already outlined in Section 3.4.1 in which the plastic area is derived from subtracting the elastic area, A_e , from the total area, A . The elastic area, A_e , is evaluated by first determining the slope of the linear relationship between the experimentally measured values of load and CMOD. This can be accomplished by either determining the linear regression of the

$P - \text{CMOD}$ data in the linear region of the load-displacement curve or by using the elastic compliance function for the tested specimen geometry. To specify this feature, use the command

```
use elastic compliance {on  
off}
```

where the option **off** is the one recommended in most analysis since it captures more closely the actual load-displacement behavior during the fracture test (note that the elastic compliance functions implemented in **FRACTUS2D** derived from plane-strain analysis as described in Appendix B).

When using a linear regression of the $P - \text{CMOD}$ data in the linear region of the load-displacement curve (option **off**) in the above command, the user must also specify the range of $P - \text{CMOD}$ data over which the linear regression is performed. The command to define the linear region of the $P - \text{CMOD}$ records is

```
maximum elastic cmod at < number >
```

where **number** defines a CMOD-value which does not need to match a specific displacement record written in the MTS test data file previously described. Once an adequate CMOD-value is specified by the user, **FRACTUS2D** will simply perform a least square fitting over the user-defined range to determine the linear slope of $P - \text{CMOD}$ data. *To enhance the accuracy in the evaluation of the linear elastic slope of the $P - \text{CMOD}$ curve, it is recommended to use only the few initial $P - \text{CMOD}$ data in the linear region. This can be generally accomplished by specifying a low value for the maximum elastic CMOD. While this CMOD value obviously depends on the material and fracture of the tested specimen, CMOD-values of ≈ 0.1 mm are often adopted.*

8.5.3 Fracture Toughness Evaluation Procedure

The expressions for η -factors implemented in **FRACTUS2D** derive primarily from previous work of Ruggieri and co-workers [43, 61, 62, 63, 64, 65, 66]. These expressions were developed for homogeneous materials and weld centerline notched specimens with a relatively narrow range of mismatch conditions in a plane-strain, 2D framework for conventional C(T) specimens, 3P and 4P bend geometries and SE(T) configurations under clamp and pin-load conditions - see Appendix C for details. In general, these η -factor equations agree well with other previously published solutions, including ASTM E1820 [38] for conventional C(T) and 3P SE(B) specimens. However, it may prove perhaps necessary in some cases to have the J -integral evaluated on the basis of a different set of η -factor expressions, particularly when following ASTM E1820 standards [38]. This feature is invoked with the command

```
fracture toughness procedure {namef  
astm}
```

where the option **namef** is the default procedure and defines the fracture toughness evaluation procedure and associated η -factor expressions developed by Ruggieri and co-workers [61, 62, 63, 64, 65, 66, 43] given in Appendixes C and D. *As currently implemented in **FRACTUS2D**, the option **astm** applies only for conventional C(T) and 3P SE(B) specimens described in ASTM E1820 [38].*

8.5.4 User-Defined η -Factors

As already introduced before, the expressions for η -factors implemented in **FRACTUS2D** were developed primarily for homogeneous materials and weld centerline notched specimens with a relatively narrow range of mismatch conditions in a plane-strain, 2D framework - see Appendixes C and D for details. In general, these η -factor equations provide sufficiently accurate and conservative estimates of fracture toughness. In some practical cases, however, it may prove useful (and perhaps necessary) to incorporate a more adequate and representative η -value into the evaluation procedure of fracture toughness such as, for example, when testing welded fracture specimens with large groove welds or testing dissimilar welds with specific mismatch conditions. In such cases, the user can define a specific value for the η -factor to be used in the evaluation procedure for fracture toughness, more specifically the J -integral as it is based on the plastic area under the load-displacement curve. The command to input the η -factor has the form

```
input eta-factor {on      eta_cmod < number >
                  off}
```

*It is important to note that, since the evaluation procedure for cleavage fracture toughness implemented in **FRACTUS2D** is entirely based on CMOD data, only η -factors based on CMOD, here denoted as η_J^{CMOD} , should be specified as input. Moreover, the specification of a proper η_J^{CMOD} requires its careful evaluation as **FRACTUS2D** does not check its validity or consistency.*

8.5.5 Test Data Units

The MTS system requires an initial test setup to perform the fracture toughness experiment on the test specimen. Most often, the recorded load and displacement are set in metric units, with load set in kN and displacements in mm. However, in some occasions, a different test setup is used, in which case different units may have been assigned to the load-displacement records. To specify the correct units utilized in the test setup, use the command

```
test data units load {kN
                      N}
```

As currently implemented in **FRACTUS2D**, only the load unit needs to be specified (kN or N) as the CMOD (and LLD) records provided by the MTS system are always expressen in mm. Since the default load unit manipulated by **FRACTUS2D** is kN, this command can be ommited by the user when this unit was used in the test setup.

8.6 Illustrative Example

The following example illustrates the **FRACTUS2D** input file to evaluate the J_c -value from experimentally measured records of load and CMOD for a standard SE(B) specimen with $a/W = 0.5$ made of an A572 steel at -20°C .

```

c
c      Fracture Toughness Test
c
c      Evaluation of Fracture Toughness Parameters J
c      Based on eta-factors Using Experimentally
c      Measured Load vs. CMOD records
c
c      ASTM A572 Steel @ T=-20C
c
c      1-T SE(B) Specimen with a/W=0.5 S/W=4 3P
c
c
c      crack analysis type fracture toughness test
c
c
c      crack configuration {
        structure sebaw5_cp23
        fracture specimen geometry 3p seb
        specimen thickness 25.4
        specimen width 50.8
        specimen span 203.2
        initial crack size 25.4 }
c
c      test data description {
        get files from directory sebaw5_CP23
        input test data from file CP23_load_cmod
        assign cmod to column 4
        assign load to column 2
        number of data points at fracture 52}
c
c
c      analysis parameters {
        use elastic compliance off
        maximum elastic cmod at 0.1 ! elastic cmod of 0.1 mm
        yield stress 379 ! yield stress @ -20C
        tensile stress 644 ! tensile strength @ -20C
        poisson ratio 0.3
        young modulus 204392 }
c
c      end

```

Figure 8.2: Illustrative example of **FRACTUS2D** input file to evaluate the J_c -value from experimentally measured records of load and CMOD for a standard SE(B) specimen with $a/W = 0.5$ made of an A572 steel at -20°C .

9

Fracture Resistance Testing

9.1 Analysis Type Definition

Evaluation of cleavage fracture toughness based on load *vs.* displacement data provided by the MTS system is requested with the command

```
crack analysis type fracture resistance testing
```

The above command line must be the first command interpreted by the input processor. The `crack analysis type` command initiates the input sequence to specify information about the specimen geometry, the test data output from the MTS system and general parameters related to the fracture toughness test procedure.

9.2 Blocks of Subcommands

To perform evaluation of fracture toughness following the definition of the analysis type, the next blocks of subcommands must be specified in the following order (see illustrative example in Chapter ??):

- crack configuration
- test data description
- analysis parameters

9.3 Crack Configuration

9.3.1 Specimen Identification

The definition of fracture toughness test begins with specification of an alphanumeric identifier for the fracture specimen. The syntax for assigning a name to the specimen employed in the analysis is as follows:

```
structure < name : label >
```

9.3.2 Fracture Specimen Geometry

FRACTUS2D currently supports the following fracture specimen geometries: 1) compact tension specimen - C(T); 2) three-point bend specimen - 3P SE(B) ; 3) four-point bend specimen - 4P SE(B); 4)

clamped and pin-loaded single notch edge tensile specimens - SE(T). The specimen geometry utilized in the fracture tests must be specified so that the correct evaluation procedures routines for J_c -values (or, equivalently, CTODvalues) are invoked in **FRACTUS2D**. The specimen geometry is defined with a command having the form

fracture specimen (geometry)	{ 3p seb 4p seb ct pin_loaded set clamped set }
------------------------------	--

When analyzing a precracked Charpy V-notch (PCVN) specimen under 3P or, eventually, under 4P bending, specify a specimen geometry corresponding to a 3P SE(B) or 4P SE(B) configuration. **FRACTUS2D** will invoke the same routines applicable to an SE(B) specimen in the case of a PCVN configuration or any other similar bend configuration.

9.3.3 Specimen Dimensions

Evaluation of fracture toughness (cleavage fracture instability or crack growth resistance) requires determination of fracture test parameters, such as the η -factor and the stress intensity factor, K_I , for the analyzed test geometry which, in turn, depend upon the specimen dimensions. The commands to define the specimen dimensions and geometry are:

```
specimen thickness < number >
```

```
specimen width < number >
```

```
initial crack size < number >
```

The initial crack size, a_0 , usually refers to the *post-mortem* measurement of the actual fatigue precrack based on a convenient average technique, such as the 9-point average procedure specified in ASTM E1820 [38]. However, the routines and procedures implemented into **FRACTUS2D** do not distinguish between the actual initial crack size and any other user-specified value, such as the nominal machined notch size. Consequently, the user should specify an appropriate and, possibly, the best value defining the initial crack size, a_0 , for subsequent use in the analysis to determine J or CTOD.

For SE(B) and SE(T) specimens, the evaluation procedure of fracture toughness also requires specification of the specimen span for bend geometries and the load point distance (also known as *day-light distance* between grips or pins) for SE(T) geometries. Each of these dimensions is specified using the commands

```
specimen span < number >
```

```
specimen day light < number >
```

As currently implemented in **FRACTUS2D**, the specimen inner span for 4-point bend specimens is set to half the specimen span, $D = S/2$ - refer to Appendix A.

9.3.4 Specimen Side Groove

Experimental procedures to evaluate fracture toughness most often recommend equipping the specimen with side grooves to maintain high constraint levels over the crack front [60]. Moreover, 3-D finite element analyses by Nevalainen and Dodds [60] have shown that side grooves tend to make the J -integral at the crack tip more uniform across the specimen crack front, thereby mitigating the effects of low J -values near the specimen surfaces. The input command to specify the side-groove depth machined into the test specimen (which thus defines the specimen net thickness) is:

```
side groove depth < number >
```

In the above command, the side-groove depth is defined as the fraction of total thickness reduction. For example, a 20 % side groove (10 % each side) corresponds to a $0.2B$ in total thickness reduction with B denoting the specimen thickness - consequently, the side groove depth is 0.2.

9.4 Test Data Description

9.4.1 Test Data File Name

To facilitate manipulation of the input file and to improve data management and organization, users should specify the directory where the MTS input file for the tested specimens is located through the command:

```
get files from directory < directory name : label >
```

Once the directory is defined, the MTS file name is specified using the following command syntax:

```
input test data from file < file name : label >
```

in which the test data MTS file is a text (ASCII) file containing basically the evolution of applied force (load) with increased displacement (CMOD and LLD) as recorded by the MTS system - see next section.

9.4.2 MTS Data File Structure

The test data file provided by the MTS system is basically a text (ASCII) file in which each line of the test data file contains records of step number, step segment¹, time, applied force (load) and corresponding displacements (CMOD and LLD) as shown in Fig. 9.1. The raw data file generated by the MTS system actually contains several initial lines with key information and test parameters related to the fracture toughness test procedure. The user should edit this raw test data file and produce another text file

¹The step segment describes: *i*) *Ramp* when the displacement is increasing, *ii*) *Extended Crack* when the crack has extended a small amount, *iii*) a number of *Unloading* and *Reloading* cycles.

containing *only* records of time, applied force (load) and displacements as displayed in Fig. 9.1 (observe that the characters, **Step**, **Step Segment**, **Time**, **Force**, **Displ_1** and **Displ_2** are provided in the input test data file only for clarity).

Depending on the MTS setup at the start of the fracture resistance test, the CMOD data can commonly be assigned to either column 3 or column 4 in the test data file. Since the present implementation of **FRACTUS2D** determines *J*-values and CTOD values *only* from experimentally measured load-CMOD records, the user must specify the column of records corresponding to load and CMOD data through the commands:

```
assign cmod to column < integer >
```

```
assign load to column < integer >
```

Moreover, the fracture resistance test protocol requires that several slow unloading-loading cycles at each *k*-th unloading step (see Chapter 4) to increase the evaluation accuracy in the slope of the unloading region which, in turn, will affect the accuracy of the compliance and crack length estimate (see discussion in Joyce [37]). Since each fracture resistance test may require the use of different numbers of unloading steps in connection with a given number of unloading-loading cycles previously setup at the start of the fracture resistance test, the user must specify these parameters using the following commands:

```
number of unloading steps < integer >
```

```
reloading cycles < integer >
```

As currently implemented, the maximum number of reloading cycle is 3, whereas a number of reloading cycles of 2 is most often adopted.

Step	Step Segment	Time	Force	Displ_1	Displ_2
12	Ramp	1131.34	90.8491	0.198452	0.813100
12	Ramp	1131.84	90.9060	0.199176	0.814424
12	Ramp	1132.34	91.0825	0.200242	0.818397
12	Ramp	1132.84	91.1727	0.201087	0.820605
.....					
12	Ramp	1144.34	92.5086	0.225621	0.879162
12	Ramp	1144.84	92.5450	0.226472	0.880559
12	Ramp	1145.34	92.6167	0.227608	0.883813
12	Ramp	1145.84	92.6716	0.228551	0.885329
12	Extend Crack	1146.51	92.5906	0.229631	0.887398
12	Extend Crack	1147.01	92.4739	0.230145	0.887308
12	Extend Crack	1147.51	92.3227	0.230396	0.887604
12	Extend Crack	1148.01	92.2767	0.230708	0.887418
.....					
12	Extend Crack	1154.51	91.8058	0.232830	0.886937
12	Extend Crack	1155.01	91.7885	0.232870	0.887644
12	Extend Crack	1155.51	91.7430	0.232949	0.887298
12	Extend Crack	1156.01	91.8083	0.233156	0.887988
12	Unload #1	1158.02	90.1782	0.230941	0.872148
12	Unload #1	1159.63	88.5765	0.228618	0.853896
12	Unload #1	1161.23	86.9480	0.226115	0.831914
12	Unload #1	1162.84	85.3736	0.223503	0.810853
.....					
12	Unload #1	1183.71	64.5187	0.197710	0.648181
12	Unload #1	1185.31	62.9090	0.195799	0.634982
12	Unload #1	1186.92	61.3079	0.193840	0.624468
12	Unload #1	1188.53	59.6998	0.191931	0.612569
12	Reload #1	1190.13	61.2509	0.194138	0.621995
12	Reload #1	1191.74	62.8472	0.196358	0.633517
12	Reload #1	1193.34	64.4372	0.198626	0.645332
12	Reload #1	1194.95	66.0388	0.200792	0.655550
.....					
12	Reload #1	1215.82	86.8833	0.226786	0.808973
12	Reload #1	1217.42	88.4822	0.228689	0.823517
12	Reload #1	1219.03	90.0922	0.230636	0.839006
12	Reload #1	1220.63	91.6767	0.233104	0.855162
12	Unload #2	1222.24	90.1634	0.230995	0.845510
12	Unload #2	1223.85	88.5610	0.228602	0.832272
12	Unload #2	1225.45	86.9699	0.226264	0.818230
12	Unload #2	1227.06	85.3657	0.224041	0.803828
.....					
12	Unload #2	1247.93	64.5280	0.198153	0.648350
12	Unload #2	1249.53	62.9269	0.196178	0.637139
12	Unload #2	1251.14	61.3041	0.194326	0.625807
12	Unload #2	1252.74	59.7172	0.192360	0.614286
12	Reload #2	1254.35	61.2421	0.194388	0.624469
12	Reload #2	1255.96	62.8320	0.196762	0.635340
12	Reload #2	1257.56	64.4379	0.199103	0.646137
12	Reload #2	1259.17	66.0344	0.201289	0.656104
.....					
12	Reload #2	1280.04	86.8732	0.227295	0.812292
12	Reload #2	1281.64	88.4635	0.229263	0.824017
12	Reload #2	1283.25	90.0894	0.231256	0.838642
12	Reload #2	1284.85	91.6917	0.233584	0.857242

Figure 9.1: Structure of the MTS data file for fracture toughness testing in which Displ_1 and Displ_2 can define either CMOD or LLD records.

9.5 Analysis Parameters

9.5.1 Material Properties

A specific set of mechanical properties must be assigned to the analysis to evaluate the fracture toughness value, including the J -integral and CTOD. *This set of mechanical properties must correspond to the properties of the tested material at the test temperature.* The commands to specify the material properties have the form

```
yield stress < number >

tensile strength < number >

young modulus < number >

poisson ratio < number >
```

In particular, specification of the tensile strength is required in all CTOD-related calculations as the flow stress, defined in the present work as $\sigma_f = (\sigma_{ys} + \sigma_{uts})/2$, enters directly into the J – CTOD relationship dimensionless constant, m - see previous Eq. (3.35). Moreover, since **FRACTUS2D** sets the Poisson's ratio to a default value of 0.3, specification of ν may be omitted in the analysis.

9.5.2 Fracture Resistance Evaluation Procedure

The expressions for η -factors and elastic compliance funtions implemented in **FRACTUS2D** derive primarily from previous work of Ruggieri and co-workers [57, 43, 61, 62, 63, 64, 65, 66, 67]. These expressions were developed for homogeneous materials and weld centerline notched specimens with a relatively narrow range of mismatch conditions in a plane-strain, 2D framework for conventional C(T) specimens, 3P and 4P bend geometries and SE(T) configurations under clamp and pin-load conditions - see Appendix B-D for details. In general, these η -factor equations elastic compliance functions agree well with other previously published solutions, including ASTM E1820 [38] for conventional C(T) and 3P SE(B) specimens, and Shen and co-workers [68, 69, 70, 71]. The fracture resistance evaluation procedure is specified with the command

```
unloading compliance procedure namef
```

where the option **namef** defines the fracture toughness evaluation procedure and associated η -factor expressions developed by Ruggieri and co-workers [57, 61, 62, 63, 64, 65, 66, 43, 67] given in Appendixes C and D.

To evaluate the fracture resistance curve for a weld centerline notched specimen, the user may also specify η -factors more applicable to welds with strength mismatch between the weld metal and the base plate. The input commands are

weld strength mismatch $\begin{cases} \text{on} \\ \text{off} \end{cases}$

`mismatch ratio < number >`

where the default option is `off`. When invoking the use of η -factors incorporating the effect of weld strength mismatch, the mismatch ratio, M_y , must also be specified - see Appendix D. As currently implemented in **FRACTUS2D**, the η -factors for weld centerline notched specimen are applicable in the range $1.0 \leq M_y \leq 1.5$.

9.5.3 Crack Extension Correction

As described in Chapter 4, because the area under the actual load-displacement curve for a growing crack differs significantly from the corresponding area for a stationary crack (which the deformation definition of J is based on) [2, 39, ?], the measured load-displacement records must be corrected for crack extension to obtain accurate estimates of J -values with increased crack growth (see further details in [39]). The command to invoke crack growth correction has the form

crack growth correction $\begin{cases} \text{on} \\ \text{off} \end{cases}$

where the default option is `on`. As shown in Mathias et al. [66], the J -resistance curves corrected for crack growth are lower ($\approx 10 \sim 20\%$) than the corresponding curves with no crack growth correction thereby resulting in more conservative fracture toughness measures.

9.5.4 Initialization Procedure

Section 4.4.2 describes an initialization procedure applicable to the measured fracture resistance data in which an improved value for the initial crack size, a_{0q} , is determined rather than the initial fatigue crack length, a_0 . Within this procedure, the original J vs. crack length data is fitted to a 3rd-degree polynomial to yield a_{0q} with the fitting procedure performed over data for which $P < P_{max}$ (see Section 4.4.2). The command to invoke the initialization procedure is

initialization procedure $\begin{cases} \text{on} \\ \text{off} \end{cases}$ initial step < integer >

where the default option is `off`.

In the above command, the initial load step (in connection with the load step associated with the maximum load, P_{max}) defines the range over which the crack length, a , versus J data is fitted to establish a polynomial dependence of crack size (as determined from the uncompliance procedure) with the experimentally measured crack driving force thereby enabling the determination of a_{0q} - see details in Section 4.4.2. As currently implemented, **FRACTUS2D** does not automatically determine a best value for the initial load step so this parameter should be carefully evaluated by the user. In general, the initial load step should be chosen as the load step at which no spurious apparent *negative* crack growth is observed

during the initial part of loading.

9.5.5 Test Data Units

The MTS system requires an initial test setup to perform the fracture toughness experiment on the test specimen. Most often, the recorded load and displacement are set in metric units, with load set in kN and displacements in mm. However, in some occasions, a different test setup is used, in which case different units may have been assigned to the load-displacement records. To specify the correct units utilized in the test setup, use the command

```
test data units load {kN  
N}
```

As currently implemented in **FRACTUS2D**, only the load unit needs to be specified (kN or N) as the CMOD (and LLD) records provided by the MTS system are always expressen in mm. Since the default load unit manipulated by **FRACTUS2D** is kN, this command can be ommited by the user when this unit was used in the test setup.

9.6 Illustrative Example

The following example illustrates the **FRACTUS2D** input file to evaluate the *J*-resistance curves for an Inconel 625 girth weld using a clamped SE(T) specimen with $a/W = 0.25$.

```

c
c      J-R Curve
c
c      Computation of J-R curve for an SE(T) specimen
c      using unloading compliance method
c
c      Inconel625 Girth WEld
c
c
c      crack analysis type resistance curve
c
c
c      crack configuration {
        structure SET_HW10_CP02
        fracture specimen clamped set
        specimen thickness 15.0
        side groove reduction 0.15 !
        specimen width 15
        specimen load point distance 150
        initial crack size 3.76
        final crack size   8.5      }
c
c      test data description {
        get files from directory CP02
        input test data from file SET02_Load_CMOD
        assign load to column 2
        assign cmod to column 3
        number of unloading steps 43
        reloading cycles 2  }
c
c
c      analysis parameters {
        crack extension correction off
        ctod resistance curve on
        unloading compliance procedure namef
        weld strength mismatch off
        initialization procedure on initial step 5
        yield stress 500.52
        tensile stress 700.46
        poisson ratio 0.3
        young modulus 200000  }
c
end

```

Figure 9.2: Illustrative example of **FRACTUS2D** input file to evaluate the J-resistance curves for an Inconel 625 girth weld using a clamped SE(T) specimen with $a/W = 0.25$.

A

Fracture Specimen Geometries

A.1 Homogeneous Fracture Specimens

Figures A.1-A.3 provide the geometry and principal dimensions of the fracture specimens currently implemented in **FRACTUS2D**, including the compact tension specimen, C(T), the three-point and four-point single edge notched bend geometry, 3P and 4P SE(B), and the single edge notched tension specimen under clamp and pin-load conditions, SE(T)_C and SE(T)_P. The C(T) and 3P SE(B) specimens follow the geometry and dimensions specified in ASTM E1820 standard [38] as well as in other related standards, such as ISO 15653 [42] and BS 7448 [72]. The 4P SE(B) and the SE(T) configurations are not fully standardized yet (refer to BS 8571 [?] for further details on the clamped SE(T) specimen) but the geometry adopted here for these specimens follow the most common configurations recently employed by several test procedures and testing programs. The following nomenclature is adopted to define each specimen geometry:

a	crack size
W	specimen width
S	specimen span
D	specimen inner span for the 4P bend specimen
H	clamp or pin-load distance for the SE(T) specimen

A.2 Weld Centerline Fracture Specimens

Figures A.4-A.6 provide the geometry and principal dimensions of the fracture specimens with weld centerline cracks currently implemented in **FRACTUS2D**, including the compact tension specimen, C(T), the standard three-point single edge notched bend geometry, 3P SE(B), and the single edge notched tension specimen under clamp and pin-load conditions, SE(T)_C and SE(T)_P. The C(T) and 3P SE(B) specimens follow the geometry and dimensions specified in ASTM E1820 standard [38] as well as in other related standards, such as ISO 15653 [42] and BS 7448 [72]. The SE(T) configurations are not fully standardized yet (refer to BS 8571 [?] for further details on the clamped SE(T) specimen) but the geometry adopted here for these specimens follow the most common configurations recently employed by several test procedures and testing programs. In the following specimen configurations, the weld joint geometry is idealized as a square groove weld with groove width, $2h$.

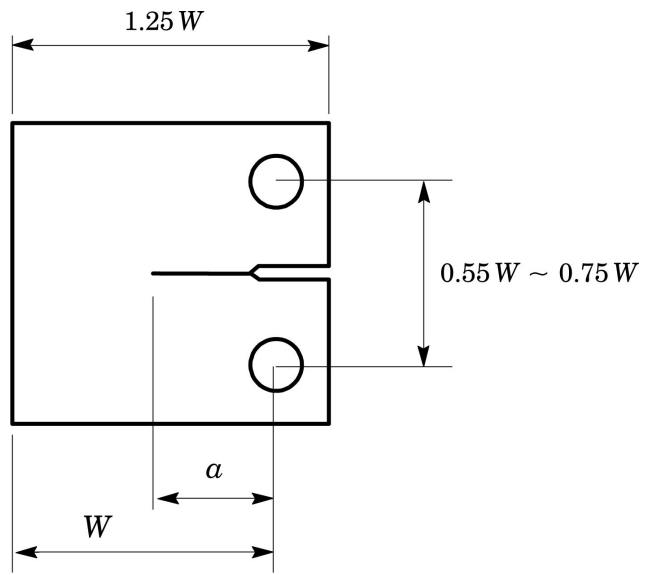


Figure A.1: *Conventional compact tension C(T) specimen.*

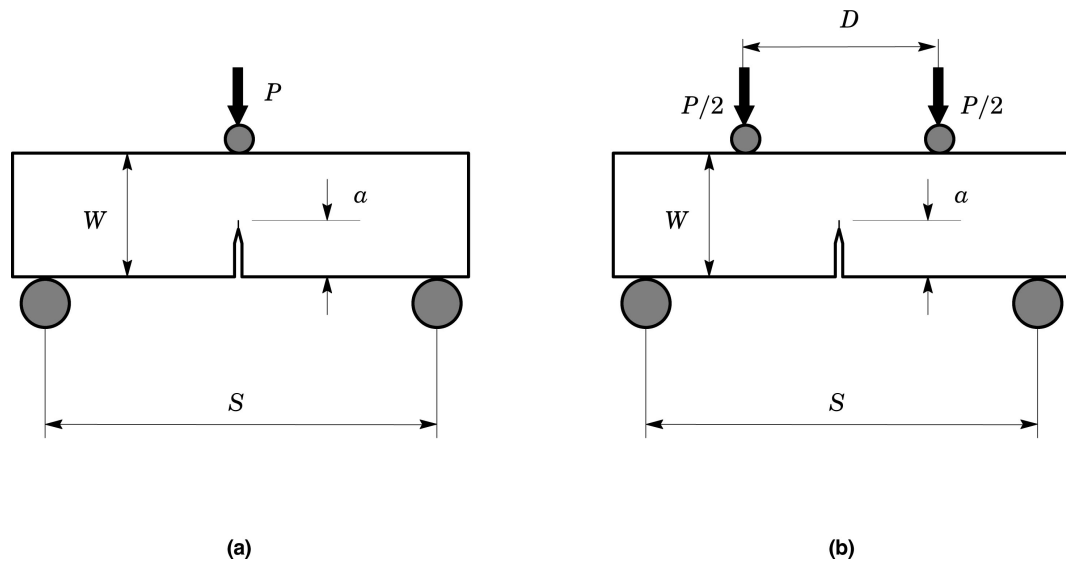


Figure A.2: (a) *Conventional 3P SE(B) specimen.* (b) *4P SE(B) specimen with $D = S/2$.*

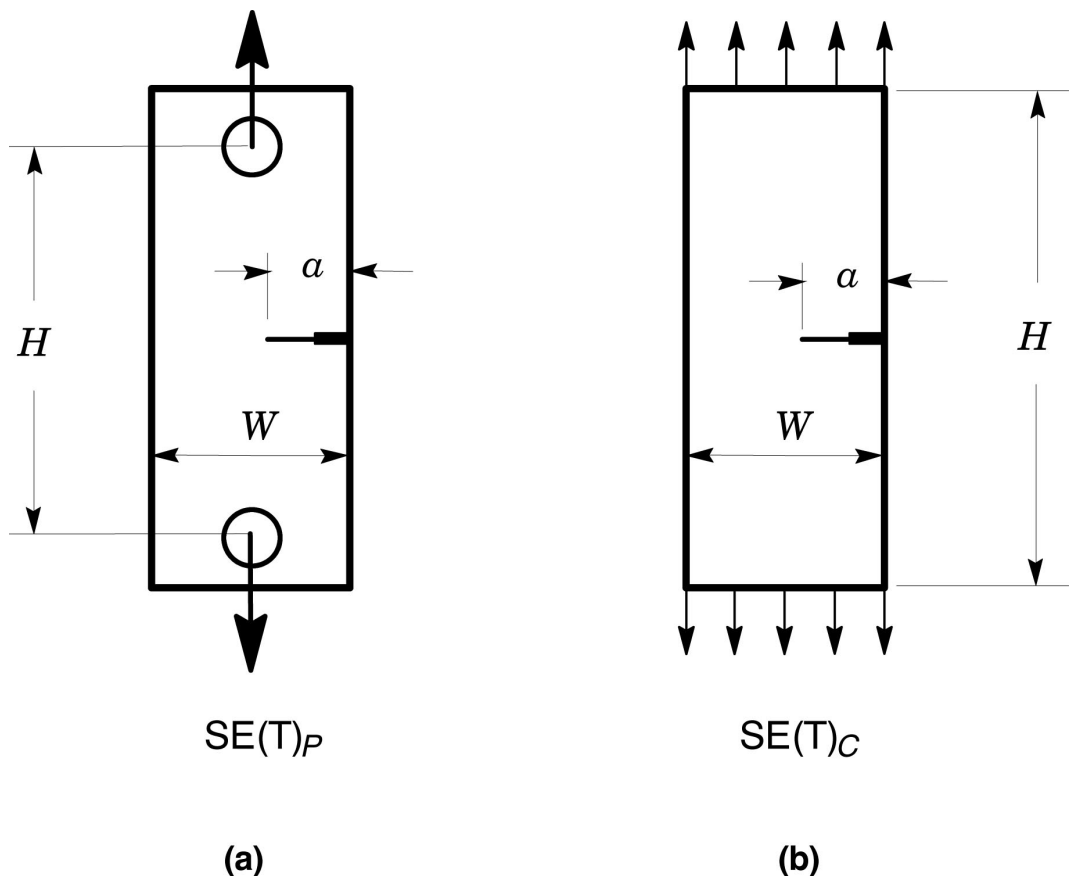


Figure A.3: (a) Pin-loaded SE(T) specimen. (b) Clamped SE(T) specimen.

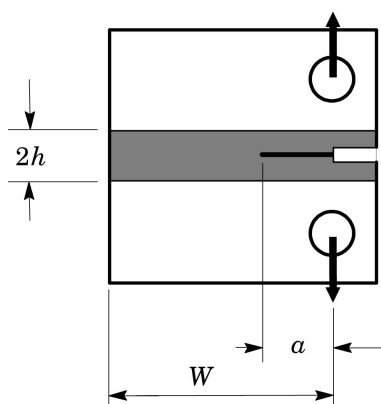


Figure A.4: Conventional compact tension C(T) specimen with weld centerline crack and groove weld width, $2h$.

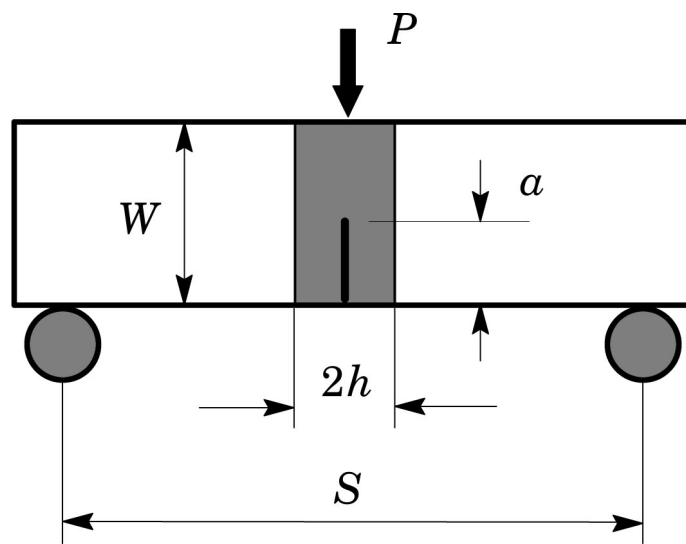


Figure A.5: Conventional 3P SE(B) specimen with weld centerline crack and groove weld width, $2h$.

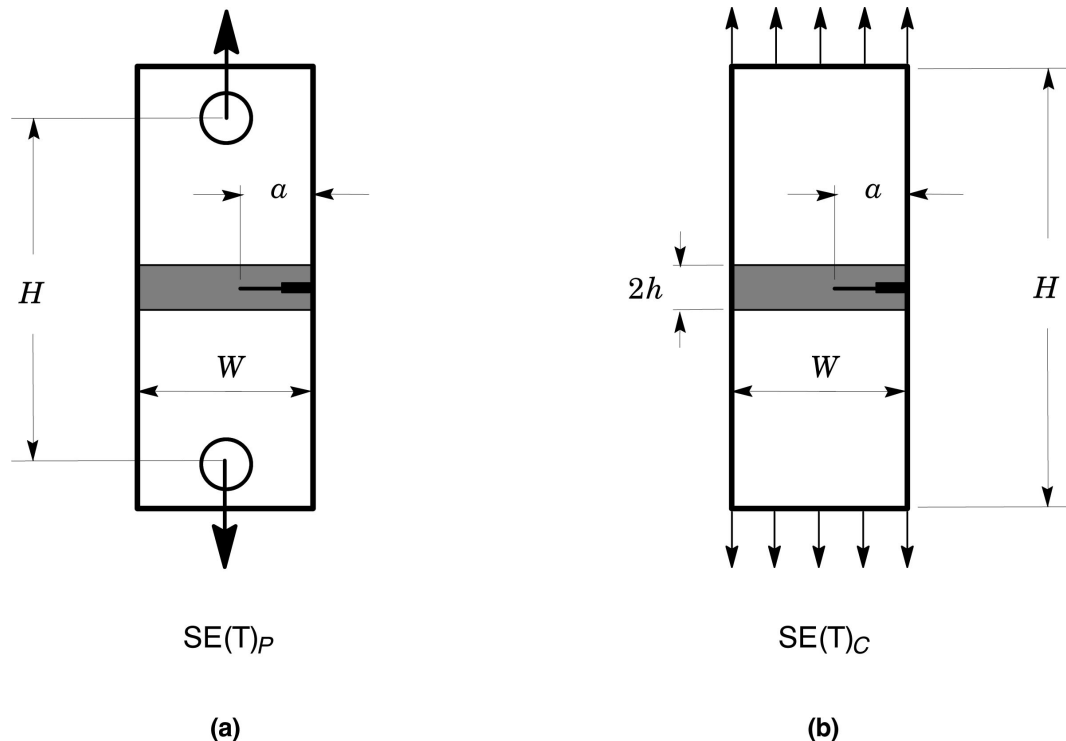


Figure A.6: Tensile loaded configurations with weld centerline crack and groove weld width, $2h$: (a) Pin-loaded SE(T) specimen. (b) Clamped SE(T) specimen.

B

Compliance Solutions for Fracture Specimens

The relationship between displacement, as generally characterized by the load line displacement (LLD or Δ) or, equivalently, the crack mouth opening displacement (CMOD or V), and applied load corresponding to linear elastic behavior defines the elastic compliance for a cracked body, denoted as C , illustrated in Fig. C.1, including standard and non-standard fracture specimens. With increased crack size, a , the ratio $C_\Delta = \Delta/P$ (or, equivalently, $C_V = V/P$) increases, as depicted in Fig. C.1(b), which simply reflects a decreasing stiffness of the cracked body (since this quantity is the inverse of the compliance). These changes in the relationship between load and crack displacement provide a simple and yet highly effective, indirect method to accurately estimate crack length and to measure the amount of crack growth in routine fracture testing using a variety of fracture specimen geometries, such as J -resistance curve testing [38, 66, 57] and fatigue crack growth testing [73]. Here, development of accurate and wide-range expressions relating C and crack size represents a key step in compliance-based crack length measurement techniques.

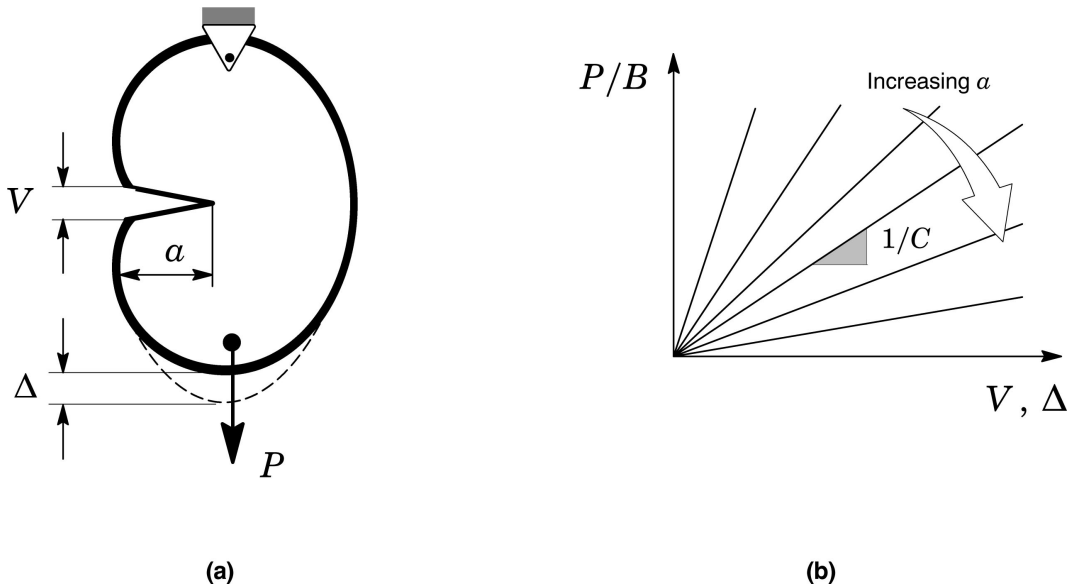


Figure C.1: (a) Arbitrary cracked body with thickness B subjected to remote loading, P , in which V defines the crack mouth opening displacement (CMOD) and Δ represents the load-line displacement (LLD); b) Linear relationship between applied load normalized by thickness and displacement with varying crack size.

For the crack configurations defined in previous Fig. A.1-A.3, the normalized specimen compliance

based on CMOD for the CT) and SE(T) configurations is most often expressed as

$$\mu_{CT} = \mu_{SET} = \left[1 + \sqrt{E' B_e C} \right]^{-1} \quad (\text{C.1})$$

whereas for the 3P and 4P bend specimens, the normalized specimen compliance based on CMOD can be expressed as

$$\mu_{SEB} = \left[1 + \sqrt{4E' B_e C W / S} \right]^{-1} \quad (\text{C.2})$$

in which the effective thickness, B_e , is defined by

$$B_e = B - \frac{(B - B_N)^2}{B} \quad (\text{C.3})$$

where B_N is the net specimen thickness at the side groove roots ($B_N = B$ if the specimen has no side grooves where B is the specimen gross thickness). The above expression (C.2) reduces to previous Eq. (C.1) in case of the standard 3-point bend geometry with $S = 4W$.

This section provides compliance solutions in terms of CMOD derived from recent plane-strain analyses conducted by Souza and Ruggieri [67] on the specimen geometries described in Appendix A. The following relationships defining the dependence of the specimen compliance on a/W yield plane-strain μ -values which provide conservative estimates of crack extension.

B.1 Compact Tension Specimen - C(T)

For the conventional compact tension specimen displayed in previous Fig. A.1, the compliance relationships are

$$\begin{aligned} \mu = & 0.2487 - 0.2593(a/W) - 0.1304(a/W)^2 + 0.5478(a/W)^3 \\ & - 0.7212(a/W)^4 + 0.3205(a/W)^5 \end{aligned} \quad (\text{C.4})$$

and

$$\begin{aligned} a/W = & 1.0216 - 5.3474\mu + 23.9166\mu^2 - 223.4974\mu^3 \\ & + 954.6388\mu^4 - 1458.8273\mu^5 \end{aligned} \quad (\text{C.5})$$

which are valid in the range of $0.1 \leq a/W \leq 0.8$.

B.2 3P Single Edge Notched Bend Specimen - 3P SE(B)

For the 3P SE(B) specimen shown in previous Fig. A.2(a), the following set of equations describe the compliance relationships

$$\begin{aligned} \mu = & 0.5035 - 1.9663(a/W) + 5.8823(a/W)^2 - 11.0250(a/W)^3 \\ & + 10.4590(a/W)^4 - 3.9101(a/W)^5 \end{aligned}, \quad \text{all } S/W \quad (\text{C.6})$$

and

$$a/W = 1.0033 - 4.0437\mu + 4.7902\mu - 13.7062\mu^3 + 59.6424\mu^4 - 71.7480\mu^5 , \quad \text{all } S/W \quad (\text{C.7})$$

which are valid in the range of $0.1 \leq a/W \leq 0.8$.

B.3 4P Single Edge Notched Bend Specimen - 4P SE(B)

For the 4P SE(B) specimen defined in previous Fig. A.2(b), the compliance relationships are

$$\mu = 0.5844 - 1.9692(a/W) + 5.2353(a/W)^2 - 8.9261(a/W)^3 + 7.4811(a/W)^4 - 2.3611(a/W)^5 , \quad \text{all } S/W \quad (\text{C.8})$$

and

$$a/W = 1.3177 - 10.2567\mu + 65.6950\mu - 271.2962\mu^3 + 549.9747\mu^4 - 420.7141\mu^5 , \quad \text{all } S/W \quad (\text{C.9})$$

which are valid in the range of $0.1 \leq a/W \leq 0.8$.

B.4 Pin-Loaded Single Edge Notched Tension Specimen - SE(T)_P

For the pin-loaded SE(T) specimen displayed in previous Fig. A.3(a), the compliance functions are given by Ruggieri [74] as

$$\mu = 0.7334 - 2.0350(a/W) + 5.0122(a/W)^2 - 9.3635(a/W)^3 + 8.8877(a/W)^4 - 3.2771(a/W)^5 , \quad \text{all } H/W \quad (\text{C.10})$$

and

$$a/W = 1.0030 - 2.6950\mu + 4.6439\mu - 10.4488\mu^3 + 13.1959\mu^4 - 5.5209\mu , \quad \text{all } H/W \quad (\text{C.11})$$

which are valid in the range of $0.1 \leq a/W \leq 0.8$.

B.5 Clamped Single Edge Notched Tension Specimen - SE(T)_C

For the clamped SE(T) specimen displayed in previous Fig. A.3(b), the following set of equations describe the compliance relationships

$$\mu = 0.7342 - 2.0519(a/W) + 5.3531(a/W)^2 - 9.7498(a/W)^3 + 9.2488(a/W)^4 - 3.4388(a/W)^5 , \quad H/W = 6 \quad (\text{C.12})$$

$$\begin{aligned}\mu = & 0.7234 - 2.0575(a/W) + 5.2243(a/W)^2 - 9.4590(a/W)^3 \\ & + 8.8792(a/W)^4 - 3.2403(a/W)^5\end{aligned}, \quad H/W = 10 \quad (\text{C.13})$$

and

$$\begin{aligned}a/W = & 2.1509 - 13.2405\mu + 48.8649\mu - 110.8908\mu^3 \\ & + 131.1808\mu^4 - 61.2957\mu\end{aligned}, \quad H/W = 6 \quad (\text{C.14})$$

and

$$\begin{aligned}a/W = & 1.7548 - 10.7686\mu + 43.1621\mu - 108.2553\mu^3 \\ & + 139.5816\mu^4 - 70.3533\mu\end{aligned}, \quad H/W = 10 \quad (\text{C.15})$$

which are valid in the range of $0.1 \leq a/W \leq 0.8$.

C

η -Factors for Homogeneous Fracture Specimens

Following the previous development to evaluate the J -integral from experimentally measured load-displacement records outlined in Chapter 4, this section presents the η -factor solutions for the fracture specimen geometries currently implemented in **FRACTUS2D**. Here, we note again that A_p (and consequently, η_J) can be defined in terms of load-load line displacement (LLD or Δ) data or load-crack mouth opening displacement (CMOD or V) data. For definiteness, the corresponding plastic η -factors are denoted η_{J-LLD} and η_{J-CMOD} . The polynomial fittings provided here derive from plane-strain finite element analyses conducted by Ruggieri and co-workers [61, 63, 64, 65, 66, 75, 76] on numerical models for the specimen geometries described in Appendix A. Thus, the following relationships defining the dependence of the plastic η -factors on a/W yield plane-strain η -values which generally provide conservative estimates of J (see Souza and Ruggieri [65] and Ruggieri [63] for further discussion).

C.1 Compact Tension Specimen - C(T)

For the conventional compact tension specimen displayed in previous Fig. A.1, the plastic η -factors are given by Savioli and Ruggieri [64] and Mathias et al. [66] as

$$\eta_J^{\text{CMOD}} = -2.264 + 18.244(a/W) - 26.430(a/W)^2 + 12.124(a/W)^3 \quad (\text{B.1})$$

and

$$\eta_J^{\text{LLD}} = -1.699 + 19.807(a/W) - 30.118(a/W)^2 + 14.099(a/W)^3 \quad (\text{B.2})$$

which are valid in the range of $0.45 \leq a/W \leq 0.7$.

C.2 3P Single Edge Notched Bend Specimen - 3P S

$$\eta_J^{\text{CMOD}} = 1.195 + 0.931(a/W) - 4.227(a/W)^2 + 3.072(a/W)^3 - 0.352M_y - 0.049M_y^2 \quad (\text{B.3})$$

E(B)

For the 3P SE(B) specimen displayed in previous Fig. A.2(a), Barbosa and Ruggieri [76] provide the following set of equations for the η -factors

$$\eta_J^{\text{CMOD}} = 3.710 - 2.782(a/W) + 1.095(a/W)^2 \quad , \quad S/W = 4 \quad (\text{B.4})$$

$$\eta_J^{\text{CMOD}} = 5.166 - 2.501(a/W) + 0.235(a/W)^2 \quad , \quad S/W = 6 \quad (\text{B.5})$$

$$\eta_J^{\text{CMOD}} = 6.865 - 2.477(a/W) - 0.662(a/W)^2 \quad , \quad S/W = 8 \quad (\text{B.6})$$

and

$$\eta_J^{\text{LLD}} = 0.668 + 6.198(a/W) - 10.355(a/W)^2 + 5.694(a/W)^3 \quad , \quad \text{all } S/W \quad (\text{B.7})$$

which are valid in the range of $0.1 \leq a/W \leq 0.8$.

C.3 4P Single Edge Notched Bend Specimen - 4P SE(B)

For the 4P SE(B) specimen displayed in previous Fig. A.2(b), the following set of equations for the η -factors are given by Barbosa and Ruggieri [76]

$$\eta_J^{\text{CMOD}} = 1.816 - 0.518(a/W) - 0.434(a/W)^2 \quad , \quad S/W = 4 \quad (\text{B.8})$$

$$\eta_J^{\text{CMOD}} = 2.749 - 0.867(a/W) - 0.578(a/W)^2 \quad , \quad S/W = 6 \quad (\text{B.9})$$

$$\eta_J^{\text{CMOD}} = 3.673 - 1.122(a/W) - 0.831(a/W)^2 \quad , \quad S/W = 8 \quad (\text{B.10})$$

and

$$\eta_J^{\text{LLD}} = -0.070 + 5.019(a/W) - 7.742(a/W)^2 + 3.910(a/W)^3 \quad , \quad \text{all } S/W \quad (\text{B.11})$$

which are valid in the range of $0.1 \leq a/W \leq 0.8$.

C.4 Pin-Loaded Single Edge Notched Tension Specimen - SE(T)_P

For the pin-loaded SE(T) specimen displayed in previous Fig. A.3(a), the plastic η -factors are given by Ruggieri [61] as

$$\begin{aligned} \eta_J^{\text{CMOD}} = & 0.692 + 3.627(a/W) - 22.180(a/W)^2 + 62.945(a/W)^3 \\ & - 79.000(a/W)^4 + 35.180(a/W)^5 \end{aligned} \quad , \quad \text{all } H/W \quad (\text{B.12})$$

and

$$\begin{aligned} \eta_J^{\text{LLD}} = & -3.106 + 52.026(a/W) - 243.885(a/W)^2 + 578.751(a/W)^3 \\ & - 646.996(a/W)^4 + 268.769(a/W)^5 \end{aligned} \quad , \quad \text{all } H/W \quad (\text{B.13})$$

which are valid in the range of $0.2 \leq a/W \leq 0.7$.

C.5 Clamped Single Edge Notched Tension Specimen - SE(T)_C

For the clamped SE(T) specimen displayed in previous Fig. A.3(b), the following set of equations for the η -factors are given by Ruggieri [61] and Mathias et al. [66]

$$\begin{aligned}\eta_J^{\text{CMOD}} = & 1.081 - 2.219(a/W) + 11.897(a/W)^2 - 35.689(a/W)^3 \\ & + 46.633(a/W)^4 - 21.792(a/W)^5\end{aligned}, \quad H/W = 6 \quad (\text{B.14})$$

$$\begin{aligned}\eta_J^{\text{CMOD}} = & 1.067 - 1.767(a/W) + 7.808(a/W)^2 - 18.269(a/W)^3 \\ & + 15.295(a/W)^4 - 3.083(a/W)^5\end{aligned}, \quad H/W = 10 \quad (\text{B.15})$$

and

$$\begin{aligned}\eta_J^{\text{LLD}} = & -1.027 + 19.906(a/W) - 72.889(a/W)^2 + 126.378(a/W)^3 \\ & - 107.534(a/W)^4 + 35.801(a/W)^5\end{aligned}, \quad H/W = 6 \quad (\text{B.16})$$

$$\begin{aligned}\eta_J^{\text{LLD}} = & -0.623 + 9.336(a/W) - 4.584(a/W)^2 - 47.963(a/W)^3 \\ & + 87.697(a/W)^4 - 44.875(a/W)^5\end{aligned}, \quad H/W = 10 \quad (\text{B.17})$$

which are valid in the range of $0.2 \leq a/W \leq 0.7$.

D

η -Factors for Weld Centerline Fracture Specimens

While the procedure to evaluate the J -integral from experimentally measured load-displacement records previously outlined in Chapter 4 was primarily developed for homogeneous materials, its extension to weld metal systems and welded testpieces, including specifically weld centerline fracture specimens, becomes relatively straightforward. For a given specimen geometry, mismatch between the weld metal and base plate strength affects the macroscopic mechanical behavior of the specimen in terms of its load-displacement response with a potentially strong impact on the coupling relationship between J and the near-tip stress fields. This section presents the η -factor solutions based on CMOD for the weld centerline fracture specimen geometries and currently implemented in **FRACTUS2D**. The polynomial fittings provided here derive from plane-strain finite element analyses conducted by Ruggieri and co-workers [43, 62, 64, 66] on numerical models for the specimen geometries described in Appendix A. Moreover, in the following relationships, the mismatch ratio, M_y , is defined as

$$M_y = \frac{\sigma_{ys}^{WM}}{\sigma_{ys}^{BM}} \quad (\text{B.1})$$

where σ_{ys}^{BM} and σ_{ys}^{WM} denote the yield stress for the base plate and weld metal. In general, the plastic η -factors for weld centerline fracture specimens do not depend sensitively on the weld groove width, $2h$. Consequently, the following set of equations for η -factors will improve the accuracy of experimentally measured J -values from testing welded fracture specimens in the range $0.1 \leq h/W \leq 0.2$ - see further details in Paredes and Ruggieri [62] and Savioli and Ruggieri [64].

D.1 Compact Tension Specimen - C(T)

For the conventional compact tension specimen with a weld centerline crack shown in previous Fig. A.4, the plastic η -factors are given by Savioli and Ruggieri [64] and Mathias et al. [66] as

$$\eta_J^{\text{CMOD}} = -3.864 + 29.086(a/W) - 46.404(a/W)^2 + 24.415(a/W)^3 - 0.252M_y - 0.106M_y^2 \quad (\text{B.1})$$

which are valid in the range of $0.45 \leq a/W \leq 0.7$ and $1.0 \leq M_y \leq 1.5$.

D.2 3P Single Edge Notched Bend Specimen - 3P SE(B)

For the conventional 3P SE(B) geometry with a weld centerline crack and $S/W = 4$ displayed in previous Fig. A.5, Donato et al. [43] and Mathias et al. [66] provide the plastic η -factors as

$$\begin{aligned}\eta_J^{\text{CMOD}} = & -3.882 + 0.222(a/W) - 5.012(a/W)^2 + 4.021(a/W)^3 \\ & - 0.407M_y - 0.050M_y^2 \quad , \quad S/W = 4\end{aligned}\tag{B.2}$$

which are valid in the range of $0.1 \leq a/W \leq 0.7$ and $1.0 \leq M_y \leq 1.5$.

D.3 Pin-Loaded Single Edge Notched Tension Specimen - SE(T)_P

For the pin-loaded SE(T) specimen with a weld centerline crack shown in previous Fig. A.6(a), a convenient fitting of the results provided by Paredes and Ruggieri [62] yields the plastic η -factors as

$$\begin{aligned}\eta_J^{\text{CMOD}} = & 1.536 - 2.692(a/W) + 6.727(a/W)^2 - 4.933(a/W)^3 \\ & - 0.318M_y + 0.040M_y^2 \quad , \quad \text{all } H/W\end{aligned}\tag{B.3}$$

which are valid in the range of $0.2 \leq a/W \leq 0.7$ and $1.0 \leq M_y \leq 1.5$.

D.4 Clamped Single Edge Notched Tension Specimen - SE(T)_C

For the clamped SE(T) specimen with a weld centerline crack and $H/W = 10$ displayed in previous Fig. A.6(b), a convenient fitting of the results provided by Paredes and Ruggieri [62] yields the plastic η -factors as

$$\begin{aligned}\eta_J^{\text{CMOD}} = & 1.195 + 0.931(a/W) - 4.227(a/W)^2 + 3.072(a/W)^3 \\ & - 0.352M_y - 0.049M_y^2 \quad , \quad H/W = 10\end{aligned}\tag{B.4}$$

which are valid in the range of $0.2 \leq a/W \leq 0.7$ and $1.0 \leq M_y \leq 1.5$.

Bibliography

- [1] J. W. Hutchinson, Fundamentals of the phenomenological theory of nonlinear fracture mechanics, *Journal of Applied Mechanics* 50 (1983) 1042–1051.
- [2] T. L. Anderson, *Fracture Mechanics: Fundaments and Applications - 3rd Edition*, CRC Press, Boca Raton, FL, 2005.
- [3] R. H. Dodds, C. Shih, T. Anderson, Continuum and micro-mechanics treatment of constraint in fracture, *International Journal of Fracture* 64 (1993) 101–133.
- [4] A. M. Al-Ani, J. W. Hancock, J -dominance of short cracks in tension and bending, *Journal of Mechanics and Physics of Solids* 39 (1991) 23–43.
- [5] C. Betegon, J. W. Hancock, Two-parameter characterization of elastic-plastic crack tip fields, *Journal of Applied Mechanics* 58 (1991) 104–113.
- [6] D. M. Parks, Advances in characterization of elastic-plastic crack-tip fields, in: A. S. Argon (Ed.), *Topics in Fracture and Fatigue*, Springer Verlag, 1992, pp. 59–98.
- [7] N. O'Dowd, C. Shih, Family of crack-tip fields characterized by a triaxiality parameter: Part I - Structure of fields, *Journal of the Mechanics and Physics of Solids* 39 (1991) 989–1015.
- [8] N. O'Dowd, C. Shih, Family of crack-tip fields characterized by a triaxiality parameter: Part II - Fracture applications, *Journal of Mechanics and Physics of Solids* 40 (1992) 939–963.
- [9] S. Yang, Y. J. Chao, M. A. Sutton, High order asymptotic crack tip fields in a power-law hardening material, *Engineering Fracture Mechanics* 45 (1993) 1–20.
- [10] Y. J. Chao, X. K. Chao, J - $A\mathcal{Q}$ characterization of crack-tip fields: Extent of J - $A\mathcal{Q}$ dominance and size requirements, *International Journal of Fracture* 89 (1998) 285–307.
- [11] U. Zerbst, R. A. Ainsworth, K.-H. Schwalbe, Basic principles of analytical flaw assessment methods, *International Journal of Pressure Vessel and Piping* 77 (2000) 855–867.
- [12] C. S. Wiesner, S. J. Maddox, W. Xu, G. A. Webster, F. M. Burdekin, R. M. Andrews, J. D. Harrison, Engineering critical analyses to BS 7910 - the UK guide on methods for assessing the acceptability of flaws in metallic structures, *International Journal of Pressure Vessel and Piping* 77 (2000) 883–893.
- [13] T. L. Anderson, D. A. Osage, API 579: A comprehensive fitness-for-service guide, *International Journal of Pressure Vessel and Piping* 77 (2000) 953–963.

- [14] British Energy Generation Limited, Assessment of the integrity of structures containing defects, R6 Procedure (2009).
- [15] British Institution, Guide to methods for assessing the acceptability of flaws in metallic structures, BS 7910 (2013).
- [16] American Petroleum Institute, Fitness-for-service, API RP-579-1 / ASME FFS-1 (2016).
- [17] E. U. B.-E. Programme, Structural integrity assessment procedures for european industry, SINTAP, Tech. Rep. EU Project BE 95-1462 (1999).
- [18] B. Healy, A. Gullerud, K. Koppenhoefer, A. Roy, S. RoyChowdhury, J. Petti, M. Walters, B. Bichon, K. Cochran, A. Carlyle, J. Sobotka, M. Messner, R. H. Dodds, WARP3D: 3-D nonlinear finite element analysis of solids for fracture and fatigue processes, Tech. rep., University of Illinois at Urbana-Champaign, <http://code.google.com/p/warp3d> (2014).
- [19] Dassault Systèmes Simulia Corp., ABAQUS Standard - V. 6.12, Providence, RI, USA (2012).
- [20] W. Sorem, R. Dodds, S. Rolfe, Effects of crack depth on elastic plastic fracture toughness, International Journal of Fracture 47 (1991) 105–126.
- [21] C. Ruggieri, R. H. Dodds, A transferability model for brittle fracture including constraint and ductile tearing effects: A probabilistic approach, International Journal of Fracture 79 (1996) 309–340.
- [22] R. G. Savioli, C. Ruggieri, Experimental study on the cleavage fracture behavior of an ASTM A285 Grade C pressure vessel steel, ASME Journal of Pressure Vessel Technology 137 (2) (2014) 1–7.
- [23] C. Ruggieri, R. G. Savioli, R. H. Dodds, An engineering methodology for constraint corrections of elastic-plastic fracture toughness - Part II:: Effects of specimen geometry and plastic strain on cleavage fracture predictions, Engineering Fracture Mechanics 146 (2015) 185–209.
- [24] V. S. Barbosa, C. Ruggieri, Fracture toughness testing using non-standard bend specimens - Part II: Experiments and evaluation of t_0 reference temperature for a low alloy structural steel, Engineering Fracture Mechanics 195 (2018) 297–312.
- [25] W. Ramberg, W. R. Osgood, Description of stress-strain curves by three-parameters, Technical Report NACA-TN-902, National Advisory Committee for Aeronautics (1943).
- [26] S. G. Larsson, A. J. Carlsson, Influence of non-singular stress terms and specimen geometry on small scale yielding at crack-tips in elastic-plastic materials, Journal of the Mechanics and Physics of Solids 21 (1973) 447–473.
- [27] J. R. Rice, Limitations to the small scale yielding approximation for crack tip plasticity, Journal of the Mechanics and Physics of Solids 22 (1974) 17–26.
- [28] Z. Z. Du, J. W. Hancock, The effect of non-singular stresses on crack-tip constraint, Journal of Mechanics and Physics of Solids 39 (1991) 555–567.
- [29] M. L. Williams, On the stress distribution at the base of a stationary crack, Journal of Applied Mechanics 24 (1957) 109–114.

- [30] E. Trovato, C. Ruggieri, Micromechanics characterization of constraint and ductile tearing effects in small scale yielding fracture, *International Journal of Solids and Structures* 38 (2001) 2171–2187.
- [31] S. Cravero, C. Ruggieri, Correlation of fracture behavior in high pressure pipelines with axial flaws using constraint designed test specimens - Part I: Plane-strain analyses, *Engineering Fracture Mechanics* 72 (2005) 1344–1360.
- [32] H. A. Ernst, P. C. Paris, J. D. Landes, Estimations on J -integral and tearing modulus T from a single specimen record, in: R. Roberts (Ed.), *Fracture Mechanics: Thirteenth Conference*, ASTM STP 743, American Society for Testing and Materials, Philadelphia, 1981, pp. 476–502.
- [33] C, Stability analysis of J -controlled crack growth, in: J. D. Landes, J. A. Begley, G. A. Clarke (Eds.), *Elastic-Plastic Fracture*, ASTM STP 668, American Society for Testing and Materials, Philadelphia, 1979, pp. 37–64.
- [34] M. F. Kanninen, C. H. Popelar, *Advanced Fracture Mechanics*, Oxford University Press, New York, 1985.
- [35] J. D. G. Sumpter, C. E. Turner, Method for laboratory determination of j_c , in: J. L. Swedlow, M. L. Williams (Eds.), *Cracks and Fracture*, ASTM STP 601, American Society for Testing and Materials, Philadelphia, 1976, pp. 3–18.
- [36] J. R. Rice, P. C. Paris, J. G. Merkle, Some further results of J -integral analysis and estimates, in: J. Kaufman, J. Swedlow, H. Corten, J. Srawley, R. Heyer, E. Wessel, G. Irwin (Eds.), *Progress in Flaw Growth and Fracture Toughness Testing*, ASTM STP 536, American Society for Testing and Materials, Philadelphia, 1973, pp. 231–245.
- [37] J. A. Joyce, Manual on elastic-plastic fracture: Laboratory test procedure, *ASTM Manual Series MNL* 27, ASTM International (1996).
- [38] American Society for Testing and Materials, Standard test method for measurement of fracture toughness, *ASTM E1820-20* (2020).
- [39] S. Cravero, C. Ruggieri, Further developments in J evaluation procedure for growing cracks based on LLD and CMOD data, *International Journal of Fracture* 148 (2007) 387–400.
- [40] British Standard, Fracture mechanics toughness tests - Part 1. Method for determination of K_{Ic} , critical CTOD and critical J values of metallic materials, BS 7448-1:1991 (1991).
- [41] International Organization for Standardization, Metallic materials - unified method of test for the determination of quasistatic fracture toughness, ISO 12135-2002 (2002).
- [42] International Organization for Standardization, Metallic materials - method of test for the determination of quasistatic fracture toughness of welds, ISO 15653-2010 (2010).
- [43] G. H. B. Donato, R. Magnabosco, C. Ruggieri, Effects of weld strength mismatch on J and CTOD estimation procedure for SE(B) specimens, *International Journal of Fracture* 159 (2009) 1–20.
- [44] M. T. Kirk, R. H. Dodds, J and CTOD estimation equations for shallow cracks in single edge notch bend specimens, *Journal of Testing and Evaluation* 21 (1993) 228–238.

- [45] C. F. Shih, Relationship between the J -integral and the crack opening displacement for stationary and extending cracks, *Journal of the Mechanics and Physics of Solids* 29 (1981) 305–326.
- [46] J. W. Hutchinson, Singular behavior at the end of a tensile crack in a hardening material, *Journal of the Mechanics and Physics of Solids* 16 (1968) 13–31.
- [47] J. R. Rice, G. F. Rosengren, Plane strain deformation near a crack tip in a power-law hardening material, *Journal of the Mechanics and Physics of Solids* 16 (1968) 1–12.
- [48] N. E. Dowling, *Mechanical Behavior of Materials: Engineering Methods for Deformation, Fracture and Fatigue*, 2nd Edition, Prentice Hall, New Jersey, 1999.
- [49] C. F. Shih, J. W. Hutchinson, Fully plastic solutions and large scale yielding estimates for plane stress crack problems, *Transactions of ASME Journal of Engineering Materials and Technology - Series H* 98 (1976) 289–295.
- [50] M. S. G. Chiodo, C. Ruggieri, J and CTOD estimation procedure for circumferential surface cracks in pipes under bending, *Engineering Fracture Mechanics* 77 (2010) 415–436.
- [51] M. T. Kirk, Y.-Y. Wang, Wide range CTOD estimation formulae for SE(B) specimens, in: W. G. Reuter, J. H. Underwood, J. Newman (Eds.), *Fracture Mechanics*, ASTM STP 1256, American Society for Testing and Materials, Philadelphia, 1995, pp. 126–141.
- [52] P. C. Paris, H. Tada, A. Zahoor, H. Ernst, The theory of instability of the tearing mode of elastic-plastic crack growth, in: J. D. Landes, J. A. Begley, G. A. Clarke (Eds.), *Elastic-Plastic Fracture*, ASTM STP 668, American Society for Testing and Materials, Philadelphia, 1979, pp. 5–36.
- [53] J. C. Newman, M. A. James, U. Zerbst, A review of the CTOA/CTOD fracture criterion, *Engineering Fracture Mechanics* 70 (2003) 371–385.
- [54] M. T. Heath, *Scientific Computing: An Introductory Survey*, 2nd Edition, The McGraw-Hill Companies, New York, NY, 2002.
- [55] J. R. Rice, A path independent integral and the approximate analysis of strain concentration by notches and cracks, *Journal of Applied Mechanics (Transactions of the American Society of Mechanical Engineers)* 35 (1968) 379–386.
- [56] H. Tada, P. C. Paris, G. R. Irwin, *The Stress Analysis of Cracks Handbook*, 3rd Edition, American Society of Mechanical Engineers, 2000.
- [57] S. Cravero, C. Ruggieri, Estimation procedure of J -resistance curves for SE(T) fracture specimens using unloading compliance, *Engineering Fracture Mechanics* 74 (2007) 2735–2757.
- [58] X. K. Zhu, B. N. Leis, J. A. Joyce, Experimental estimation of J - R curves from load-CMOD record for SE(B) specimens, *Journal of ASTM International* 5 (5) (2008) 1–15.
- [59] W. H. Press, S. A. Teukolsky, W. T. Vetterling, B. P. Flannery, *Numerical Recipes in FORTRAN: The Art of Scientific Computing*, 2nd Edition, Cambridge University Press, Cambridge, 1992.
- [60] M. Nevalainen, R. H. Dodds, Numerical investigation of 3-D constraint effects on brittle fracture in SE(B) and C(T) specimens, *International Journal of Fracture* 74 (1995) 131–161.

- [61] C. Ruggieri, Further results in J and CTOD estimation procedures for SE(T) fracture specimens - Part I: Homogeneous materials, *Engineering Fracture Mechanics* 79 (2012) 245–265.
- [62] M. Paredes, C. Ruggieri, Further results in J and CTOD estimation procedures for SE(T) fracture specimens - Part II: weld centerline cracks, *Engineering Fracture Mechanics* 89 (2012) 24–39.
- [63] C. Ruggieri, Low constraint fracture toughness testing using SE(T) and SE(B) specimens, *International Journal of Pressure Vessels and Piping* 156 (2017) 23–39.
- [64] R. G. Savioli, C. Ruggieri, J and CTOD estimation formulas for C(T) fracture specimens including effects of weld strength overmatch, *International Journal of Fracture* 179 (2013) 109–127.
- [65] R. F. Souza, C. Ruggieri, Revised η -factors and J -CTOD relationships for SE(B) fracture specimens including 3-D effects and implications for fracture toughness measurements, *Materials Performance and Characterization* 2 (2) (2015) 34–54, ASTM International.
- [66] L. L. S. Mathias, D. F. B. Sarzosa, C. Ruggieri, Effects of specimen geometry and loading mode on crack growth resistance curves of a high-strength pipeline girth weld, *International Journal of Pressure Vessels and Piping* 111-112 (2013) 106–119.
- [67] R. F. Souza, C. Ruggieri, Revised wide range compliance solutions for selected standard and non-standard fracture test specimens based on crack mouth opening displacement, *Engineering Fracture Mechanics* 178 (2017) 77–92.
- [68] G. Shen, R. Bouchard, J. A. Gianetto, W. R. Tyson, Fracture toughness evaluation of high-strength steel pipe, in: ASME PVP 2008 Pressure Vessel and Piping Division Conference, American Society of Mechanical Engineers, Chicago, IL, 2008.
- [69] G. Shen, W. R. Tyson, Crack size evaluation using unloading compliance in single-specimen single-edge notched tension fracture toughness testing, *Journal of Testing and Evaluation* 37 (4) (2009) 347–357.
- [70] G. Shen, W. R. Tyson, Evaluation of CTOD from J -integral for SE(T) specimens, in: Pipeline Technology Conference (PTC 2009), Ostend, Belgium, 2009.
- [71] G. Shen, J. A. Gianetto, W. R. Tyson, Measurements of $J-R$ curves using single specimen technique on clamped SE(T) specimens, in: 19th International Offshore and Polar Engineering Conference (ISOPE), Osaka, Japan, 2009.
- [72] British Institution, Guide to methods for assessing the acceptability of flaws in metallic structures, BS 7910 (2013).
- [73] American Society for Testing and Materials, Standard test method for measurement of fatigue crack growth rates, ASTM E647-15 (2015).
- [74] C. Ruggieri, FRACTUS2D V4.0: Numerical computation of fracture mechanics parameters for 2-D cracked solids, Tech. rep., University of Sao Paulo, (In Portuguese) (2013).
- [75] G. H. B. Donato, C. Ruggieri, Estimation procedure for J and CTOD fracture parameters using three-point bend specimens, in: 6th International Pipeline Conference (IPC 2006) , Calgary, Canada, 2006.

- [76] V. S. Barbosa, C. Ruggieri, Fracture toughness testing using non-standard bend specimens - Part I: Constraint effects and development of test procedure, *Engineering Fracture Mechanics* 195 (2018) 279–296.